



Photochemical Model Estimated Relationships Between Offshore Wind Energy Project Precursor Emissions and Downwind Air Quality (O₃ and PM_{2.5}) Impacts

EPA-454/R-22-007
December 2022

Photochemical Model Estimated Relationships Between Offshore Wind Energy Project
Precursor Emissions and Downwind Air Quality (O₃ and PM_{2.5}) Impacts

U.S. Environmental Protection Agency
Office of Air Quality Planning and Standards
Air Quality Assessment Division
Research Triangle Park, NC

BACKGROUND

This document is intended to provide information for permitting authorities and permit applicants relating precursor emissions from offshore wind energy projects to ozone (O₃) and secondarily formed particulate matter less than 2.5 microns in diameter (PM_{2.5}) impacts. Primarily emitted PM_{2.5} should be estimated with tools intended for that purpose. Section 4.2.2.3 of the *Guideline on Air Quality Models* (the “*Guideline*,” published as Appendix W to 40 CFR part 51) states that the impacts of offshore primary pollutants should be modeled using the Offshore and Coastal Dispersion (OCD) model (or other case specific alternative model approved by EPA) for distances out to 50 km (section 8.1.2) from the source. The *Guideline* recommends a two-tiered approach for addressing single-source impacts on O₃ and secondary PM_{2.5} (U.S. Environmental Protection Agency, 2021). The first tier (or Tier 1) involves use of appropriate and technically credible relationships between emissions and ambient impacts developed from existing modeling studies deemed sufficient for evaluating impacts from a project. The second tier (or Tier 2) involves more sophisticated case-specific application of chemical transport modeling (e.g., with an Eulerian grid or Lagrangian model) (U.S. Environmental Protection Agency, 2021).

The document is intended to provide relationships between precursors and maximum downwind impacts of O₃ and PM_{2.5} for the purposes of developing a technically credible Tier 1 demonstration tool for sources offshore of the Atlantic coast. Specifically, the emissions sources in this assessment represent areas offshore of the United States that have been leased for the purpose of constructing wind energy projects. This approach is similar to Modeled Emission Rates for Precursors (MERPs), which is also a Tier 1 demonstration tool (U.S. Environmental Protection Agency, 2019b) under the Prevention of Significant Deterioration (PSD) permitting program that provides a simple way to relate maximum downwind impacts with a critical air quality threshold (e.g., a significant impact level or SIL) (U.S. Environmental Protection Agency, 2018). Relationships between emissions and downwind impacts of primarily emitted PM_{2.5} are provided for distances beyond 50 km for permit related assessments where that information may be useful (e.g., Class I increment for the PSD program). New relationships between emissions and downwind impacts were needed to represent the offshore chemical and physical environment which was not reasonably reflected in the existing Tier 1 MERPs database.

O₃ formation is a complicated, nonlinear process that depends on meteorological conditions in addition to volatile organic compounds (VOC) and nitrogen oxides (NO_x) concentrations (Seinfeld and Pandis, 2008). Warm temperatures, clear skies (abundant levels of solar radiation), and stagnant air masses (low wind speeds) increase O₃ formation potential (Seinfeld and Pandis, 2008). In the case of PM_{2.5}, total mass is often categorized into two groups: primary (i.e., emitted directly as PM_{2.5} from sources) and secondary (i.e., PM_{2.5} formed in the atmosphere by precursor emissions from sources). PM_{2.5} sulfate, nitrate, and ammonium are predominantly the result of chemical reactions of the oxidized products of sulfur dioxide (SO₂) and NO_x emissions and direct ammonia (NH₃) emissions (Seinfeld and Pandis, 2008). PM_{2.5} organic aerosol (primary and secondary), nitrate, and ammonium are also impacted by semivolatile partitioning that is influenced by both the meteorological conditions and the chemical environment.

EPA believes that use of photochemical models for estimating single source secondary pollutant impacts is scientifically appropriate (U.S. Environmental Protection Agency, 2019b, 2021). Photochemical models treat emissions, chemical transformation and partitioning, transport, and deposition using time and space variant meteorology. These modeling systems simulate primarily emitted species and secondarily formed pollutants such as O₃ and PM_{2.5} (Kelly et al., 2019; Simon et al., 2012). Even though single source emissions are injected into a grid volume, photochemical transport models have been shown to

adequately capture single source impacts when compared with downwind in-plume measurements (Baker and Kelly, 2014; Baker and Woody, 2017).

Some photochemical models have been instrumented with source apportionment capabilities which tracks emissions from specific sources through chemical transformation, transport, and deposition processes to estimate source-specific impacts to predicted air quality at downwind receptors (Kwok et al., 2015; Kwok et al., 2013). Source apportionment has been used to differentiate the air quality impact from single sources on model predicted O₃ and PM_{2.5} (Baker and Foley, 2011; Baker and Kelly, 2014; Baker et al., 2016; Baker and Woody, 2017). Photochemical grid model source apportionment and source sensitivity simulation of single-source downwind impacts compare well against field study primary and secondary ambient in-plume measurements (Baker and Kelly, 2014; Baker and Woody, 2017; ENVIRON International Corporation, 2012). This work indicates photochemical grid models using source apportionment or source sensitivity approaches provide meaningful estimates of single source impacts.

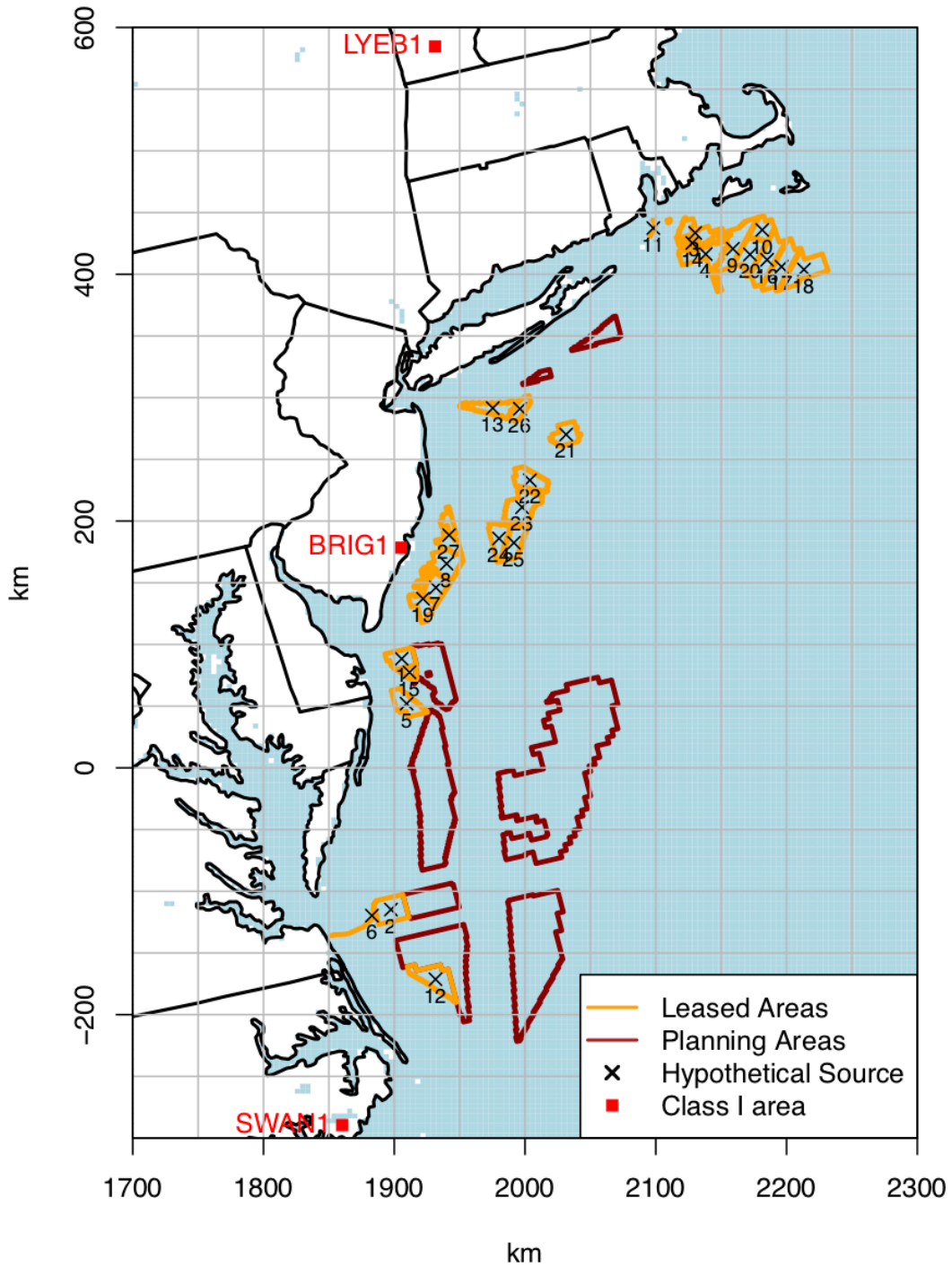
This document presents an overview of EPA photochemical modeling of hypothetical offshore emissions sources with 2017 National Emission Inventory (NEI) based emissions on downwind O₃ and secondary PM_{2.5}. Ozone contributions were estimated using Ozone Source Apportionment Technology and PM_{2.5} contributions using Particulate Source Apportionment Technology as implemented in the CAMx photochemical model (Ramboll, 2022). The contribution from each of these emissions sources to model predicted O₃ and inorganic PM_{2.5} ions (sulfate, nitrate, ammonium) were tracked using reactive tracers which track impacts of chemistry, atmospheric transport and deposition in the photochemical model (Kwok et al., 2015; Kwok et al., 2013; Ramboll, 2022). Primary emitted PM_{2.5} was tracked with inert tracers which track impacts of atmospheric transport and deposition in the photochemical model. All precursor impacts on PM_{2.5} and O₃ are tracked separately (e.g., NO_x to O₃, VOC to O₃, etc.).

MODEL CONFIGURATION & APPLICATION

Wind farm construction and operation includes the use of multiple categories of commercial marine vessels. Category 1 (C1) and Category 2 (C2) vessels have marine diesel engines above 800 horsepower (hp) with displacement less than 30 liters per cylinder. Category 3 (C3) engines are those at or above 30 liters per cylinder, typically these are the largest engines rated at 3,000 to 100,000 hp. C3 engines are typically used for propulsion on ocean-going vessels. C1 and C2 marine diesel engines typically range in size from about 700 to 11,000 hp. These engines are used to provide propulsion power on many kinds of vessels including tugboats, towboats, supply vessels, fishing vessels, and other commercial vessels in and around ports. They are also used as stand-alone generators for auxiliary electrical power on many types of vessels.

The locations tracked for contribution are shown in Figure 1. These locations were selected based on a review of areas offshore that were leased to private entities for the purpose of wind farm construction and operation.

Figure 1. Location of hypothetical emissions sources tracked for contribution as part of this project. The gray lines indicate nominal distance increments of 50 km and do not represent grid cell size used for the photochemical model applications.



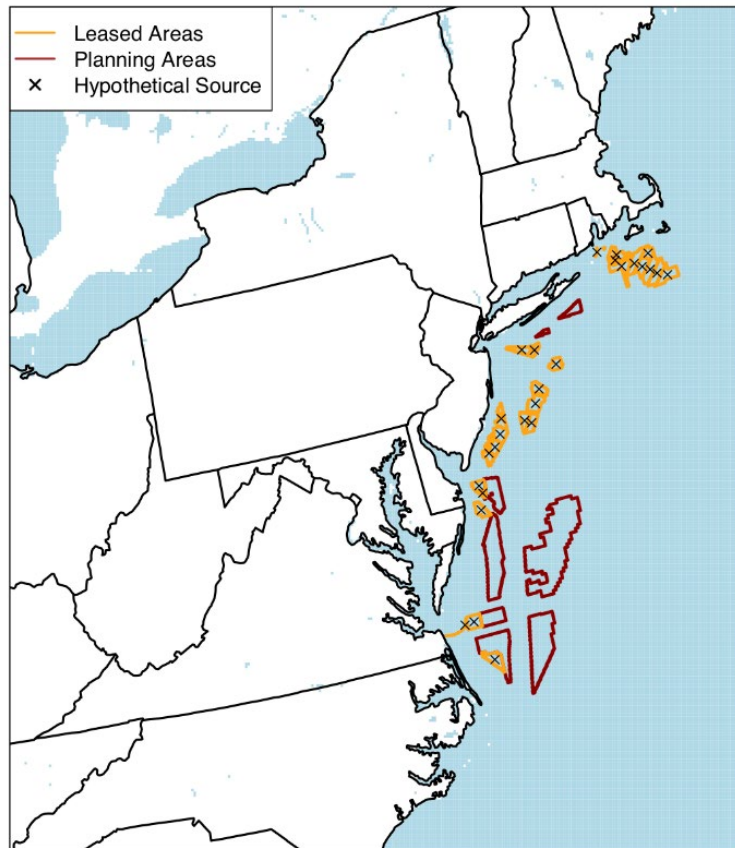
Annual emission totals in tons per year (tpy) were provided for total primarily emitted PM_{2.5}, coarse fraction PM, VOC, NH₃, SO₂, and NO_x for each hypothetical source. Primarily emitted PM_{2.5} was tracked with 4 separate emission rates for each source: 20, 215, 1100, and 3700 tpy. Primarily emitted coarse fraction PM was tracked with 2 separate emission rates for each source: 215 and 870 tpy. An emission rate of 5,000 tpy was used for NO_x and 50 tpy for SO₂ and VOC. Ammonia emissions were 5 tpy based on the 2017 NEI totals for commercial marine vessels. The hypothetical sources were assigned a surface level stack height. NO_x, VOC, and primary PM emissions were speciated consistent with profiles used for the commercial marine sector. Temporal profiles were unique to each hypothetical source location and based on nearby commercial marine vessel activity reported in the 2017 AIS database (NOAA Office for Coastal Management, 2022).

Model Configuration

Annual 2017 photochemical model simulations were performed for a domain covering the contiguous United States with 12 km sized grid cells (Figure 2). Each simulation tracked a different combination of pollutants. All simulations were conducted using version 7.20 of the Comprehensive Air Quality Model with Extensions (CAMx) photochemical grid model (www.camx.com). This CAMx application includes ISORROPIA inorganic chemistry (Nenes et al., 1998), gas phase reactions based on the Carbon Bond (CB6r5) mechanism (Ramboll, 2016, 2022), and aqueous phase reactions (Ramboll, 2022). Chemical boundary inflow was extracted from a photochemical model simulation for 2017 with a larger geographic domain covering the northern hemisphere (U.S. Environmental Protection Agency, 2019a).

A total of 35 layers were used to represent the vertical atmosphere to 50 mb with thinner layers nearer the surface (the height of the layer closest to the surface is approximately 20 m). The meteorological model configuration, application, and evaluation are available in a separate document (U.S. Environmental Protection Agency, 2022). Baseline emissions include anthropogenic sources based on the “2017gb” version of the 2017 National Emission Inventory (U.S. Environmental Protection Agency, 2020) and biogenic sources estimated with the Biogenic Emission Inventory System version 3.6.1 (Bash et al., 2016). Mobile emissions were based on the MOVES2014b model. Wildland fire emissions were day specific for 2017 (U.S. Environmental Protection Agency, 2020).

Figure 2. Photochemical model domain. The location of offshore leased and planning areas are also shown as well as hypothetical sources modeled as part of this assessment.



Model Application

The photochemical model was applied for the entire year of 2017 at 12 km grid resolution. A total of 27 hypothetical offshore emissions sources were included in addition to the 2017 NEI emissions and tracked for contribution to air quality impacts using source apportionment. Table 1 shows the relationship between precursor emissions and contribution to modeled primary and secondary pollutants. The model was applied so that primary and secondary precursors were tracked for contribution to modeled $PM_{2.5}$ components. NO_x emissions were tracked for contribution to $PM_{2.5}$ nitrate ion, NH_3 emissions were tracked for contribution to $PM_{2.5}$ ammonium ion, and SO_2 emissions were tracked for contribution to $PM_{2.5}$ sulfate ion.

Primarily emitted elemental carbon, organic aerosol, and crustal components were tracked to model predicted $PM_{2.5}$ emitted as primary only. Primarily emitted coarse PM components were tracked to model predicted coarse PM. The contribution to $PM_{2.5}$ nitrate does not include primarily emitted $PM_{2.5}$ nitrate and the contribution to $PM_{2.5}$ sulfate does not include primarily emitted $PM_{2.5}$ sulfate.

Table 1. Relationship between emissions species and tracked primary and secondarily formed PM_{2.5} and O₃ in the modeling system.

Precursor	Tagged Pollutant
SO ₂	Secondarily formed PM _{2.5} sulfate ion
NO _x	Secondarily formed PM _{2.5} nitrate ion
NH ₃	Secondarily formed PM _{2.5} ammonium ion
Primary PM _{2.5}	Primary PM _{2.5} : FCRS, FPRM, PEC, POA
Coarse PM	Primary coarse PM: CCRS, CPRM
VOC	Ozone
NO _x	Ozone

MODEL PERFORMANCE EVALUATION

Particulate Matter

An operational model performance evaluation for the speciated components of PM_{2.5} (e.g., sulfate, nitrate, elemental carbon, organic carbon, etc.) was conducted using 2017 monitoring data in order to estimate the ability of the modeling system to predict ambient concentrations. The evaluation of PM_{2.5} component species includes comparisons of predicted and observed concentrations of sulfate (SO₄), nitrate (NO₃), elemental carbon (EC), and organic carbon (OC). Chemically speciated PM_{2.5} ambient measurements for 2017 were obtained from the Chemical Speciation Network (CSN) and the Interagency Monitoring of PROtected Visual Environments (IMPROVE). The CSN sites are generally located within urban areas and the IMPROVE sites are typically in rural/remote areas. The measurements at CSN and IMPROVE sites represent 24-hour average concentrations. In calculating the model performance metrics, the modeled hourly species predictions were aggregated to the averaging times of the measurements.

Model performance statistics were calculated for observed/predicted pairs of all daily concentrations measured in 2017 (Simon et al., 2012). Aggregated metrics and number (N) of prediction-observation pairs are shown by chemical specie in Table 2. PM_{2.5} ammonium ion is not measured at most IMPROVE monitors, so metrics were not generated for that network. Model performance was compared to the performance found in recent regional PM_{2.5} model applications for other assessments. Overall, the mean bias (bias) and mean error (error) statistics are within the range or close to that found by other groups in recent applications (Kelly et al., 2019; Simon et al., 2012; Wilson et al., 2019). The average bias and error for PM_{2.5} organic carbon are slightly larger than other recent assessments and are related to overestimation of organic aerosol in the continental scale model simulation used to provide boundary inflow conditions. This performance feature is not expected to systematically impact primary or secondary PM_{2.5} or O₃ predictions for the offshore wind sources modeled as part of this assessment.

Overall, the model performance results provide confidence that this application of CAMx provides a scientifically credible approach for estimating PM_{2.5} concentrations for the purposes of this assessment.

Table 2. Aggregated model performance metrics for speciated components of PM_{2.5} for the IMPROVE and CSN monitor networks.

Specie	Network	N	Mean Bias ($\mu\text{g}/\text{m}^3$)	Mean Error ($\mu\text{g}/\text{m}^3$)	Normalized Mean Bias (%)	Normalized Mean Error (%)	r^2
PM2.5 sulfate ion	CSN	6,725	0.32	0.50	33	50	0.31
PM2.5 sulfate ion	IMPROVE	3,506	0.20	0.36	22	41	0.44
PM2.5 nitrate ion	CSN	6,712	0.55	0.77	70	97	0.38
PM2.5 nitrate ion	IMPROVE	3,508	0.38	0.51	97	129	0.28
PM2.5 elemental carbon	CSN	6,502	-0.02	0.28	-3	46	0.24
PM2.5 elemental carbon	IMPROVE	3,582	0.00	0.10	-2	40	0.58
PM2.5 organic carbon	CSN	6,510	2.77	2.82	139	141	0.33
PM2.5 organic carbon	IMPROVE	3,591	1.58	1.61	122	125	0.49

Ozone

An operational model performance evaluation for eight-hour daily maximum (MDA8) ozone was conducted in order to estimate the ability of the modeling system to replicate the 2017 base year concentrations. Ozone measurements were taken from 2017 monitoring site data in the Air Quality System (AQS). The ozone metrics covered in this evaluation include eight-hour average daily maximum ozone bias and error (Simon et al., 2012). The evaluation principally consists of statistical assessments of model versus observed pairs that are paired in time and space. Aggregated metrics and number (N) of prediction-observation pairs are shown in Table 3.

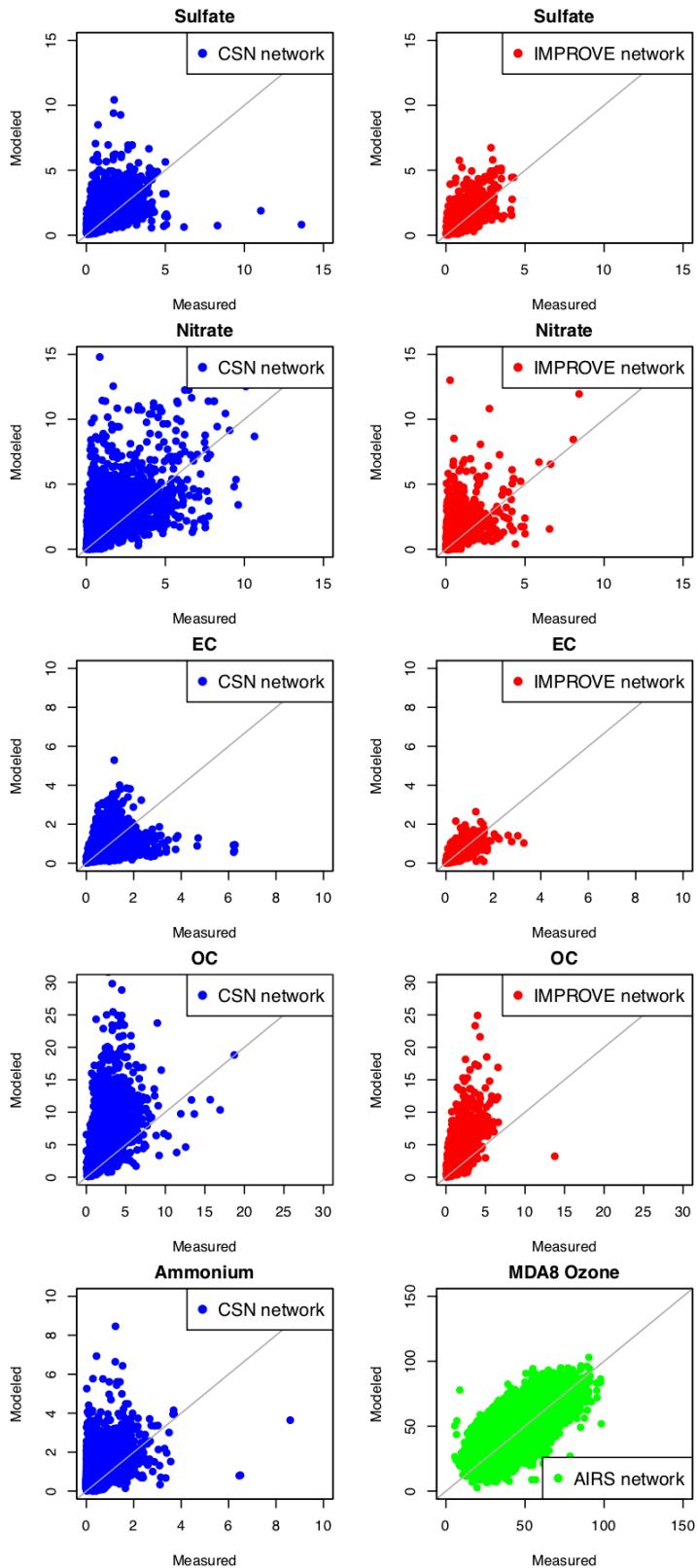
Table 3. Aggregated model performance metrics for MDA8 O₃. Metrics are shown for all prediction-observation pairs, pairs where the model predictions exceed 60 ppb, and pairs where the observations exceed 60 ppb.

Averaging Time & Specie	Data Subset	N	Mean Bias (ppb)	Mean Error (ppb)	Normalized Mean Bias (%)	Normalized Mean Error (%)	r^2
MDA8O3	ALL	76,475	2.28	7.44	5	17	0.49
MDA8O3	MODEL > 60	8,593	9.43	10.50	17	19	0.19
MDA8O3	OBS > 60	4,519	-2.66	7.15	-4	11	0.19

Only prediction-observation pairs from April through October were included in the aggregated metrics. This ozone model performance includes all prediction-observation pairs, a subset of prediction-observation pairs where observed ozone exceeded 60 ppb, and a subset of prediction-observation pairs where predicted ozone exceeded 60 ppb. This cutoff was applied to evaluate the model on days of elevated ozone which are more policy relevant. Overall, the mean bias (bias) and mean error (error) statistics are within the range or close to that found by other groups in recent applications (Simon et al., 2012; Wilson et al., 2019). The model performance results provide confidence that this application of CAMx provides a scientifically credible approach for estimating O₃ mixing ratios for the purposes of this assessment.

Model predictions paired with observation data for multiple species are provided in Figure 3. PM_{2.5} species are shown separately for the IMPROVE and CSN monitor networks. PM_{2.5} ammonium ion is only shown for the CSN network because it is not measured at sites in the IMPROVE network.

Figure 3. Paired observations with model predictions. Comparisons shown for PM_{2.5} species: sulfate ion, nitrate ion, elemental carbon, organic carbon, ammonium ion, and hourly O₃.

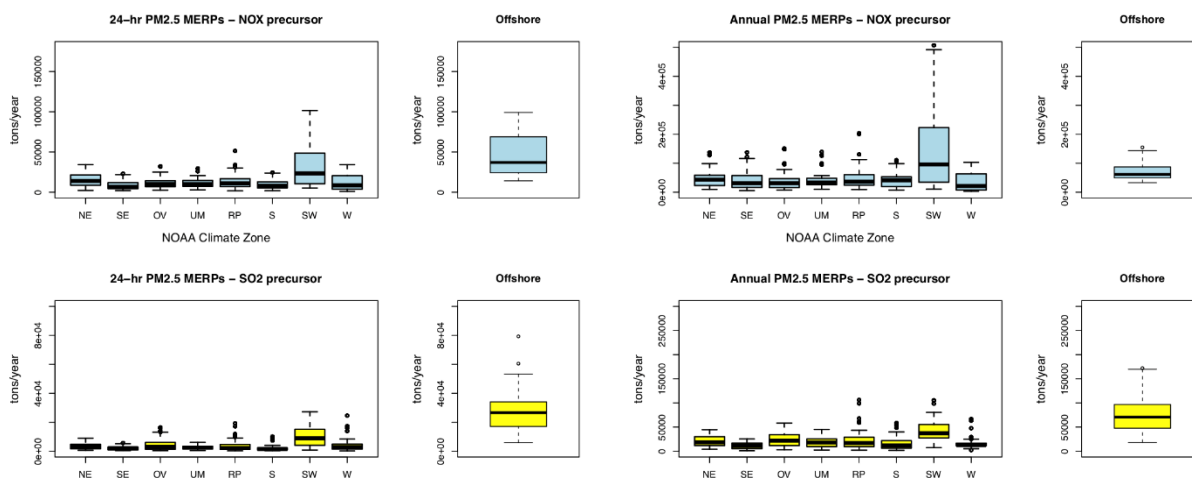


SOURCE IMPACT OVERVIEW

Ammonia reacts with sulfuric acid to form aerosol and with nitric acid to form ammonium nitrate when meteorological conditions are favorable (Seinfeld and Pandis, 2008). Ammonia has been measured in oceanic environments (Nair and Yu, 2020) but tends to be more abundant over land due to the larger amounts of sources.

The distribution of emission rates of NO_x and SO_2 that form $\text{PM}_{2.5}$ equivalent to the SIL are shown in Figure 4. This comparison includes hypothetical sources modeled over land (U.S. Environmental Protection Agency, 2019b) and offshore sources modeled as part of this assessment. The land-based distributions are differentiated by climate zone.

Figure 4. The distribution of emission rates equivalent to the relevant SIL level for daily average $\text{PM}_{2.5}$ (left) and annual average $\text{PM}_{2.5}$ (right) for hypothetical single sources modeled over land and the sources modeled offshore in this assessment. Results are shown for $\text{PM}_{2.5}$ nitrate ion (top row) and $\text{PM}_{2.5}$ sulfate ion (bottom row).



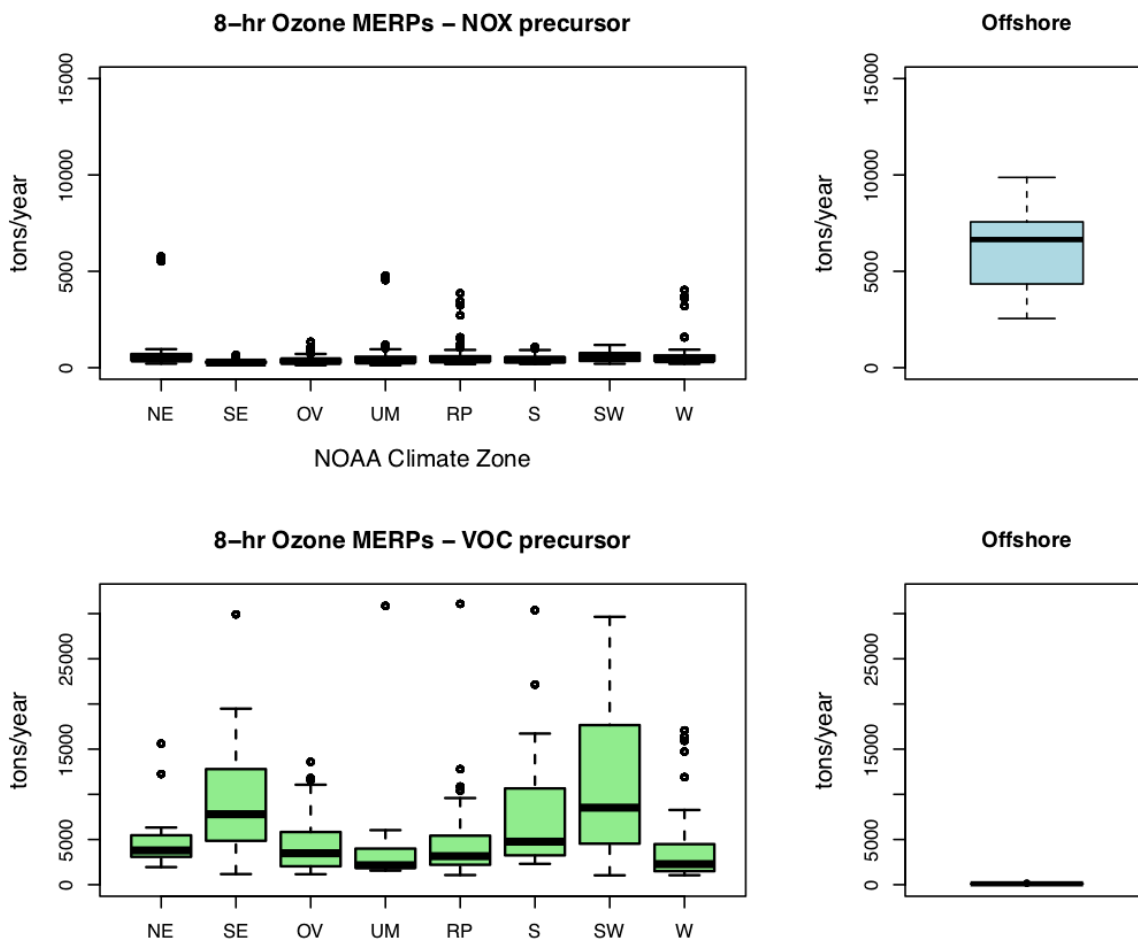
Based on the information shown in Figure 4, the offshore sources modeled in this assessment indicate that much greater SO_2 emissions are needed to form $\text{PM}_{2.5}$ sulfate ion equivalent of the SIL compared to over-land sources. Offshore emissions of NO_x needed to form $\text{PM}_{2.5}$ nitrate ion equivalent to the SIL are like the southwestern U.S. where ammonia emissions are more scarce compared to other regions. This is most pronounced for the daily form of the NAAQS.

Other anions (such as sodium or calcium) already in the aerosol phase can also react with nitric acid resulting in nitrate condensing into the particle phase. This switching would have limited (or small) influence on aerosol mass because the water content would not be identical for NO_3 and Cl and the molar mass of NO_3 and Cl is different. This type of anion substitution can also lead to the release of sequestered hydrochloric acid that could participate in atmospheric reactions and increase the anthropogenic contribution to aerosol at the expense of geogenic (e.g., sea salt) sources.

Figure 5 shows the distribution of NO_x and VOC emissions needed to generate a modeled MDA8 O_3 impact equivalent to the SIL for over land hypothetical sources (U.S. Environmental Protection Agency,

2019b) and offshore sources modeled as part of this assessment. The results shown in Figure 5 suggests areas offshore of the Atlantic coast tend to be much more conducive to MDA8 O₃ formation from VOC than NO_x emissions. This is likely due to the sparse nature of chemically reactive VOC offshore compared to over land where biogenic VOC is typically abundant, especially in the eastern U.S.

Figure 5. The distribution of emission rates equivalent to the relevant SIL level for MDA8 O₃ for hypothetical single sources modeled over land and the sources modeled offshore in this assessment. Results are shown for NO_x (top row) and VOC (bottom row).

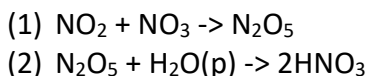


Oceanic emissions of halogens in aerosol and gas phase forms can influence the lifetime of NO_x, O₃, and some inorganic particulates. Some of these processes are included as part of the chemical mechanism developed for the photochemical model. However, others are more novel and have not been fully implemented. The potential impacts of chemical and physical processes related to oceanic emissions on O₃ and PM_{2.5} model predictions follow.

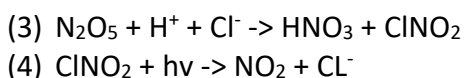
A chlorine mediated nitrate photolysis pathway could allow for NO_x recycling in the marine environment (Kasibhatla et al., 2018). This process is highly uncertain but could be a source of nitrous acid (HONO)

and NO_x in remote areas (Zhang et al., 2020). Both iodine and bromine chemistry can affect NO_x in the marine environment but would not be expected to have a large impact on NO_x.

NO_x can react in the atmosphere to form N₂O₅ (Equation 1) and be converted to nitric acid (HNO₃) (Equation 2) through heterogeneous chemistry and subsequently removed from participation in O₃ formation reactions (McDuffie et al., 2018).



Another heterogeneous N₂O₅ hydrolysis pathway (Equation 3) can act as a reservoir for NO₂ overnight and potentially result in regenerated NO₂ at sunrise (Equation 4) (McDuffie et al., 2018).



In environments without chlorine, 2 nitric acid molecules form from N₂O₅ heterogeneous reactions, which have a short atmospheric lifetime. In marine environments with chlorine emissions, N₂O₅ heterogeneous reactions make one nitric acid and one ClONO₂. The ClONO₂ photolyzes during the daytime to form Cl⁻ and NO₂. These marine environment processes can act as a nighttime NO_x reservoir which would then regenerate NO₂ on sunrise (McDuffie et al., 2018).

However, it is important to consider that the presence of chlorine speeds up the N₂O₅ hydrolysis reaction (Equation 3) rate (Bertram and Thornton, 2009). Therefore, it is not clear how much NO₂ would convert to HNO₃ rather than ClONO₂ in the presence of chlorine containing aerosol.

Photochemical modeling that incorporates the full suite of chemical reactions would be needed to fully understand the implications of the various reactions and processes noted in this section. However, important chemical and physical processes are included in the modeling system and the impacts provided here are considered a reasonable representation of O₃ and PM_{2.5} impacts from precursors for the intended purpose of supporting permit program related demonstrations.

PRODUCTS

PM_{2.5} nitrate impacts were linked to secondary formation attributed to NO_x emissions only and therefore these outputs do not include the impacts from primarily emitted PM_{2.5} nitrate. PM_{2.5} sulfate impacts were linked to secondary formation attributed to SO₂ emissions only and similarly do not include the impacts from primarily emitted PM_{2.5} sulfate. PM_{2.5} ammonium impacts were linked to secondary formation attributed to NH₃ emissions only and do not include the impacts from primarily emitted PM_{2.5} ammonium.

The modeled contributions from each source were processed to match metrics relevant for permit program related demonstrations. PM_{2.5} impacts were estimated as annual average and annual maximum daily average. O₃ impacts were estimated as maximum daily average of 8-hr rolling averages for April through October. The air quality impacts were then normalized by precursor emissions as a function of distance bins from the hypothetical source to develop transfer coefficients. These transfer coefficients

were intended to be paired with project specific emissions to develop an approximation of project specific air quality impacts by distance. Since the modeling was done using 12 km sized grid cells, no information is available for source impacts at distances less than the size of the grid cell.

The relationship between estimated project impacts, project emissions, and transfer coefficients is shown in Equation 1.

$$\text{Equation (1) } \textit{Air quality impact} = \textit{Project Emissions} \times \textit{Transfer Coefficient}$$

Where the screening level air quality impact would have units $\mu\text{g}/\text{m}^3$ for $\text{PM}_{2.5}$ and ppb for MDA8 O_3 calculations. The project emissions should be expressed as tons per year. The transfer coefficients are provided in for each precursor to secondary pollutant in Tables 4 to 15. The transfer coefficients are expressed as $(\mu\text{g}/\text{m}^3)/\text{tpy}$ for $\text{PM}_{2.5}$ and ppb/tpy for O_3 calculations.

It is expected that the screening level air quality impacts would be compared to appropriate SIL and increment values (U.S. Environmental Protection Agency, 2018, 2019b, 2021). These screening level air quality impacts could also be used in combination with appropriate estimates of ambient air and nearby sources as part of a cumulative demonstration comparison with NAAQS levels (U.S. Environmental Protection Agency, 2018, 2019b, 2021). Offshore projects should select the values from the table for areas that represent that particular project. If a new offshore project has a location that was not included in this assessment the applicant should consult with the appropriate Regional Office to discuss how this information might be used for that situation.

Table 4. Transfer coefficients (ppb/tpy) relating NO_x emissions (tpy) with maximum MDA8 O₃ impacts (ppb) at distance bins downwind for each hypothetical source.

SOURCE	LAT	LONG	NO _x to O ₃ coefficients (ppb/tpy) by distance from the source (km)							
			< 15	15 to 30	30 to 50	50 to 100	100 to 150	150 to 200	200 to 250	> 250
1	38.674	-74.701	1.41E-04	1.27E-04	1.34E-04	1.23E-04	1.50E-04	1.23E-04	1.24E-04	9.53E-05
2	36.908	-75.349	2.33E-04	3.59E-04	3.35E-04	2.78E-04	2.08E-04	2.08E-04	1.76E-04	1.59E-04
3	41.154	-71.080	1.22E-04	7.17E-05	5.48E-05	6.02E-05	6.88E-05	6.94E-05	6.37E-05	6.02E-05
4	40.985	-71.045	1.37E-04	8.58E-05	7.19E-05	9.13E-05	1.01E-04	9.63E-05	8.56E-05	6.08E-05
5	38.347	-74.761	2.58E-04	2.59E-04	2.53E-04	1.90E-04	1.76E-04	1.50E-04	1.50E-04	1.21E-04
6	36.896	-75.522	1.36E-04	2.95E-04	2.42E-04	2.70E-04	1.84E-04	1.81E-04	1.69E-04	1.58E-04
7	39.122	-74.242	1.06E-04	5.92E-05	4.84E-05	1.07E-04	1.02E-04	9.75E-05	8.55E-05	8.64E-05
8	39.273	-74.093	1.40E-04	1.33E-04	7.85E-05	7.58E-05	9.84E-05	9.56E-05	7.87E-05	8.33E-05
9	40.969	-70.792	1.01E-04	5.50E-05	5.85E-05	6.76E-05	7.37E-05	6.90E-05	7.49E-05	5.32E-05
10	41.043	-70.482	1.20E-04	9.35E-05	6.09E-05	1.39E-04	1.26E-04	7.90E-05	7.17E-05	6.76E-05
11	41.269	-71.436	1.06E-04	1.47E-04	1.63E-04	1.48E-04	1.06E-04	8.62E-05	6.82E-05	4.34E-05
12	36.339	-75.127	2.75E-04	3.08E-04	3.92E-04	3.60E-04	3.46E-04	2.66E-04	1.72E-04	1.65E-04
13	40.295	-73.315	1.76E-04	2.07E-04	1.96E-04	1.67E-04	1.38E-04	8.70E-05	7.16E-05	5.63E-05
14	41.089	-71.133	1.26E-04	9.36E-05	5.75E-05	6.74E-05	7.56E-05	7.49E-05	6.24E-05	5.54E-05
15	38.565	-74.665	1.33E-04	5.51E-05	1.03E-04	1.24E-04	1.47E-04	1.43E-04	1.45E-04	1.10E-04
16	40.824	-70.523	9.69E-05	6.26E-05	5.54E-05	1.33E-04	1.40E-04	1.33E-04	1.21E-04	1.14E-04
17	40.747	-70.416	1.31E-04	7.77E-05	8.80E-05	1.76E-04	1.87E-04	1.78E-04	1.61E-04	1.35E-04
18	40.682	-70.228	1.31E-04	1.16E-04	1.65E-04	1.74E-04	1.91E-04	1.90E-04	1.85E-04	1.21E-04
19	39.065	-74.379	1.79E-04	1.27E-04	8.06E-05	9.92E-05	1.04E-04	9.45E-05	9.02E-05	8.90E-05
20	40.895	-70.658	1.19E-04	5.21E-05	3.29E-05	8.88E-05	9.59E-05	9.72E-05	9.88E-05	8.91E-05
21	39.976	-72.740	2.03E-04	2.22E-04	2.67E-04	3.29E-04	3.72E-04	1.82E-04	1.19E-04	1.12E-04
22	39.718	-73.170	1.49E-04	2.13E-04	2.80E-04	3.06E-04	2.55E-04	1.29E-04	1.26E-04	9.22E-05
23	39.541	-73.304	1.73E-04	2.73E-04	2.62E-04	2.72E-04	2.27E-04	1.27E-04	7.50E-05	6.88E-05
24	39.361	-73.579	1.07E-04	8.42E-05	7.95E-05	8.34E-05	1.08E-04	1.00E-04	9.74E-05	1.01E-04
25	39.304	-73.461	1.28E-04	9.98E-05	1.01E-04	1.07E-04	1.06E-04	9.26E-05	1.02E-04	9.65E-05
26	40.242	-73.079	1.06E-04	1.57E-04	1.58E-04	1.93E-04	1.33E-04	1.05E-04	7.08E-05	7.16E-05
27	39.472	-74.004	8.58E-05	8.05E-05	1.10E-04	1.37E-04	9.91E-05	9.27E-05	7.85E-05	8.22E-05

Table 5. Transfer coefficients (ppb/tpy) relating VOC emissions (tpy) with maximum MDA8 O₃ impacts (ppb) at distance bins downwind for each hypothetical source.

POL	SOURCE	LAT	LONG	VOC to O ₃ coefficients (ppb/tpy) by distance from the source (km)							
				< 15	15 to 30	30 to 50	50 to 100	100 to 150	150 to 200	200 to 250	> 250
O3V	1	38.674	-74.701	1.29E-02	4.94E-03	4.95E-03	2.18E-03	6.58E-04	4.99E-04	4.15E-04	3.27E-04
O3V	2	36.908	-75.349	1.02E-02	7.43E-03	4.64E-03	2.48E-03	1.84E-03	9.99E-04	5.45E-04	3.66E-04
O3V	3	41.154	-71.080	1.23E-02	7.19E-03	4.62E-03	1.51E-03	1.00E-03	6.60E-04	3.39E-04	2.54E-04
O3V	4	40.985	-71.045	1.35E-02	7.24E-03	5.22E-03	1.47E-03	5.91E-04	4.19E-04	3.24E-04	2.99E-04
O3V	5	38.347	-74.761	8.91E-03	5.05E-03	2.51E-03	1.83E-03	1.02E-03	5.39E-04	3.29E-04	3.07E-04
O3V	6	36.896	-75.522	1.14E-02	6.79E-03	4.78E-03	2.34E-03	1.18E-03	6.96E-04	4.47E-04	3.28E-04
O3V	7	39.122	-74.242	9.97E-03	4.79E-03	3.44E-03	2.06E-03	7.25E-04	5.03E-04	2.96E-04	2.78E-04
O3V	8	39.273	-74.093	9.04E-03	4.68E-03	1.73E-03	1.55E-03	9.17E-04	5.20E-04	2.74E-04	2.56E-04
O3V	9	40.969	-70.792	1.01E-02	5.53E-03	4.69E-03	3.02E-03	1.03E-03	5.47E-04	3.33E-04	3.06E-04
O3V	10	41.043	-70.482	1.20E-02	9.23E-03	5.57E-03	4.19E-03	1.08E-03	5.34E-04	3.60E-04	3.15E-04
O3V	11	41.269	-71.436	8.82E-03	1.00E-02	4.33E-03	2.90E-03	7.85E-04	4.95E-04	4.20E-04	2.04E-04
O3V	12	36.339	-75.127	1.11E-02	9.49E-03	5.22E-03	3.66E-03	1.60E-03	1.03E-03	5.83E-04	4.09E-04
O3V	13	40.295	-73.315	5.60E-03	3.18E-03	3.83E-03	1.77E-03	5.45E-04	4.93E-04	3.05E-04	2.47E-04
O3V	14	41.089	-71.133	1.25E-02	9.01E-03	3.39E-03	2.26E-03	9.11E-04	5.24E-04	3.09E-04	2.76E-04
O3V	15	38.565	-74.665	1.28E-02	4.73E-03	2.95E-03	1.84E-03	7.49E-04	5.11E-04	4.22E-04	3.33E-04
O3V	16	40.824	-70.523	9.16E-03	5.78E-03	3.38E-03	2.28E-03	9.49E-04	5.49E-04	4.36E-04	4.43E-04
O3V	17	40.747	-70.416	1.14E-02	5.97E-03	3.77E-03	2.73E-03	1.04E-03	7.27E-04	5.51E-04	5.08E-04
O3V	18	40.682	-70.228	9.23E-03	6.48E-03	3.99E-03	3.97E-03	1.25E-03	7.51E-04	5.60E-04	4.95E-04
O3V	19	39.065	-74.379	1.06E-02	4.22E-03	2.47E-03	1.59E-03	7.04E-04	5.13E-04	3.19E-04	2.90E-04
O3V	20	40.895	-70.658	1.13E-02	3.63E-03	2.54E-03	1.68E-03	7.63E-04	3.94E-04	3.15E-04	3.29E-04
O3V	21	39.976	-72.740	1.29E-02	6.25E-03	4.97E-03	3.59E-03	1.93E-03	5.98E-04	3.70E-04	2.87E-04
O3V	22	39.718	-73.170	1.03E-02	4.87E-03	2.44E-03	1.65E-03	1.18E-03	5.22E-04	3.14E-04	2.30E-04
O3V	23	39.541	-73.304	1.25E-02	5.32E-03	2.05E-03	1.58E-03	1.48E-03	5.12E-04	3.74E-04	2.88E-04
O3V	24	39.361	-73.579	7.04E-03	4.99E-03	2.62E-03	1.67E-03	1.40E-03	9.81E-04	3.30E-04	2.23E-04
O3V	25	39.304	-73.461	8.65E-03	5.90E-03	3.00E-03	2.23E-03	1.59E-03	1.10E-03	3.72E-04	2.60E-04
O3V	26	40.242	-73.079	6.43E-03	4.48E-03	2.64E-03	1.55E-03	8.07E-04	4.02E-04	2.40E-04	2.17E-04
O3V	27	39.472	-74.004	8.58E-03	5.29E-03	2.62E-03	1.89E-03	7.56E-04	5.77E-04	3.85E-04	2.00E-04

Table 6. Transfer coefficients ($(\mu\text{g}/\text{m}^3)\cdot\text{tpy}$) relating SO_2 emissions (tpy) with annual maximum daily average $\text{PM}_{2.5}$ impacts ($\mu\text{g}/\text{m}^3$) at distance bins downwind for each hypothetical source.

SOURCE	LAT	LONG	SO2 to PM25 coefficients ($(\mu\text{g}/\text{m}^3)/\text{tpy}$) by distance from the source (km)							
			< 15	15 to 30	30 to 50	50 to 100	100 to 150	150 to 200	200 to 250	> 250
1	38.674	-74.701	8.67E-05	7.16E-05	5.04E-05	2.83E-05	1.24E-05	1.19E-05	1.19E-05	1.10E-05
2	36.908	-75.349	1.08E-04	7.24E-05	6.10E-05	5.01E-05	3.82E-05	2.63E-05	1.92E-05	1.53E-05
3	41.154	-71.08	4.06E-05	2.15E-05	1.84E-05	1.43E-05	1.24E-05	1.00E-05	9.32E-06	8.76E-06
4	40.985	-71.045	8.74E-06	8.64E-06	1.05E-05	2.26E-05	2.16E-05	1.51E-05	9.16E-06	8.26E-06
5	38.347	-74.761	1.74E-04	1.07E-04	7.74E-05	4.96E-05	3.44E-05	2.45E-05	1.97E-05	1.58E-05
6	36.896	-75.522	9.34E-05	1.01E-04	9.46E-05	9.48E-05	6.58E-05	4.29E-05	3.16E-05	2.50E-05
7	39.122	-74.242	2.71E-05	2.78E-05	2.17E-05	2.17E-05	1.96E-05	1.32E-05	1.13E-05	1.04E-05
8	39.273	-74.093	1.97E-05	2.14E-05	2.89E-05	3.76E-05	2.33E-05	1.41E-05	1.09E-05	9.82E-06
9	40.969	-70.792	1.80E-05	1.90E-05	3.29E-05	4.18E-05	2.59E-05	1.54E-05	9.48E-06	8.97E-06
10	41.043	-70.482	1.96E-04	1.78E-04	1.34E-04	1.13E-04	4.46E-05	1.88E-05	1.31E-05	9.90E-06
11	41.269	-71.436	2.75E-05	3.08E-05	3.36E-05	3.13E-05	1.68E-05	1.35E-05	9.14E-06	7.81E-06
12	36.339	-75.127	1.69E-04	2.03E-04	1.44E-04	1.16E-04	5.91E-05	3.97E-05	2.81E-05	2.26E-05
13	40.295	-73.315	2.28E-05	2.16E-05	3.61E-05	5.98E-05	3.65E-05	3.11E-05	1.21E-05	9.26E-06
14	41.089	-71.133	1.41E-05	1.26E-05	1.07E-05	1.98E-05	1.96E-05	1.17E-05	8.18E-06	8.04E-06
15	38.565	-74.665	8.50E-05	4.92E-05	4.60E-05	4.10E-05	2.14E-05	1.88E-05	1.38E-05	1.24E-05
16	40.824	-70.523	4.13E-05	3.57E-05	4.79E-05	4.96E-05	3.89E-05	2.44E-05	1.04E-05	9.82E-06
17	40.747	-70.416	2.49E-05	2.00E-05	3.14E-05	2.63E-05	2.30E-05	1.75E-05	1.15E-05	8.99E-06
18	40.682	-70.228	5.57E-05	3.66E-05	3.84E-05	3.50E-05	3.36E-05	2.43E-05	1.23E-05	8.91E-06
19	39.065	-74.379	2.96E-05	3.43E-05	2.84E-05	2.12E-05	2.11E-05	1.46E-05	1.22E-05	1.01E-05
20	40.895	-70.658	1.78E-05	2.72E-05	3.93E-05	4.51E-05	3.56E-05	2.31E-05	1.03E-05	8.94E-06
21	39.976	-72.74	7.07E-06	1.13E-05	1.08E-05	1.48E-05	1.51E-05	1.47E-05	1.33E-05	1.07E-05
22	39.718	-73.17	3.90E-05	3.65E-05	2.73E-05	2.93E-05	2.95E-05	1.78E-05	1.30E-05	9.15E-06
23	39.541	-73.304	4.48E-05	5.60E-05	4.30E-05	3.43E-05	1.98E-05	1.52E-05	1.26E-05	9.27E-06
24	39.361	-73.579	2.07E-05	2.30E-05	3.62E-05	3.14E-05	1.93E-05	1.69E-05	1.31E-05	9.65E-06
25	39.304	-73.461	1.77E-05	2.68E-05	4.11E-05	3.64E-05	1.97E-05	1.70E-05	1.31E-05	9.71E-06
26	40.242	-73.079	2.36E-05	2.19E-05	2.07E-05	4.83E-05	4.07E-05	2.44E-05	1.47E-05	9.05E-06
27	39.472	-74.004	1.93E-05	4.87E-05	5.13E-05	4.74E-05	3.31E-05	1.62E-05	1.12E-05	9.34E-06

Table 7. Transfer coefficients (($\mu\text{g}/\text{m}^3$)*tpy) relating NO_x emissions (tpy) with annual maximum daily average PM_{2.5} impacts ($\mu\text{g}/\text{m}^3$) at distance bins downwind for each hypothetical source.

SOURCE	LAT	LONG	NO _x to PM _{2.5} coefficients (($\mu\text{g}/\text{m}^3$)/tpy) by distance from the source (km)							
			< 15	15 to 30	30 to 50	50 to 100	100 to 150	150 to 200	200 to 250	> 250
1	38.674	-74.7	4.25E-05	3.36E-05	2.52E-05	3.06E-05	3.07E-05	2.90E-05	1.51E-05	1.45E-05
2	36.908	-75.35	1.35E-05	1.72E-05	1.95E-05	2.91E-05	2.79E-05	2.90E-05	2.08E-05	2.23E-05
3	41.154	-71.08	2.08E-05	1.45E-05	1.24E-05	1.79E-05	1.51E-05	1.29E-05	1.05E-05	7.26E-06
4	40.985	-71.04	1.64E-05	1.69E-05	1.59E-05	1.43E-05	1.44E-05	1.10E-05	9.89E-06	6.39E-06
5	38.347	-74.76	2.76E-05	2.85E-05	4.36E-05	6.13E-05	2.99E-05	1.38E-05	1.28E-05	1.19E-05
6	36.896	-75.52	2.25E-05	2.46E-05	3.25E-05	3.30E-05	2.98E-05	2.46E-05	1.95E-05	1.97E-05
7	39.122	-74.24	2.96E-05	3.18E-05	4.64E-05	4.86E-05	8.41E-05	3.15E-05	1.57E-05	1.28E-05
8	39.273	-74.09	1.47E-05	2.72E-05	4.82E-05	4.09E-05	8.47E-05	2.14E-05	1.43E-05	1.17E-05
9	40.969	-70.79	1.74E-05	1.72E-05	1.57E-05	1.33E-05	1.30E-05	1.18E-05	1.05E-05	6.12E-06
10	41.043	-70.48	1.15E-05	7.39E-06	7.29E-06	1.49E-05	1.50E-05	1.39E-05	1.06E-05	5.75E-06
11	41.269	-71.44	4.85E-05	4.70E-05	3.46E-05	2.75E-05	1.48E-05	1.15E-05	8.84E-06	5.97E-06
12	36.339	-75.13	2.62E-05	2.29E-05	1.90E-05	2.43E-05	2.03E-05	2.39E-05	2.05E-05	1.75E-05
13	40.295	-73.32	1.46E-05	1.31E-05	2.46E-05	5.65E-05	3.89E-05	2.02E-05	1.65E-05	1.19E-05
14	41.089	-71.13	1.75E-05	1.59E-05	1.39E-05	1.66E-05	1.46E-05	1.16E-05	9.60E-06	6.38E-06
15	38.565	-74.67	2.74E-05	2.49E-05	2.59E-05	3.00E-05	2.54E-05	2.25E-05	1.14E-05	1.22E-05
16	40.824	-70.52	7.57E-06	6.67E-06	7.34E-06	9.42E-06	1.40E-05	1.24E-05	1.08E-05	5.98E-06
17	40.747	-70.42	7.19E-06	5.85E-06	7.67E-06	8.80E-06	1.29E-05	1.17E-05	9.83E-06	5.81E-06
18	40.682	-70.23	7.55E-06	6.34E-06	5.81E-06	7.04E-06	1.21E-05	1.11E-05	8.71E-06	5.77E-06
19	39.065	-74.38	3.94E-05	3.43E-05	3.90E-05	3.92E-05	7.36E-05	2.65E-05	1.52E-05	1.24E-05
20	40.895	-70.66	7.00E-06	7.54E-06	8.39E-06	1.36E-05	1.33E-05	1.13E-05	9.61E-06	5.32E-06
21	39.976	-72.74	1.49E-05	1.44E-05	1.37E-05	9.91E-06	1.98E-05	2.09E-05	1.48E-05	8.81E-06
22	39.718	-73.17	1.25E-05	1.00E-05	7.49E-06	5.06E-05	4.05E-05	3.13E-05	1.87E-05	1.19E-05
23	39.541	-73.3	9.84E-06	8.65E-06	6.92E-06	3.21E-05	3.24E-05	2.46E-05	1.52E-05	1.27E-05
24	39.361	-73.58	5.39E-06	7.32E-06	1.00E-05	2.81E-05	3.31E-05	2.44E-05	1.23E-05	1.35E-05
25	39.304	-73.46	5.85E-06	8.13E-06	8.08E-06	2.83E-05	3.28E-05	3.13E-05	1.48E-05	1.36E-05
26	40.242	-73.08	1.27E-05	1.15E-05	9.44E-06	3.96E-05	3.22E-05	2.14E-05	1.39E-05	9.03E-06
27	39.472	-74	1.72E-05	2.70E-05	2.90E-05	6.21E-05	8.04E-05	2.34E-05	1.37E-05	1.03E-05

Table 8. Transfer coefficients (($\mu\text{g}/\text{m}^3$)*tpy) relating NH_3 emissions (tpy) with annual maximum daily average $\text{PM}_{2.5}$ impacts ($\mu\text{g}/\text{m}^3$) at distance bins downwind for each hypothetical source.

SOURCE	LAT	LONG	NH3 to PM25 coefficients (($\mu\text{g}/\text{m}^3$)/tpy) by distance from the source (km)							
			< 15	15 to 30	30 to 50	50 to 100	100 to 150	150 to 200	200 to 250	> 250
1	38.674	-74.701	7.16E-03	4.19E-03	2.43E-03	9.74E-04	2.62E-04	1.01E-04	5.14E-05	2.50E-05
2	36.908	-75.349	1.05E-02	2.60E-03	1.06E-03	4.43E-04	1.64E-04	9.40E-05	6.14E-05	4.65E-05
3	41.154	-71.08	2.79E-03	6.36E-04	2.86E-04	1.68E-04	9.22E-05	5.80E-05	3.54E-05	2.20E-05
4	40.985	-71.045	2.45E-03	6.00E-04	3.09E-04	1.86E-04	1.16E-04	7.55E-05	4.59E-05	2.85E-05
5	38.347	-74.761	6.06E-03	2.91E-03	1.71E-03	7.80E-04	2.75E-04	1.21E-04	7.93E-05	4.65E-05
6	36.896	-75.522	1.36E-02	4.05E-03	1.70E-03	6.36E-04	2.80E-04	1.76E-04	1.18E-04	8.66E-05
7	39.122	-74.242	6.49E-03	3.36E-03	1.73E-03	5.43E-04	1.79E-04	7.52E-05	3.44E-05	2.67E-05
8	39.273	-74.093	6.51E-03	3.00E-03	8.34E-04	5.41E-04	1.27E-04	6.22E-05	3.21E-05	2.36E-05
9	40.969	-70.792	2.65E-03	7.16E-04	2.91E-04	2.15E-04	1.05E-04	6.67E-05	3.96E-05	2.41E-05
10	41.043	-70.482	4.45E-03	1.50E-03	4.64E-04	3.15E-04	8.05E-05	5.39E-05	3.38E-05	2.10E-05
11	41.269	-71.436	3.23E-03	7.21E-04	3.77E-04	2.84E-04	1.12E-04	5.58E-05	4.00E-05	3.08E-05
12	36.339	-75.127	7.95E-03	1.75E-03	5.22E-04	3.49E-04	1.11E-04	5.56E-05	3.92E-05	3.04E-05
13	40.295	-73.315	2.91E-03	9.17E-04	4.28E-04	1.57E-04	9.03E-05	5.06E-05	3.78E-05	2.98E-05
14	41.089	-71.133	2.40E-03	6.08E-04	3.21E-04	1.89E-04	1.06E-04	6.80E-05	4.11E-05	2.56E-05
15	38.565	-74.665	5.47E-03	2.96E-03	1.67E-03	7.39E-04	2.31E-04	1.08E-04	6.05E-05	3.06E-05
16	40.824	-70.523	3.46E-03	1.07E-03	5.34E-04	2.45E-04	1.06E-04	6.79E-05	4.12E-05	2.44E-05
17	40.747	-70.416	3.06E-03	9.49E-04	5.97E-04	2.34E-04	1.14E-04	7.99E-05	4.81E-05	2.80E-05
18	40.682	-70.228	3.02E-03	1.40E-03	5.80E-04	3.11E-04	1.10E-04	7.36E-05	4.53E-05	2.50E-05
19	39.065	-74.379	6.62E-03	3.12E-03	1.68E-03	5.90E-04	1.33E-04	5.84E-05	3.09E-05	2.46E-05
20	40.895	-70.658	2.65E-03	7.99E-04	4.73E-04	2.26E-04	1.11E-04	7.35E-05	4.31E-05	2.55E-05
21	39.976	-72.74	2.37E-03	6.42E-04	2.87E-04	1.52E-04	8.21E-05	5.02E-05	3.24E-05	2.44E-05
22	39.718	-73.17	4.09E-03	9.52E-04	4.40E-04	2.33E-04	1.24E-04	5.43E-05	3.64E-05	2.27E-05
23	39.541	-73.304	5.69E-03	1.40E-03	4.81E-04	1.99E-04	1.20E-04	5.28E-05	3.59E-05	2.38E-05
24	39.361	-73.579	4.40E-03	1.69E-03	6.83E-04	2.10E-04	1.09E-04	5.07E-05	3.34E-05	2.18E-05
25	39.304	-73.461	4.36E-03	1.77E-03	7.45E-04	2.14E-04	1.35E-04	5.17E-05	3.33E-05	2.13E-05
26	40.242	-73.079	2.94E-03	7.00E-04	2.99E-04	1.62E-04	7.51E-05	4.99E-05	3.23E-05	2.53E-05
27	39.472	-74.004	7.73E-03	3.31E-03	9.21E-04	5.39E-04	1.35E-04	7.61E-05	3.47E-05	2.35E-05

Table 9. Transfer coefficients (($\mu\text{g}/\text{m}^3$)*tpy) relating primary PM_{2.5} emissions (tpy) with annual maximum daily average PM_{2.5} impacts ($\mu\text{g}/\text{m}^3$) at distance bins downwind for each hypothetical source.

SOURCE	LAT	LONG	Primary PM25 coefficients (($\mu\text{g}/\text{m}^3$)/tpy) by distance from the source (km)							
			< 15	15 to 30	30 to 50	50 to 100	100 to 150	150 to 200	200 to 250	> 250
1	38.674	-74.701				1.02E-03	2.52E-04	9.80E-05	5.99E-05	3.44E-05
2	36.908	-75.349				5.65E-04	2.15E-04	1.23E-04	8.02E-05	6.34E-05
3	41.154	-71.08				2.23E-04	1.19E-04	7.28E-05	4.59E-05	3.02E-05
4	40.985	-71.045				2.39E-04	1.33E-04	8.48E-05	5.29E-05	3.35E-05
5	38.347	-74.761				8.37E-04	2.79E-04	1.26E-04	8.37E-05	5.21E-05
6	36.896	-75.522				6.88E-04	2.89E-04	1.68E-04	1.18E-04	9.02E-05
7	39.122	-74.242				6.27E-04	1.72E-04	8.37E-05	4.55E-05	3.20E-05
8	39.273	-74.093				5.93E-04	1.70E-04	7.16E-05	4.07E-05	2.80E-05
9	40.969	-70.792				2.33E-04	1.25E-04	7.94E-05	4.74E-05	2.81E-05
10	41.043	-70.482				3.07E-04	1.00E-04	6.87E-05	4.41E-05	2.49E-05
11	41.269	-71.436				3.45E-04	1.47E-04	6.00E-05	4.39E-05	4.28E-05
12	36.339	-75.127				4.48E-04	1.67E-04	1.03E-04	7.61E-05	5.59E-05
13	40.295	-73.315				2.29E-04	1.14E-04	5.47E-05	4.29E-05	2.92E-05
14	41.089	-71.133				2.38E-04	1.25E-04	7.67E-05	4.62E-05	2.92E-05
15	38.565	-74.665				7.89E-04	2.39E-04	1.03E-04	6.40E-05	3.90E-05
16	40.824	-70.523				2.75E-04	1.32E-04	8.61E-05	5.28E-05	2.99E-05
17	40.747	-70.416				2.85E-04	1.38E-04	1.03E-04	6.16E-05	3.42E-05
18	40.682	-70.228				2.94E-04	1.22E-04	9.23E-05	5.76E-05	3.08E-05
19	39.065	-74.379				6.36E-04	1.55E-04	8.88E-05	4.58E-05	3.43E-05
20	40.895	-70.658				2.71E-04	1.36E-04	8.97E-05	5.36E-05	3.04E-05
21	39.976	-72.74				2.20E-04	1.13E-04	6.95E-05	5.29E-05	3.51E-05
22	39.718	-73.17				2.61E-04	1.46E-04	7.12E-05	5.13E-05	3.14E-05
23	39.541	-73.304				2.91E-04	1.68E-04	8.40E-05	5.35E-05	3.27E-05
24	39.361	-73.579				2.91E-04	1.36E-04	7.64E-05	4.74E-05	2.77E-05
25	39.304	-73.461				3.59E-04	1.76E-04	6.86E-05	4.74E-05	3.02E-05
26	40.242	-73.079				2.35E-04	9.33E-05	5.38E-05	3.60E-05	2.97E-05
27	39.472	-74.004				4.67E-04	1.71E-04	7.80E-05	4.14E-05	2.82E-05

Table 10. Transfer coefficients (($\mu\text{g}/\text{m}^3$)*tpy) relating primary coarse PM emissions (tpy) with annual maximum daily average coarse PM impacts ($\mu\text{g}/\text{m}^3$) at distance bins downwind for each hypothetical source.

SOURCE	LAT	LONG	Primary Coarse PM coefficients (($\mu\text{g}/\text{m}^3$)/tpy) by distance from the source (km)							
			< 15	15 to 30	30 to 50	50 to 100	100 to 150	150 to 200	200 to 250	> 250
1	38.674	-74.701				5.37E-04	1.27E-04	6.12E-05	3.70E-05	2.63E-05
2	36.908	-75.349				3.93E-04	1.67E-04	9.39E-05	5.49E-05	3.48E-05
3	41.154	-71.08				1.92E-04	9.64E-05	5.76E-05	3.69E-05	2.68E-05
4	40.985	-71.045				2.12E-04	1.18E-04	7.29E-05	4.28E-05	2.64E-05
5	38.347	-74.761				5.28E-04	1.68E-04	7.20E-05	4.30E-05	3.43E-05
6	36.896	-75.522				4.29E-04	1.52E-04	8.53E-05	5.21E-05	3.77E-05
7	39.122	-74.242				3.13E-04	1.34E-04	6.68E-05	3.87E-05	2.74E-05
8	39.273	-74.093				3.44E-04	1.24E-04	6.08E-05	3.60E-05	2.44E-05
9	40.969	-70.792				1.77E-04	1.04E-04	6.43E-05	3.70E-05	2.46E-05
10	41.043	-70.482				1.81E-04	7.85E-05	5.27E-05	3.32E-05	2.16E-05
11	41.269	-71.436				2.98E-04	1.21E-04	5.26E-05	3.73E-05	3.36E-05
12	36.339	-75.127				3.32E-04	1.39E-04	7.09E-05	4.37E-05	2.97E-05
13	40.295	-73.315				1.73E-04	8.28E-05	4.64E-05	3.28E-05	2.47E-05
14	41.089	-71.133				2.15E-04	1.10E-04	6.57E-05	3.84E-05	2.61E-05
15	38.565	-74.665				4.64E-04	1.46E-04	6.51E-05	3.86E-05	2.86E-05
16	40.824	-70.523				2.15E-04	1.15E-04	6.61E-05	4.02E-05	2.48E-05
17	40.747	-70.416				2.24E-04	1.20E-04	7.85E-05	4.73E-05	2.76E-05
18	40.682	-70.228				1.98E-04	1.10E-04	7.27E-05	4.50E-05	2.45E-05
19	39.065	-74.379				3.89E-04	1.29E-04	7.14E-05	3.89E-05	2.95E-05
20	40.895	-70.658				1.97E-04	1.12E-04	7.14E-05	4.10E-05	2.47E-05
21	39.976	-72.74				1.60E-04	8.13E-05	5.16E-05	3.59E-05	2.73E-05
22	39.718	-73.17				2.10E-04	8.90E-05	5.29E-05	3.57E-05	2.52E-05
23	39.541	-73.304				2.26E-04	8.66E-05	6.11E-05	3.75E-05	2.22E-05
24	39.361	-73.579				2.75E-04	1.03E-04	5.86E-05	3.51E-05	2.51E-05
25	39.304	-73.461				2.75E-04	9.70E-05	5.15E-05	3.50E-05	2.52E-05
26	40.242	-73.079				1.79E-04	7.60E-05	4.71E-05	3.29E-05	2.78E-05
27	39.472	-74.004				2.80E-04	1.18E-04	5.82E-05	3.86E-05	2.63E-05

Table 11. Transfer coefficients (($\mu\text{g}/\text{m}^3$)*tpy) relating SO_2 emissions (tpy) with annual average $\text{PM}_{2.5}$ impacts ($\mu\text{g}/\text{m}^3$) at distance bins downwind for each hypothetical source.

SOURCE	LAT	LONG	SO2 to PM25 coefficients (($\mu\text{g}/\text{m}^3$)/tpy) by distance from the source (km)							
			< 15	15 to 30	30 to 50	50 to 100	100 to 150	150 to 200	200 to 250	> 250
1	38.674	-74.701	7.01E-06	5.22E-06	3.86E-06	2.37E-06	1.24E-06	9.92E-07	8.10E-07	7.36E-07
2	36.908	-75.349	5.03E-06	2.96E-06	2.35E-06	1.93E-06	1.53E-06	1.11E-06	9.84E-07	8.31E-07
3	41.154	-71.08	2.34E-06	1.63E-06	1.37E-06	1.20E-06	1.16E-06	1.04E-06	1.01E-06	6.57E-07
4	40.985	-71.045	1.14E-06	9.50E-07	9.18E-07	1.18E-06	1.15E-06	1.07E-06	1.04E-06	6.98E-07
5	38.347	-74.761	1.10E-05	8.06E-06	5.89E-06	3.78E-06	2.17E-06	1.40E-06	1.09E-06	7.75E-07
6	36.896	-75.522	4.78E-06	4.02E-06	3.64E-06	3.63E-06	2.82E-06	2.16E-06	1.68E-06	1.28E-06
7	39.122	-74.242	3.61E-06	2.87E-06	2.34E-06	1.94E-06	1.59E-06	9.98E-07	7.70E-07	6.62E-07
8	39.273	-74.093	3.28E-06	2.84E-06	2.44E-06	2.46E-06	1.50E-06	8.94E-07	7.40E-07	5.79E-07
9	40.969	-70.792	1.44E-06	1.14E-06	1.60E-06	1.94E-06	1.51E-06	1.21E-06	9.88E-07	6.48E-07
10	41.043	-70.482	7.16E-06	6.68E-06	5.18E-06	4.53E-06	2.06E-06	1.31E-06	8.43E-07	6.88E-07
11	41.269	-71.436	2.83E-06	2.22E-06	1.80E-06	1.65E-06	1.04E-06	7.07E-07	6.24E-07	6.02E-07
12	36.339	-75.127	7.36E-06	7.27E-06	4.97E-06	4.00E-06	2.08E-06	1.42E-06	1.00E-06	8.16E-07
13	40.295	-73.315	2.30E-06	1.86E-06	1.81E-06	2.87E-06	1.93E-06	1.32E-06	1.02E-06	7.93E-07
14	41.089	-71.133	1.41E-06	1.20E-06	1.09E-06	1.25E-06	1.24E-06	1.02E-06	1.00E-06	6.63E-07
15	38.565	-74.665	7.39E-06	5.68E-06	4.55E-06	3.24E-06	1.69E-06	1.28E-06	9.21E-07	7.00E-07
16	40.824	-70.523	2.01E-06	1.68E-06	2.06E-06	1.97E-06	1.42E-06	1.28E-06	7.87E-07	6.56E-07
17	40.747	-70.416	1.76E-06	1.29E-06	1.58E-06	1.43E-06	1.24E-06	1.09E-06	8.54E-07	6.69E-07
18	40.682	-70.228	3.74E-06	1.99E-06	1.87E-06	1.24E-06	1.25E-06	1.18E-06	8.64E-07	6.51E-07
19	39.065	-74.379	3.72E-06	3.35E-06	2.70E-06	2.01E-06	1.64E-06	1.09E-06	7.88E-07	6.67E-07
20	40.895	-70.658	1.15E-06	1.12E-06	1.62E-06	1.79E-06	1.38E-06	1.30E-06	8.86E-07	6.32E-07
21	39.976	-72.74	1.10E-06	9.65E-07	1.08E-06	1.12E-06	1.15E-06	1.16E-06	1.11E-06	9.33E-07
22	39.718	-73.17	2.37E-06	1.78E-06	1.33E-06	1.60E-06	1.67E-06	9.77E-07	7.70E-07	5.90E-07
23	39.541	-73.304	2.59E-06	2.41E-06	1.74E-06	1.42E-06	1.28E-06	9.26E-07	7.34E-07	5.85E-07
24	39.361	-73.579	2.08E-06	1.83E-06	1.90E-06	1.48E-06	1.25E-06	8.76E-07	6.83E-07	5.43E-07
25	39.304	-73.461	2.14E-06	1.95E-06	2.07E-06	1.66E-06	1.25E-06	9.33E-07	6.86E-07	5.29E-07
26	40.242	-73.079	2.29E-06	1.86E-06	1.65E-06	2.32E-06	2.27E-06	1.13E-06	7.93E-07	6.21E-07
27	39.472	-74.004	3.19E-06	3.47E-06	3.33E-06	3.02E-06	1.60E-06	9.95E-07	7.62E-07	6.22E-07

Table 12. Transfer coefficients (($\mu\text{g}/\text{m}^3$)*tpy) relating NO_x emissions (tpy) with annual average $\text{PM}_{2.5}$ impacts ($\mu\text{g}/\text{m}^3$) at distance bins downwind for each hypothetical source.

SOURCE	LAT	LONG	NO _x to PM ₂₅ coefficients (($\mu\text{g}/\text{m}^3$)/tpy) by distance from the source (km)							
			< 15	15 to 30	30 to 50	50 to 100	100 to 150	150 to 200	200 to 250	> 250
1	38.674	-74.701	4.99E-06	4.08E-06	4.03E-06	3.44E-06	2.78E-06	2.40E-06	1.66E-06	1.18E-06
2	36.908	-75.349	3.26E-06	2.87E-06	2.54E-06	2.17E-06	1.93E-06	2.38E-06	2.33E-06	2.35E-06
3	41.154	-71.08	3.53E-06	2.09E-06	1.43E-06	1.00E-06	7.46E-07	6.44E-07	5.44E-07	4.04E-07
4	40.985	-71.045	2.17E-06	1.52E-06	1.29E-06	9.66E-07	7.48E-07	5.70E-07	4.91E-07	3.40E-07
5	38.347	-74.761	3.90E-06	3.17E-06	2.94E-06	3.66E-06	2.17E-06	1.53E-06	1.54E-06	1.13E-06
6	36.896	-75.522	4.29E-06	3.61E-06	3.56E-06	3.06E-06	2.50E-06	2.68E-06	2.88E-06	2.85E-06
7	39.122	-74.242	3.96E-06	3.07E-06	4.07E-06	4.19E-06	4.76E-06	2.28E-06	1.83E-06	1.09E-06
8	39.273	-74.093	3.00E-06	2.28E-06	4.45E-06	3.58E-06	4.93E-06	2.02E-06	1.66E-06	9.82E-07
9	40.969	-70.792	2.33E-06	1.38E-06	1.18E-06	8.73E-07	7.47E-07	6.04E-07	5.00E-07	3.31E-07
10	41.043	-70.482	2.25E-06	1.42E-06	1.08E-06	1.01E-06	7.94E-07	6.83E-07	4.72E-07	2.44E-07
11	41.269	-71.436	6.07E-06	4.09E-06	2.68E-06	1.65E-06	1.07E-06	6.99E-07	5.16E-07	3.91E-07
12	36.339	-75.127	3.91E-06	3.26E-06	2.48E-06	1.77E-06	2.03E-06	2.05E-06	1.78E-06	1.67E-06
13	40.295	-73.315	3.11E-06	2.25E-06	2.02E-06	3.74E-06	2.97E-06	2.27E-06	1.40E-06	9.58E-07
14	41.089	-71.133	2.80E-06	1.83E-06	1.52E-06	1.00E-06	7.28E-07	5.95E-07	5.24E-07	3.60E-07
15	38.565	-74.665	3.54E-06	2.98E-06	2.51E-06	2.42E-06	2.27E-06	1.80E-06	1.39E-06	1.10E-06
16	40.824	-70.523	1.45E-06	9.60E-07	8.24E-07	8.00E-07	7.24E-07	6.23E-07	4.82E-07	2.85E-07
17	40.747	-70.416	1.39E-06	1.01E-06	8.07E-07	7.90E-07	6.67E-07	6.08E-07	4.50E-07	2.49E-07
18	40.682	-70.228	1.29E-06	9.47E-07	9.00E-07	8.03E-07	6.67E-07	6.16E-07	4.44E-07	2.64E-07
19	39.065	-74.379	4.23E-06	3.09E-06	3.38E-06	3.58E-06	4.11E-06	1.95E-06	1.63E-06	9.23E-07
20	40.895	-70.658	1.60E-06	1.10E-06	9.45E-07	7.88E-07	7.24E-07	5.96E-07	4.51E-07	2.92E-07
21	39.976	-72.74	1.89E-06	1.45E-06	1.18E-06	8.67E-07	1.65E-06	1.32E-06	1.06E-06	5.84E-07
22	39.718	-73.17	2.21E-06	1.25E-06	1.09E-06	3.46E-06	3.05E-06	2.53E-06	1.29E-06	1.08E-06
23	39.541	-73.304	1.93E-06	1.37E-06	1.12E-06	2.53E-06	2.34E-06	2.26E-06	1.03E-06	9.42E-07
24	39.361	-73.579	1.60E-06	1.12E-06	9.57E-07	2.25E-06	2.40E-06	2.12E-06	1.02E-06	8.62E-07
25	39.304	-73.461	1.66E-06	1.14E-06	8.54E-07	2.28E-06	2.32E-06	2.39E-06	1.03E-06	9.54E-07
26	40.242	-73.079	2.47E-06	1.77E-06	1.41E-06	3.02E-06	2.96E-06	2.15E-06	1.27E-06	8.03E-07
27	39.472	-74.004	3.46E-06	3.05E-06	3.55E-06	4.38E-06	5.35E-06	2.32E-06	1.85E-06	8.95E-07

Table 13. Transfer coefficients (($\mu\text{g}/\text{m}^3$)*tpy) relating NH_3 emissions (tpy) with annual average $\text{PM}_{2.5}$ impacts ($\mu\text{g}/\text{m}^3$) at distance bins downwind for each hypothetical source.

SOURCE	LAT	LONG	NH3 to PM25 coefficients (($\mu\text{g}/\text{m}^3$)/tpy) by distance from the source (km)							
			< 15	15 to 30	30 to 50	50 to 100	100 to 150	150 to 200	200 to 250	> 250
1	38.674	-74.701	2.00E-03	5.08E-04	2.46E-04	9.43E-05	2.33E-05	1.03E-05	5.32E-06	3.49E-06
2	36.908	-75.349	1.75E-03	3.77E-04	1.49E-04	5.04E-05	1.36E-05	7.12E-06	4.47E-06	3.16E-06
3	41.154	-71.08	1.24E-03	2.88E-04	1.06E-04	3.91E-05	1.60E-05	9.57E-06	5.16E-06	2.00E-06
4	40.985	-71.045	1.18E-03	2.75E-04	1.03E-04	3.96E-05	1.63E-05	8.90E-06	3.92E-06	2.09E-06
5	38.347	-74.761	1.80E-03	4.13E-04	1.87E-04	7.26E-05	2.39E-05	1.18E-05	6.46E-06	3.61E-06
6	36.896	-75.522	2.00E-03	4.24E-04	1.81E-04	6.84E-05	2.27E-05	1.17E-05	7.08E-06	4.70E-06
7	39.122	-74.242	2.01E-03	4.71E-04	2.05E-04	6.49E-05	1.63E-05	7.70E-06	5.17E-06	3.80E-06
8	39.273	-74.093	1.85E-03	4.16E-04	9.38E-05	5.79E-05	1.37E-05	7.89E-06	5.30E-06	3.86E-06
9	40.969	-70.792	1.20E-03	2.83E-04	6.30E-05	4.37E-05	1.49E-05	8.01E-06	3.26E-06	1.94E-06
10	41.043	-70.482	1.29E-03	3.15E-04	7.46E-05	5.18E-05	1.61E-05	6.92E-06	2.71E-06	1.88E-06
11	41.269	-71.436	1.39E-03	3.20E-04	6.68E-05	4.38E-05	1.35E-05	8.39E-06	5.84E-06	2.41E-06
12	36.339	-75.127	1.69E-03	2.85E-04	7.18E-05	3.26E-05	1.18E-05	5.73E-06	3.74E-06	2.30E-06
13	40.295	-73.315	1.38E-03	3.07E-04	6.79E-05	4.59E-05	1.75E-05	8.56E-06	5.32E-06	3.80E-06
14	41.089	-71.133	1.21E-03	2.85E-04	1.07E-04	4.09E-05	1.63E-05	9.35E-06	5.50E-06	1.95E-06
15	38.565	-74.665	1.78E-03	4.17E-04	1.91E-04	7.48E-05	2.30E-05	1.08E-05	5.40E-06	3.25E-06
16	40.824	-70.523	1.23E-03	2.92E-04	1.15E-04	4.76E-05	1.74E-05	6.40E-06	3.08E-06	2.11E-06
17	40.747	-70.416	1.23E-03	2.91E-04	1.20E-04	4.73E-05	1.63E-05	6.20E-06	3.57E-06	2.27E-06
18	40.682	-70.228	1.23E-03	2.99E-04	1.18E-04	4.60E-05	1.53E-05	6.24E-06	3.51E-06	2.18E-06
19	39.065	-74.379	1.88E-03	4.35E-04	1.96E-04	6.95E-05	1.78E-05	8.28E-06	5.42E-06	3.93E-06
20	40.895	-70.658	1.17E-03	2.76E-04	1.09E-04	4.51E-05	1.72E-05	7.86E-06	3.08E-06	2.10E-06
21	39.976	-72.74	1.15E-03	2.70E-04	1.02E-04	3.98E-05	1.57E-05	8.65E-06	5.46E-06	3.60E-06
22	39.718	-73.17	1.39E-03	1.77E-04	6.66E-05	3.23E-05	1.32E-05	7.26E-06	4.66E-06	3.38E-06
23	39.541	-73.304	1.44E-03	3.08E-04	1.12E-04	4.20E-05	1.57E-05	8.42E-06	4.91E-06	3.56E-06
24	39.361	-73.579	1.34E-03	2.93E-04	1.07E-04	4.00E-05	1.51E-05	8.29E-06	5.36E-06	3.83E-06
25	39.304	-73.461	1.34E-03	2.95E-04	7.84E-05	2.97E-05	1.30E-05	7.55E-06	5.03E-06	3.67E-06
26	40.242	-73.079	1.27E-03	2.86E-04	1.07E-04	4.24E-05	1.64E-05	8.95E-06	5.70E-06	3.90E-06
27	39.472	-74.004	2.04E-03	4.51E-04	9.49E-05	5.68E-05	1.38E-05	7.85E-06	5.17E-06	3.70E-06

Table 14. Transfer coefficients (($\mu\text{g}/\text{m}^3$)*tpy) relating primary $\text{PM}_{2.5}$ emissions (tpy) with annual average $\text{PM}_{2.5}$ impacts ($\mu\text{g}/\text{m}^3$) at distance bins downwind for each hypothetical source.

SOURCE	LAT	LONG	Primary PM25 coefficients (($\mu\text{g}/\text{m}^3$)/tpy) by distance from the source (km)							
			< 15	15 to 30	30 to 50	50 to 100	100 to 150	150 to 200	200 to 250	> 250
1	38.674	-74.701				1.00E-04	2.72E-05	1.12E-05	6.62E-06	5.07E-06
2	36.908	-75.349				7.66E-05	2.20E-05	1.10E-05	7.84E-06	6.32E-06
3	41.154	-71.08				4.65E-05	1.91E-05	1.14E-05	6.41E-06	2.62E-06
4	40.985	-71.045				5.28E-05	2.02E-05	1.08E-05	5.46E-06	2.52E-06
5	38.347	-74.761				9.49E-05	2.77E-05	1.32E-05	7.44E-06	5.06E-06
6	36.896	-75.522				8.30E-05	2.52E-05	1.29E-05	9.40E-06	7.03E-06
7	39.122	-74.242				6.67E-05	1.80E-05	1.02E-05	7.05E-06	5.33E-06
8	39.273	-74.093				6.68E-05	1.82E-05	1.07E-05	7.35E-06	5.47E-06
9	40.969	-70.792				5.18E-05	1.76E-05	9.41E-06	4.02E-06	2.41E-06
10	41.043	-70.482				5.99E-05	1.90E-05	8.71E-06	3.44E-06	2.44E-06
11	41.269	-71.436				5.48E-05	1.69E-05	1.04E-05	7.25E-06	3.43E-06
12	36.339	-75.127				5.36E-05	1.94E-05	9.94E-06	7.31E-06	5.18E-06
13	40.295	-73.315				5.79E-05	2.30E-05	1.11E-05	7.25E-06	5.04E-06
14	41.089	-71.133				5.02E-05	1.97E-05	1.12E-05	6.64E-06	2.45E-06
15	38.565	-74.665				8.32E-05	2.55E-05	1.13E-05	6.78E-06	4.86E-06
16	40.824	-70.523				5.51E-05	2.01E-05	8.07E-06	3.78E-06	2.60E-06
17	40.747	-70.416				5.76E-05	1.92E-05	7.60E-06	4.38E-06	2.82E-06
18	40.682	-70.228				5.21E-05	1.77E-05	7.67E-06	4.39E-06	2.83E-06
19	39.065	-74.379				8.17E-05	2.00E-05	1.11E-05	7.40E-06	5.50E-06
20	40.895	-70.658				5.49E-05	2.06E-05	9.36E-06	3.79E-06	2.67E-06
21	39.976	-72.74				5.11E-05	2.12E-05	1.17E-05	7.48E-06	4.97E-06
22	39.718	-73.17				4.30E-05	1.81E-05	1.00E-05	6.54E-06	4.80E-06
23	39.541	-73.304				5.46E-05	2.11E-05	1.15E-05	6.84E-06	5.02E-06
24	39.361	-73.579				5.08E-05	2.00E-05	1.12E-05	7.39E-06	5.40E-06
25	39.304	-73.461				3.79E-05	1.71E-05	1.01E-05	6.83E-06	5.10E-06
26	40.242	-73.079				5.27E-05	2.13E-05	1.18E-05	7.63E-06	4.87E-06
27	39.472	-74.004				6.04E-05	1.84E-05	1.07E-05	7.20E-06	5.24E-06

Table 15. Transfer coefficients (($\mu\text{g}/\text{m}^3$)*tpy) relating primary coarse PM emissions (tpy) with annual average coarse PM impacts ($\mu\text{g}/\text{m}^3$) at distance bins downwind for each hypothetical source.

SOURCE	LAT	LONG	Primary Coarse PM coefficients (($\mu\text{g}/\text{m}^3$)/tpy) by distance from the source (km)							
			< 15	15 to 30	30 to 50	50 to 100	100 to 150	150 to 200	200 to 250	> 250
1	38.674	-74.701				6.80E-05	1.69E-05	8.83E-06	5.99E-06	4.52E-06
2	36.908	-75.349				6.10E-05	1.88E-05	9.44E-06	5.82E-06	3.81E-06
3	41.154	-71.08				4.47E-05	1.79E-05	1.04E-05	5.66E-06	2.33E-06
4	40.985	-71.045				4.77E-05	1.77E-05	9.55E-06	4.67E-06	2.29E-06
5	38.347	-74.761				6.79E-05	1.76E-05	9.13E-06	6.00E-06	4.39E-06
6	36.896	-75.522				6.79E-05	1.65E-05	9.16E-06	5.74E-06	3.82E-06
7	39.122	-74.242				4.88E-05	1.62E-05	9.39E-06	6.38E-06	4.75E-06
8	39.273	-74.093				5.37E-05	1.68E-05	9.81E-06	6.65E-06	4.89E-06
9	40.969	-70.792				4.69E-05	1.55E-05	8.61E-06	3.67E-06	2.18E-06
10	41.043	-70.482				5.24E-05	1.68E-05	7.31E-06	2.96E-06	2.09E-06
11	41.269	-71.436				5.27E-05	1.61E-05	9.72E-06	6.66E-06	2.84E-06
12	36.339	-75.127				4.50E-05	1.63E-05	7.78E-06	4.55E-06	3.66E-06
13	40.295	-73.315				5.39E-05	2.11E-05	1.01E-05	6.55E-06	4.58E-06
14	41.089	-71.133				4.61E-05	1.77E-05	9.96E-06	6.08E-06	2.22E-06
15	38.565	-74.665				6.00E-05	1.74E-05	9.31E-06	6.16E-06	4.30E-06
16	40.824	-70.523				4.89E-05	1.79E-05	7.32E-06	3.33E-06	2.34E-06
17	40.747	-70.416				5.00E-05	1.75E-05	6.55E-06	3.85E-06	2.52E-06
18	40.682	-70.228				4.64E-05	1.64E-05	6.71E-06	3.86E-06	2.44E-06
19	39.065	-74.379				5.61E-05	1.86E-05	1.02E-05	6.74E-06	4.95E-06
20	40.895	-70.658				4.85E-05	1.80E-05	8.71E-06	3.34E-06	2.32E-06
21	39.976	-72.74				4.83E-05	1.95E-05	1.08E-05	6.91E-06	4.53E-06
22	39.718	-73.17				3.98E-05	1.68E-05	9.29E-06	6.03E-06	4.38E-06
23	39.541	-73.304				5.17E-05	1.98E-05	1.07E-05	6.34E-06	4.60E-06
24	39.361	-73.579				4.92E-05	1.90E-05	1.06E-05	6.91E-06	4.99E-06
25	39.304	-73.461				3.64E-05	1.62E-05	9.47E-06	6.37E-06	4.67E-06
26	40.242	-73.079				4.95E-05	1.97E-05	1.08E-05	6.95E-06	4.50E-06
27	39.472	-74.004				5.59E-05	1.69E-05	9.74E-06	6.48E-06	4.68E-06

REFERENCES

- Baker, K.R., Foley, K.M., 2011. A nonlinear regression model estimating single source concentrations of primary and secondarily formed PM_{2.5}. *Atmospheric Environment* 45, 3758-3767.
- Baker, K.R., Kelly, J.T., 2014. Single source impacts estimated with photochemical model source sensitivity and apportionment approaches. *Atmospheric Environment* 96, 266-274.
- Baker, K.R., Kotchenruther, R.A., Hudman, R.C., 2016. Estimating ozone and secondary PM_{2.5} impacts from hypothetical single source emissions in the central and eastern United States. *Atmospheric Pollution Research* 7, 122-133.
- Baker, K.R., Woody, M.C., 2017. Assessing Model Characterization of Single Source Secondary Pollutant Impacts Using 2013 SENEX Field Study Measurements. *Environmental Science & Technology* 51, 3833-3842.

Bash, J.O., Baker, K.R., Beaver, M.R., 2016. Evaluation of improved land use and canopy representation in BEIS v3. 61 with biogenic VOC measurements in California. *Geoscientific Model Development* 9, 2191.

Bertram, T., Thornton, J., 2009. Toward a general parameterization of N_2O_5 reactivity on aqueous particles: the competing effects of particle liquid water, nitrate and chloride. *Atmos. Chem. Phys.* 9, 8351-8363.

ENVIRON International Corporation, 2012. Evaluation of Chemical Dispersion Models using Atmospheric Plume Measurements from Field Experiments. EPA Contract No: EP-D-07-102.
https://www.epa.gov/sites/default/files/2020-10/documents/plume_eval_final_sep_2012v5_0.pdf.

Kasibhatla, P., Sherwen, T., Evans, M.J., Carpenter, L.J., Reed, C., Alexander, B., Chen, Q., Sulprizio, M.P., Lee, J.D., Read, K.A., 2018. Global impact of nitrate photolysis in sea-salt aerosol on NO_x , OH, and O_3 in the marine boundary layer. *Atmos. Chem. Phys.* 18, 11185-11203.

Kelly, J.T., Koplitz, S.N., Baker, K.R., Holder, A.L., Pye, H.O., Murphy, B.N., Bash, J.O., Henderson, B.H., Possiel, N.C., Simon, H., 2019. Assessing PM_{2.5} model performance for the conterminous US with comparison to model performance statistics from 2007-2015. *Atmospheric Environment* 214, 116872.

Kwok, R., Baker, K., Napelenok, S., Tonnesen, G., 2015. Photochemical grid model implementation of VOC, NO_x , and O_3 source apportionment. *Geoscientific Model Development* 8, 99-114.

Kwok, R., Napelenok, S., Baker, K., 2013. Implementation and evaluation of PM_{2.5} source contribution analysis in a photochemical model. *Atmospheric Environment* 80, 398-407.

McDuffie, E.E., Fibiger, D.L., Dubé, W.P., Lopez Hilfiker, F., Lee, B.H., Jaeglé, L., Guo, H., Weber, R.J., Reeves, J.M., Weinheimer, A.J., 2018. ClNO₂ yields from aircraft measurements during the 2015 WINTER campaign and critical evaluation of the current parameterization. *Journal of Geophysical Research: Atmospheres* 123, 994-913,015.

Nair, A.A., Yu, F., 2020. Quantification of atmospheric ammonia concentrations: A review of its measurement and modeling. *Atmosphere* 11, 1092.

Nenes, A., Pandis, S.N., Pilinis, C., 1998. ISORROPIA: A new thermodynamic equilibrium model for multiphase multicomponent inorganic aerosols. *Aquatic geochemistry* 4, 123-152.

NOAA Office for Coastal Management, 2022.
<https://coast.noaa.gov/digitalcoast/data/vesseltraffic.html>.

Ramboll, 2016. Technical Memorandum: EPA Contract EPD12044; WA 4-07; Meteorological, Photochemical, and Dispersion Modeling Support Task 7: Update Carbon Bond Chemical Mechanism.
http://www.camx.com/files/emaq4-07_task7_techmemo_r1_1aug16.pdf.

Ramboll, 2022. User's Guide Comprehensive Air Quality Model with Extensions Version 7.20.
www.camx.com.

Seinfeld, J., Pandis, S., 2008. *Atmospheric chemistry and physics*. 1997. New York.

Simon, H., Baker, K.R., Phillips, S., 2012. Compilation and interpretation of photochemical model performance statistics published between 2006 and 2012. *Atmospheric Environment* 61, 124-139.

U.S. Environmental Protection Agency, 2018. Guidance on Significant Impact Levels for Ozone and Fine Particles in the Prevention of Significant Deterioration Permitting Program.

https://www.epa.gov/sites/production/files/2018-04/documents/sils_policy_guidance_document_final_signed_4-17-18.pdf.

U.S. Environmental Protection Agency, 2019a. 2016 Hemispheric Modeling Platform Version 1: Implementation, Evaluation, and Attribution. Research Triangle Park, NC. U.S. Environmental Protection Agency. U.S. EPA.

U.S. Environmental Protection Agency, 2019b. Guidance on the Development of Modeled Emission Rates for Precursors (MERPs) as a Tier 1 Demonstration Tool for Ozone and PM_{2.5} under the PSD Permitting Program. EPA-454/R-10-003. https://www.epa.gov/sites/default/files/2020-09/documents/epa-454_r-19-003.pdf.

U.S. Environmental Protection Agency, 2020. 2017 National Emission Inventory Technical Support Document. <https://www.epa.gov/air-emissions-inventories/2017-national-emissions-inventory-nei-technical-support-document-tsd>.

U.S. Environmental Protection Agency, 2021. Guidance for Ozone and Fine Particulate Matter Permit Modeling. https://www.epa.gov/system/files/documents/2021-09/revised_draft_guidance_for_o3_pm25_permit_modeling.pdf.

U.S. Environmental Protection Agency, 2022. Meteorological Model Performance for Annual 2017 Simulation WRF v3.8. EPA-454/R-22-006. https://www.epa.gov/system/files/documents/2022-09/MET_TSD_2017.pdf.

Wilson, D., Stoeckenius, T., Brashers, B., Do, B., 2019. Air quality modeling in the Gulf of Mexico Region. New Orleans (LA): U.S. Department of the Interior, Bureau of Ocean Energy Management. Gulf of Mexico Region. OCS Study BOEM 2019-057. Prepared by the Eastern Research Group, Inc. 655 p.

Zhang, R., Gen, M., Huang, D., Li, Y., Chan, C.K., 2020. Enhanced sulfate production by nitrate photolysis in the presence of halide ions in atmospheric particles. *Environmental Science & Technology* 54, 3831-3839.

APPENDIX A

Annual Maximum MDA8 Ozone and Speciated PM_{2.5} Impacts Based on Hypothetical Emission Rates

Figure A1. Maximum MDA8 O₃ impacts from 5000 tpy of NO_x emissions from sources 1-9.

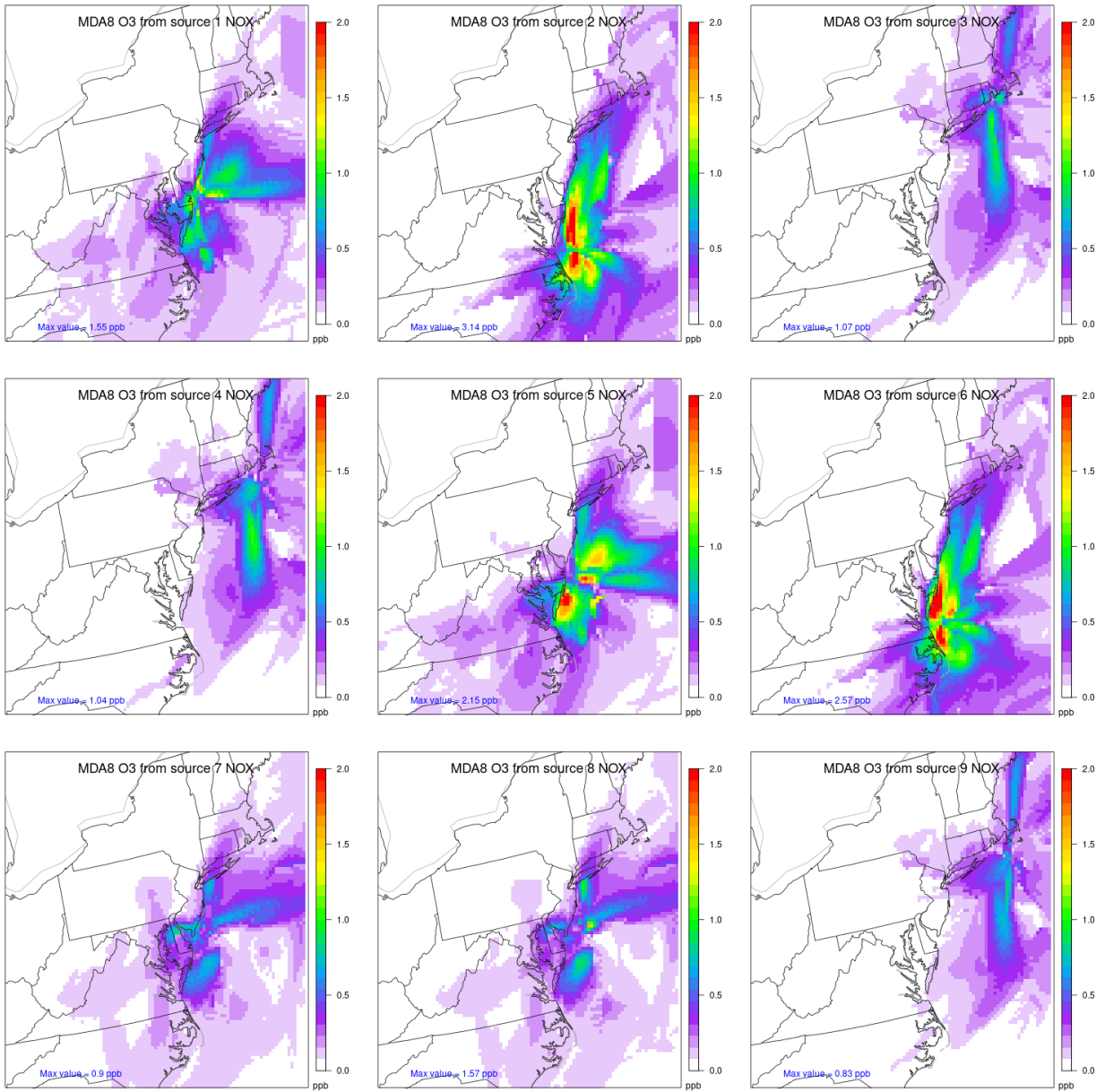


Figure A2. Maximum MDA8 O₃ impacts from 5000 tpy of NO_x emissions from sources 10-18.

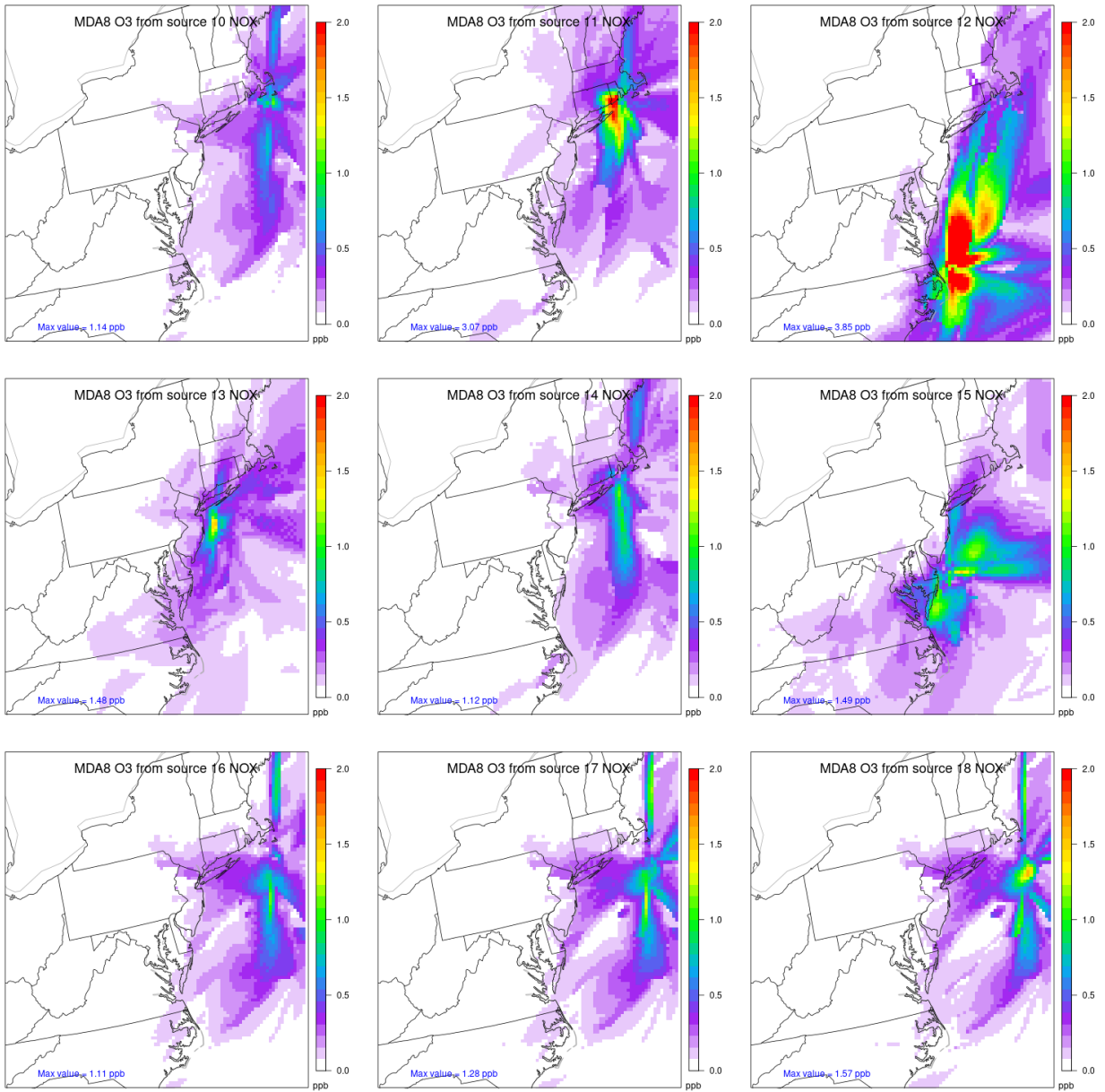


Figure A3. Maximum MDA8 O₃ impacts from 5000 tpy of NO_x emissions from sources 19-27.

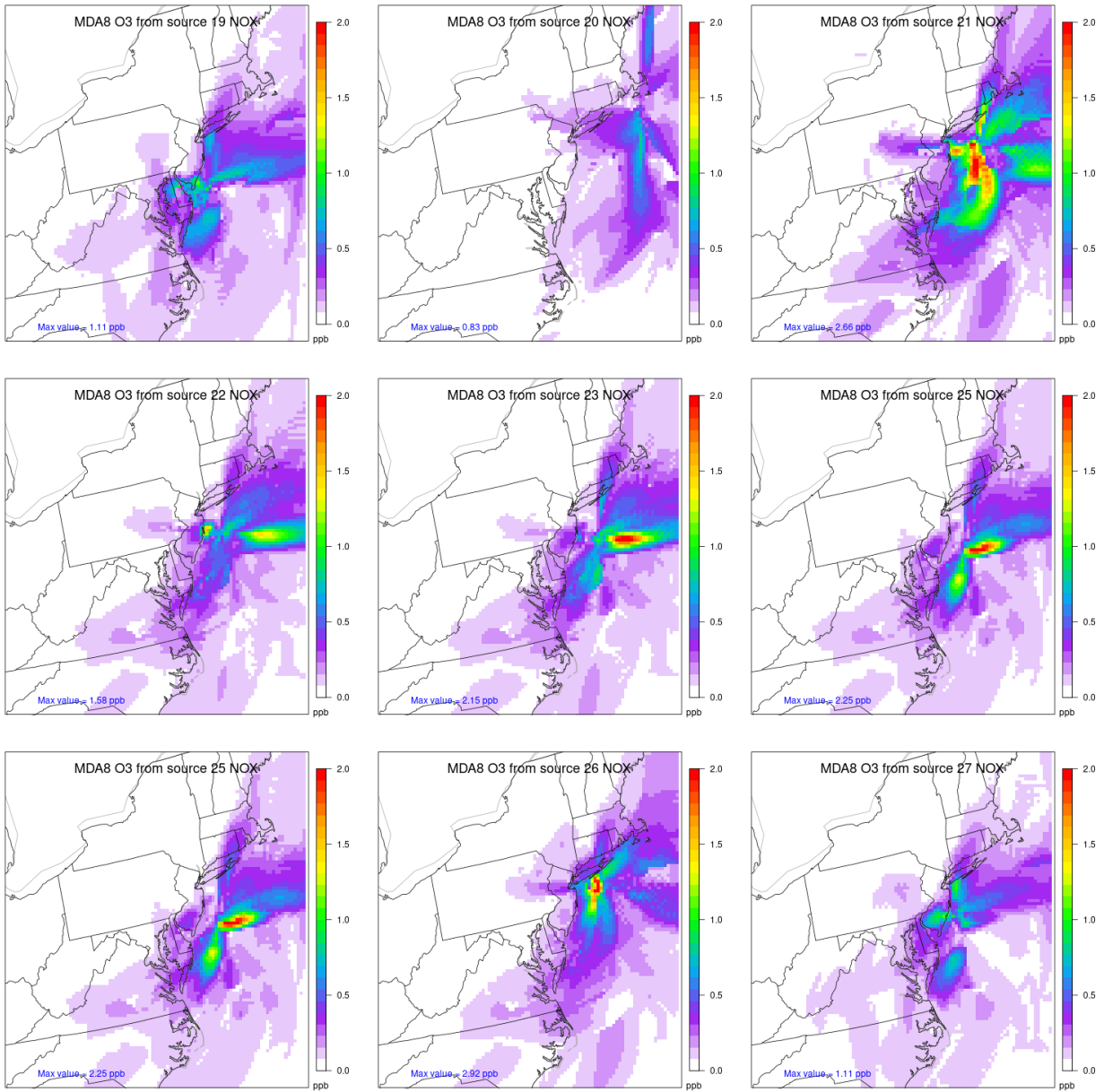


Figure A4. Maximum MDA8 O₃ impacts from 50 tpy of VOC emissions from sources 1-9.

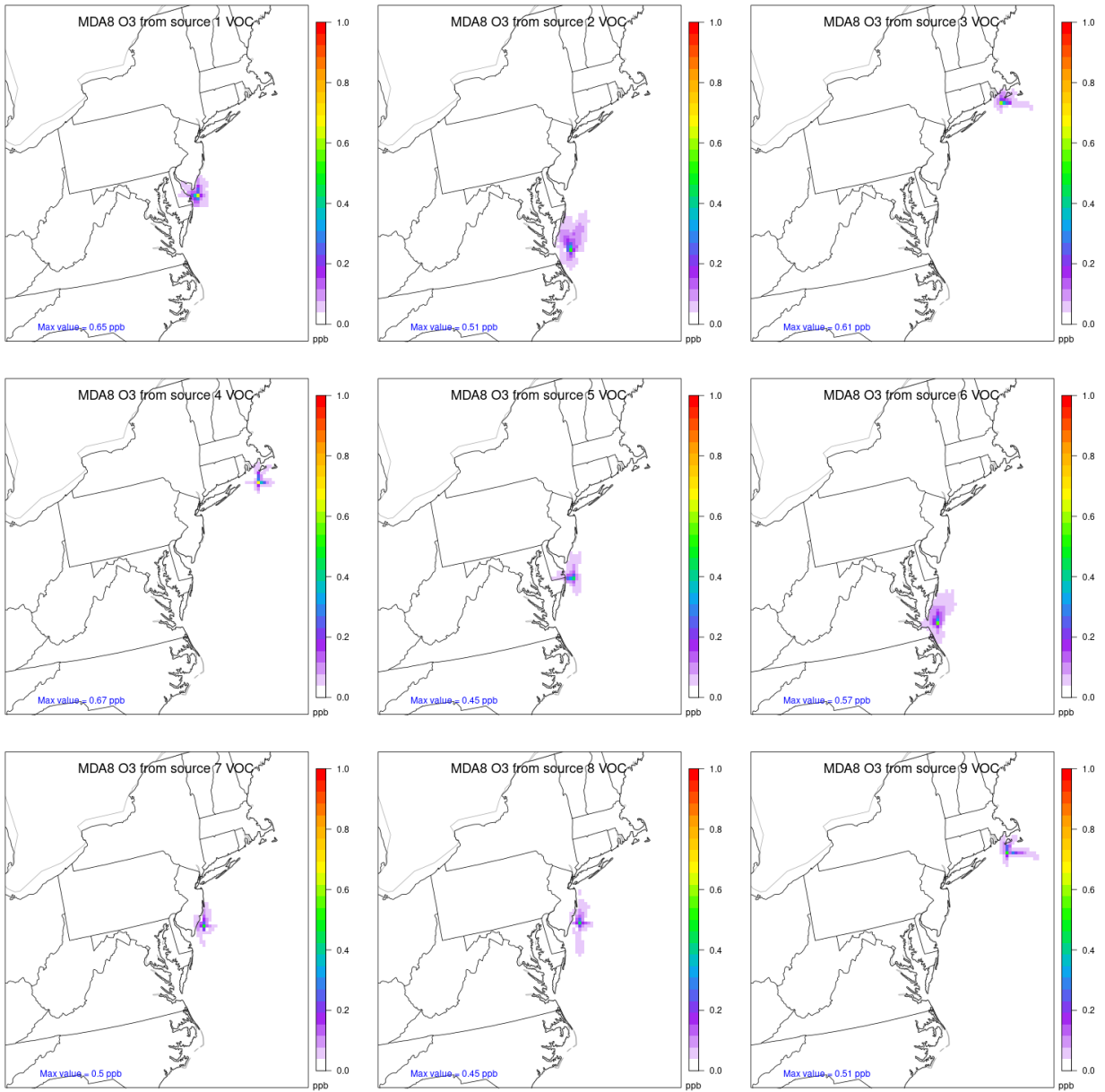


Figure A5. Maximum MDA8 O₃ impacts from 50 tpy of VOC emissions from sources 10-18.

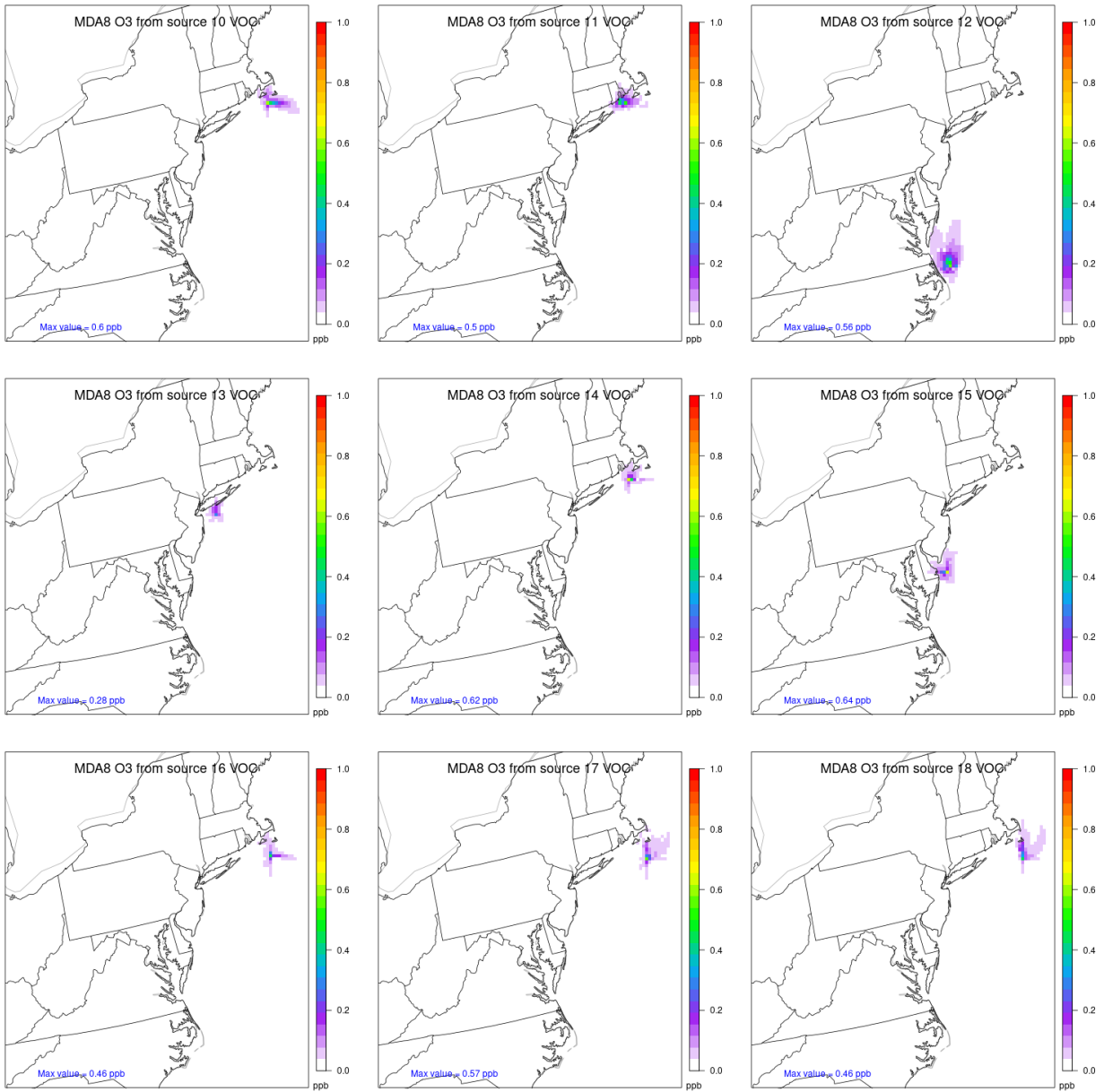


Figure A6. Maximum MDA8 O₃ impacts from 50 tpy of VOC emissions from sources 19-27.

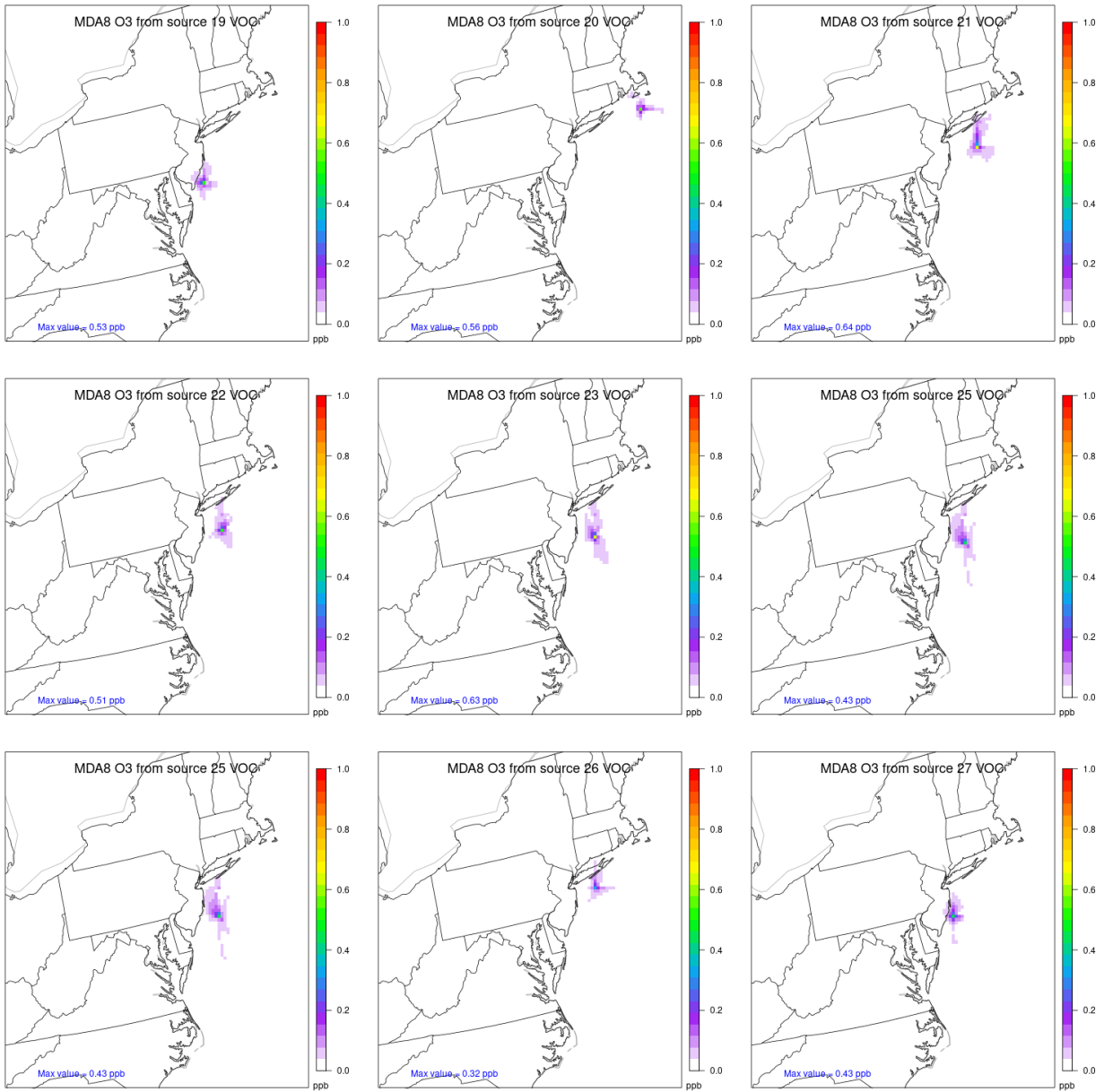


Figure A7. Annual Maximum Daily Average PM_{2.5} sulfate ion impacts from 50 tpy of SO₂ emissions from sources 1-9.

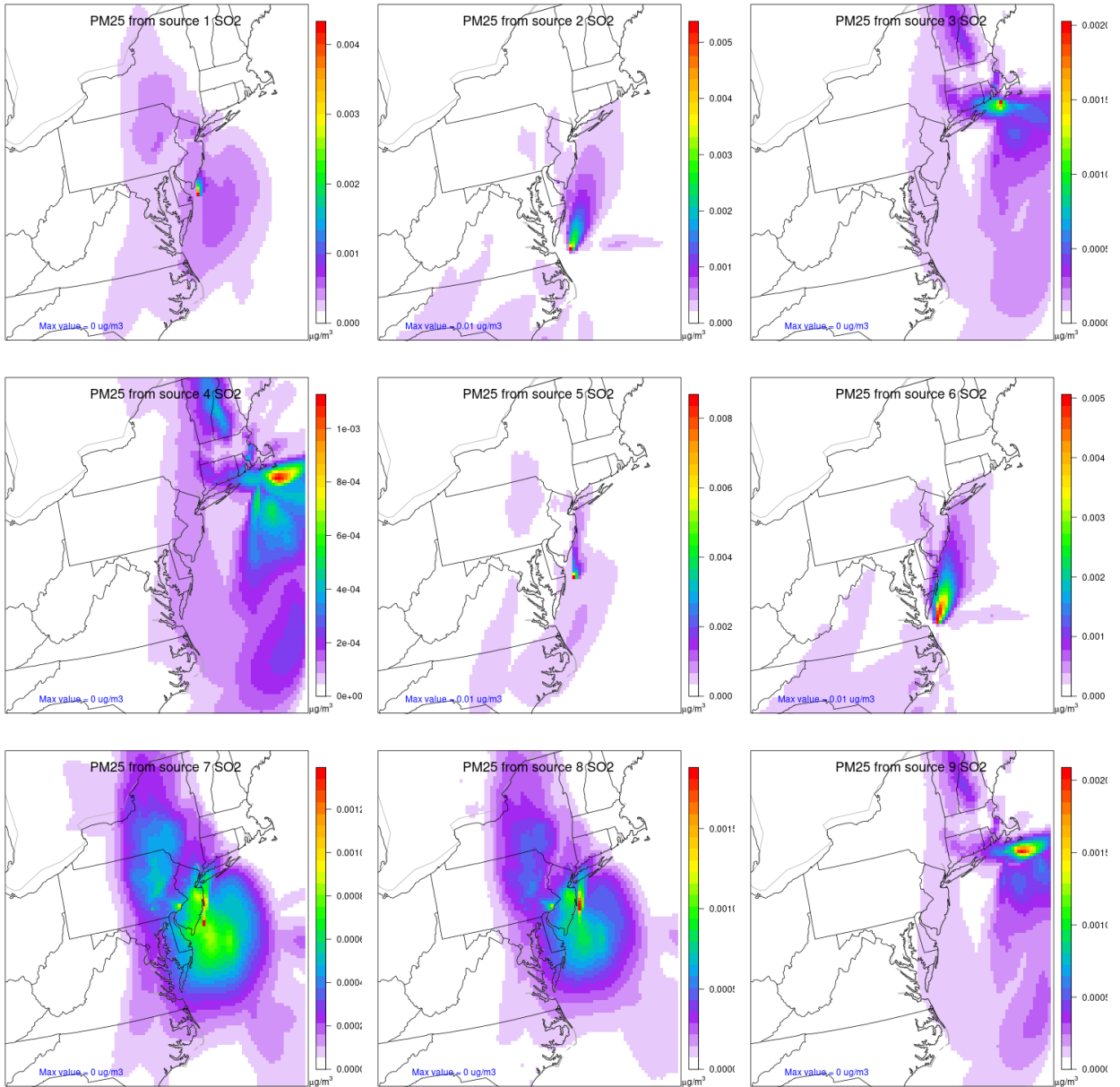


Figure A8. Annual Maximum Daily Average PM_{2.5} sulfate ion impacts from 50 tpy of SO₂ emissions from sources 10-18.

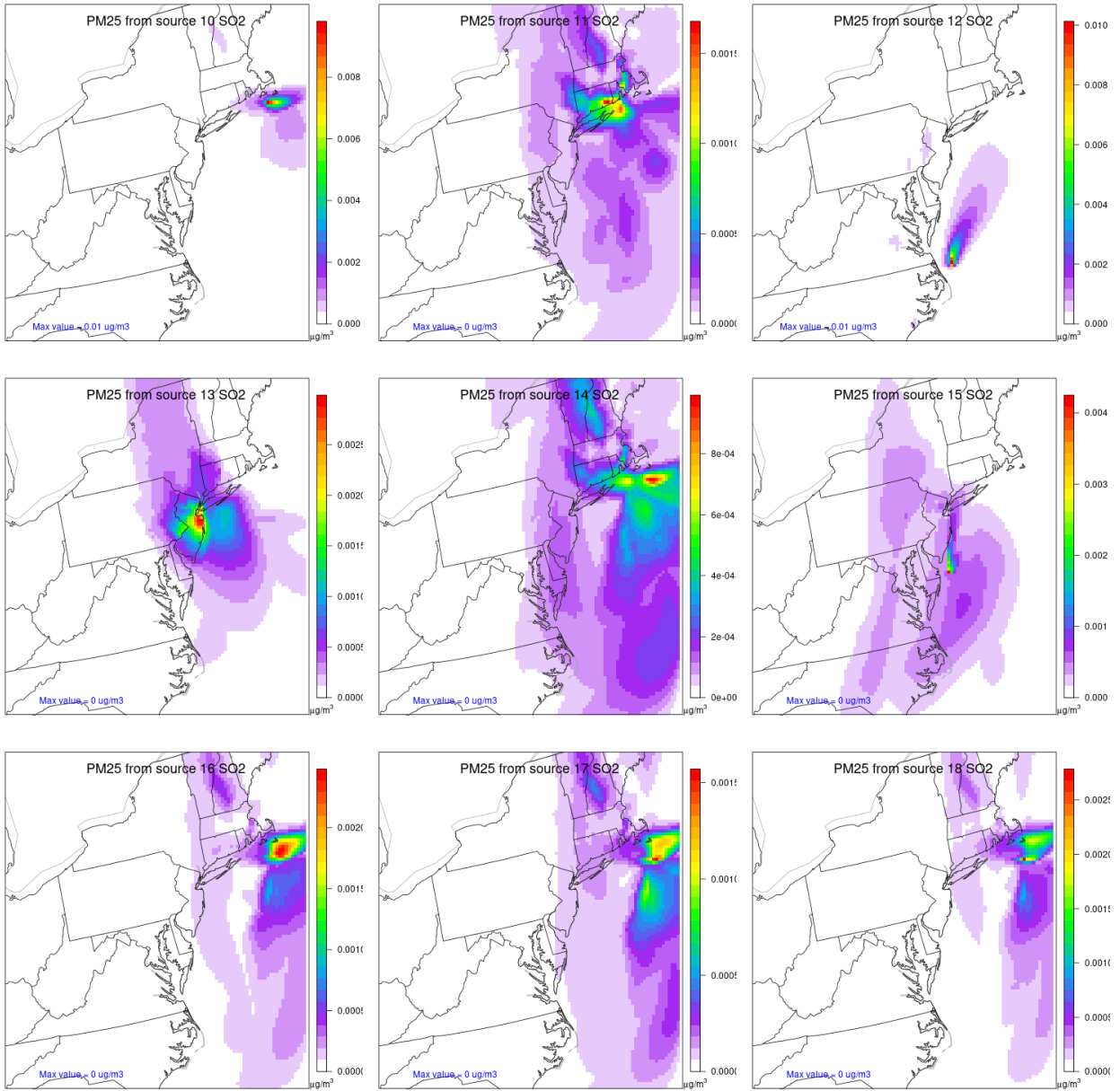


Figure A9. Annual Maximum Daily Average PM_{2.5} sulfate ion impacts from 50 tpy of SO₂ emissions from sources 19-27.

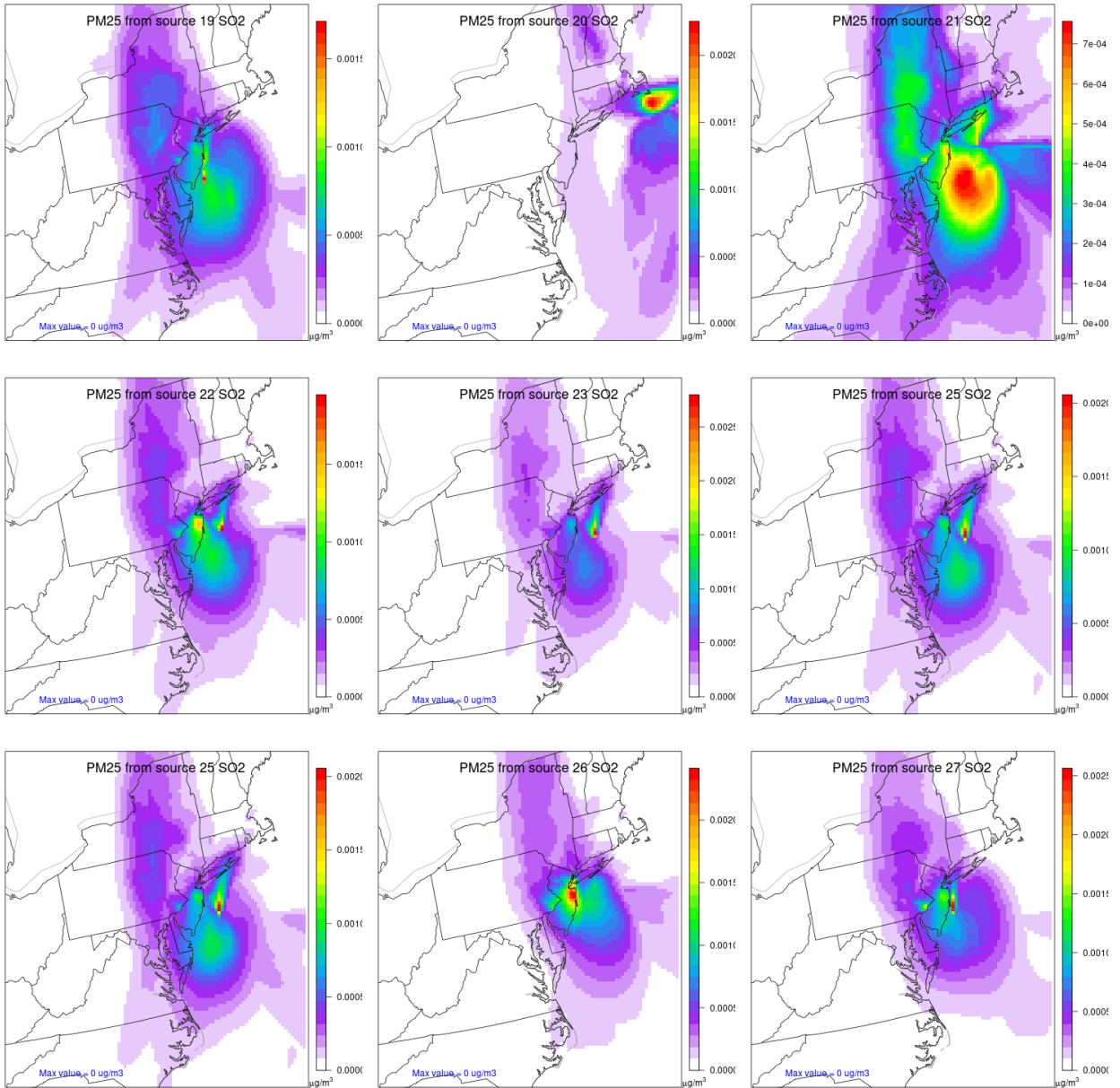


Figure A10. Annual Maximum Daily Average PM_{2.5} nitrate ion impacts from 5000 tpy of NO_x emissions from sources 1-9.

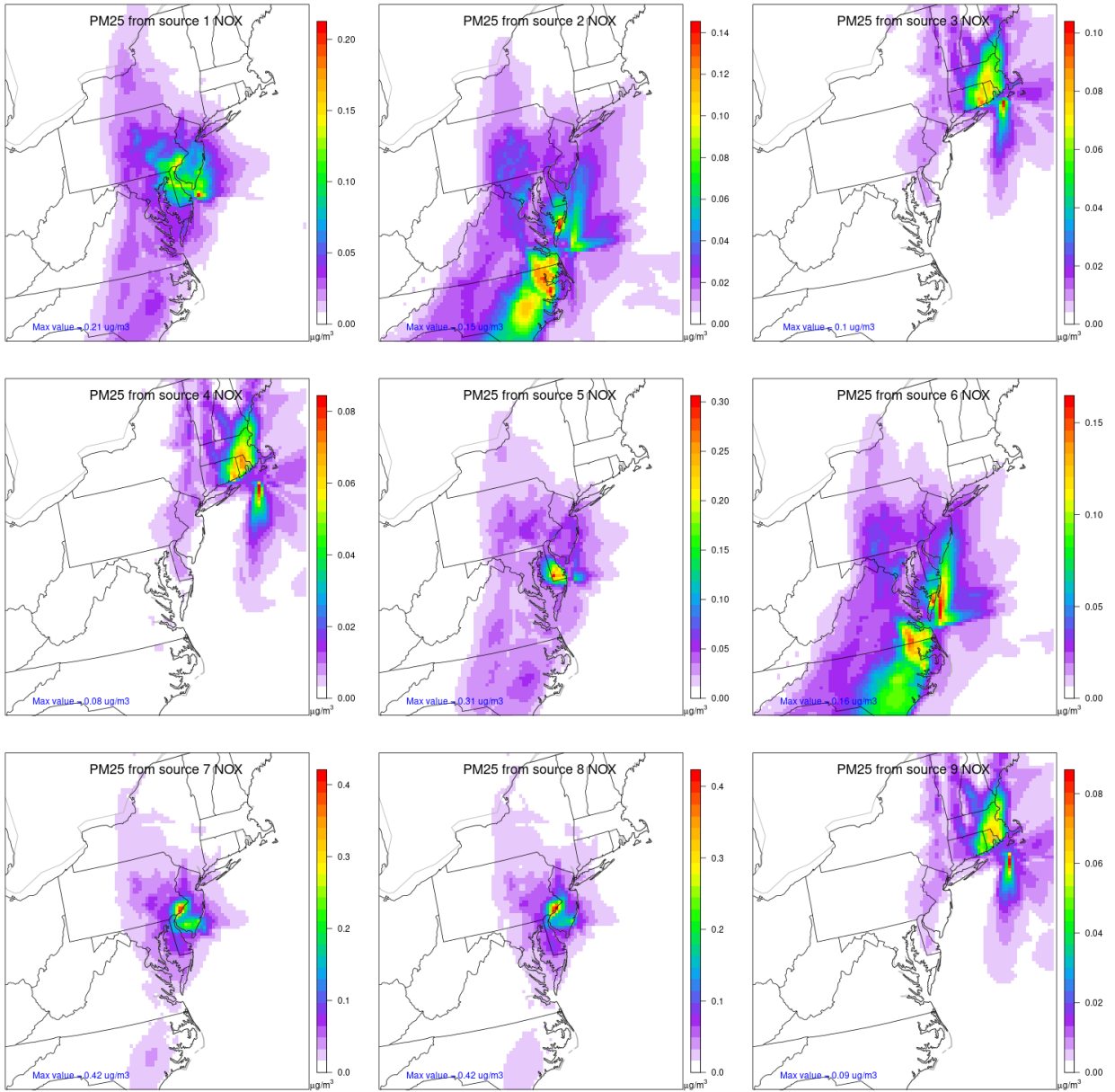


Figure A11. Annual Maximum Daily Average PM_{2.5} nitrate ion impacts from 5000 tpy of NO_x emissions from sources 10-18.

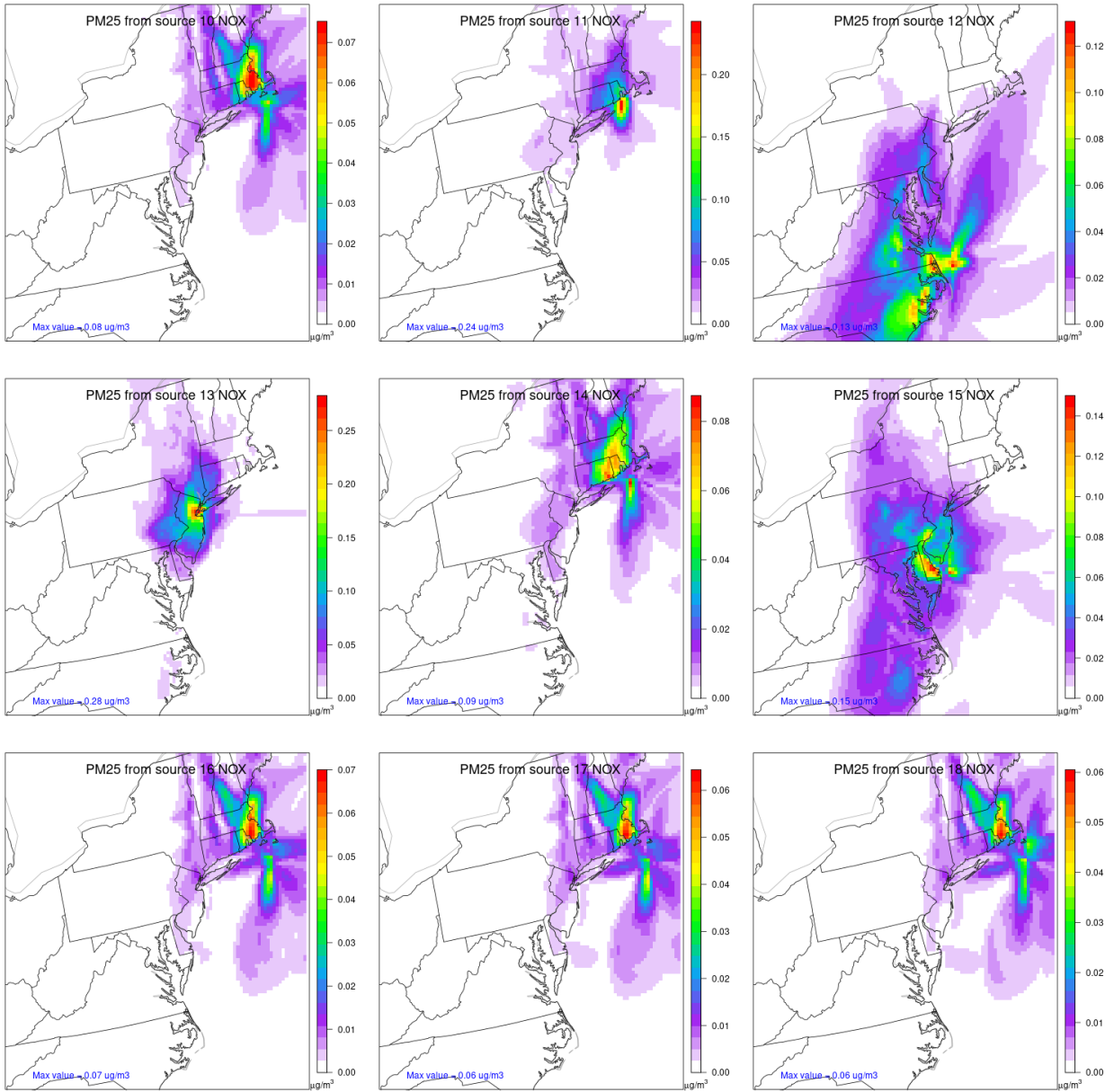


Figure A12. Annual Maximum Daily Average PM_{2.5} nitrate ion impacts from 5000 tpy of NO_x emissions from sources 19-27.

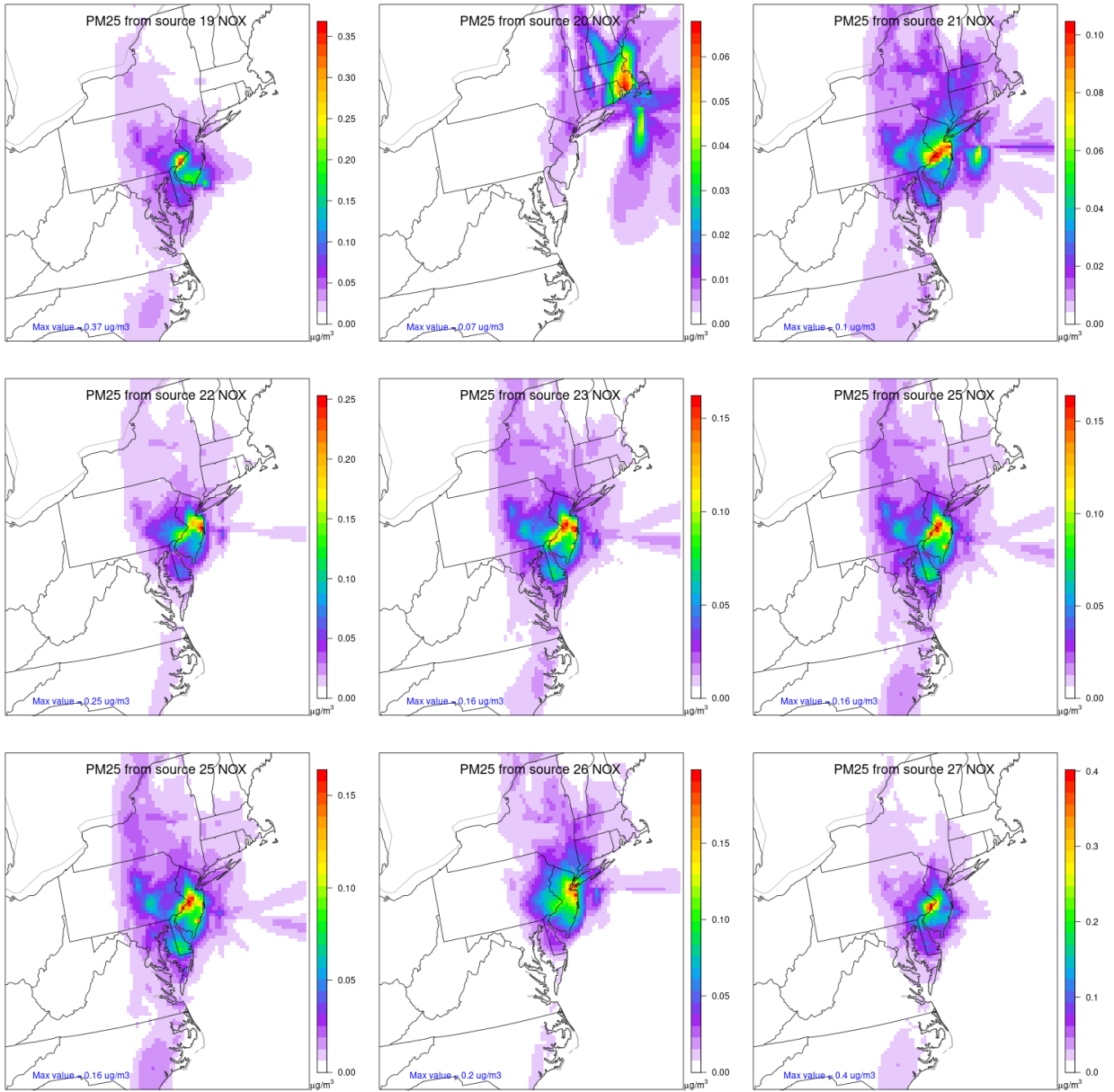


Figure A13. Annual Maximum Daily Average PM_{2.5} ammonium ion impacts from 5 tpy of NH₃ emissions from sources 1-9.

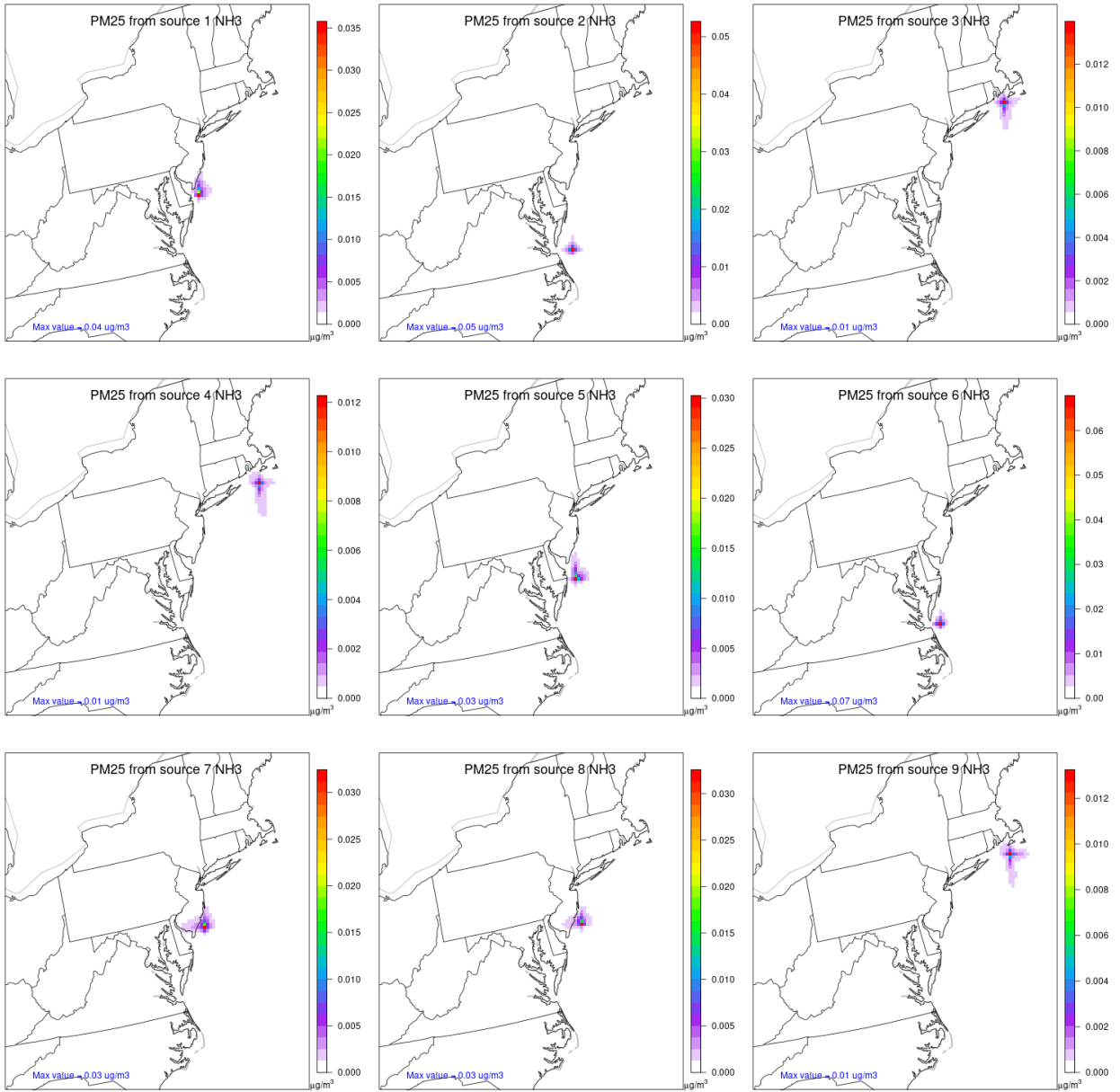


Figure A14. Annual Maximum Daily Average PM_{2.5} ammonium ion impacts from 5 tpy of NH₃ emissions from sources 10-18.

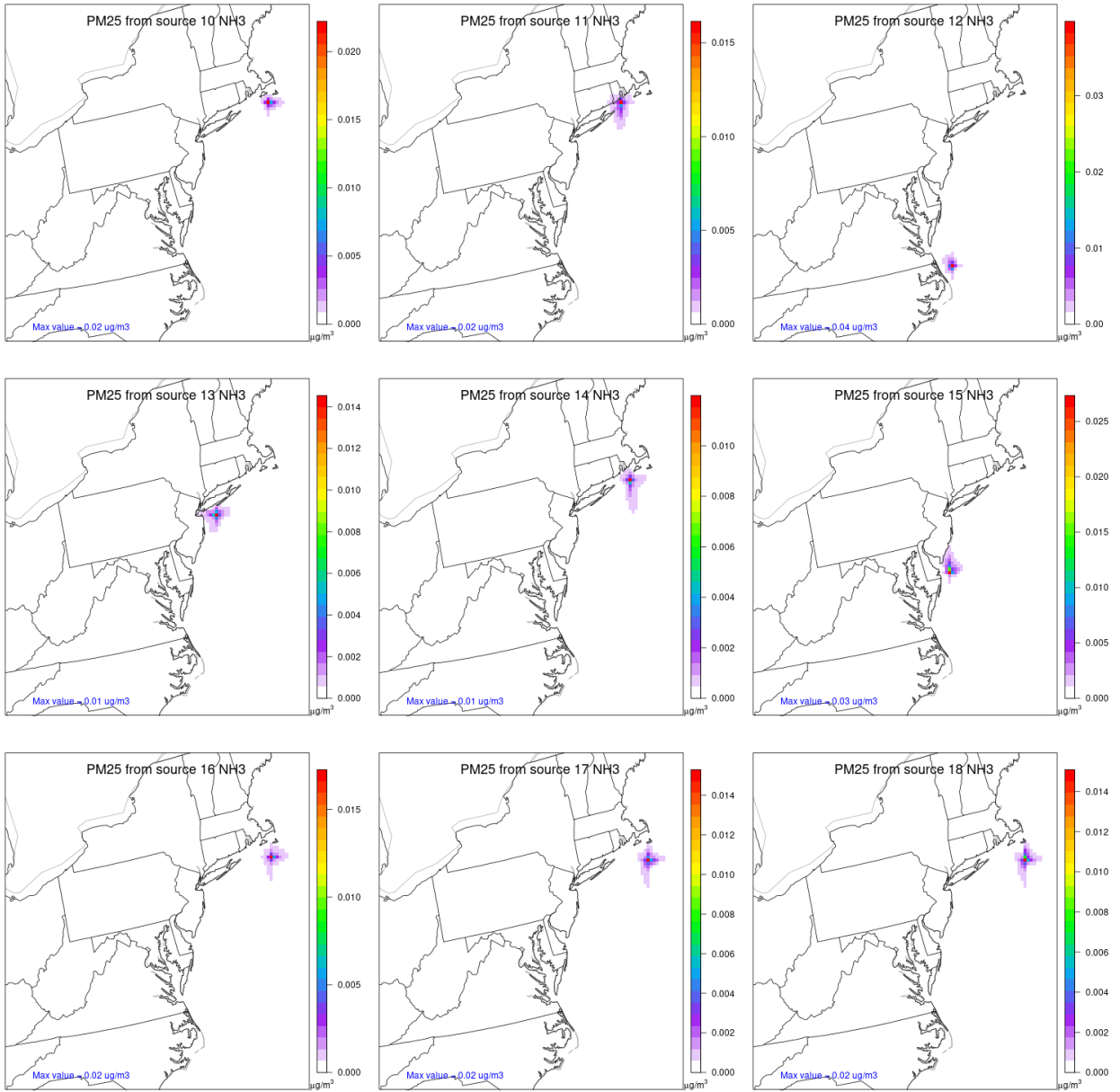


Figure A15. Annual Maximum Daily Average PM_{2.5} ammonium ion impacts from 5 tpy of NH₃ emissions from sources 19-27.

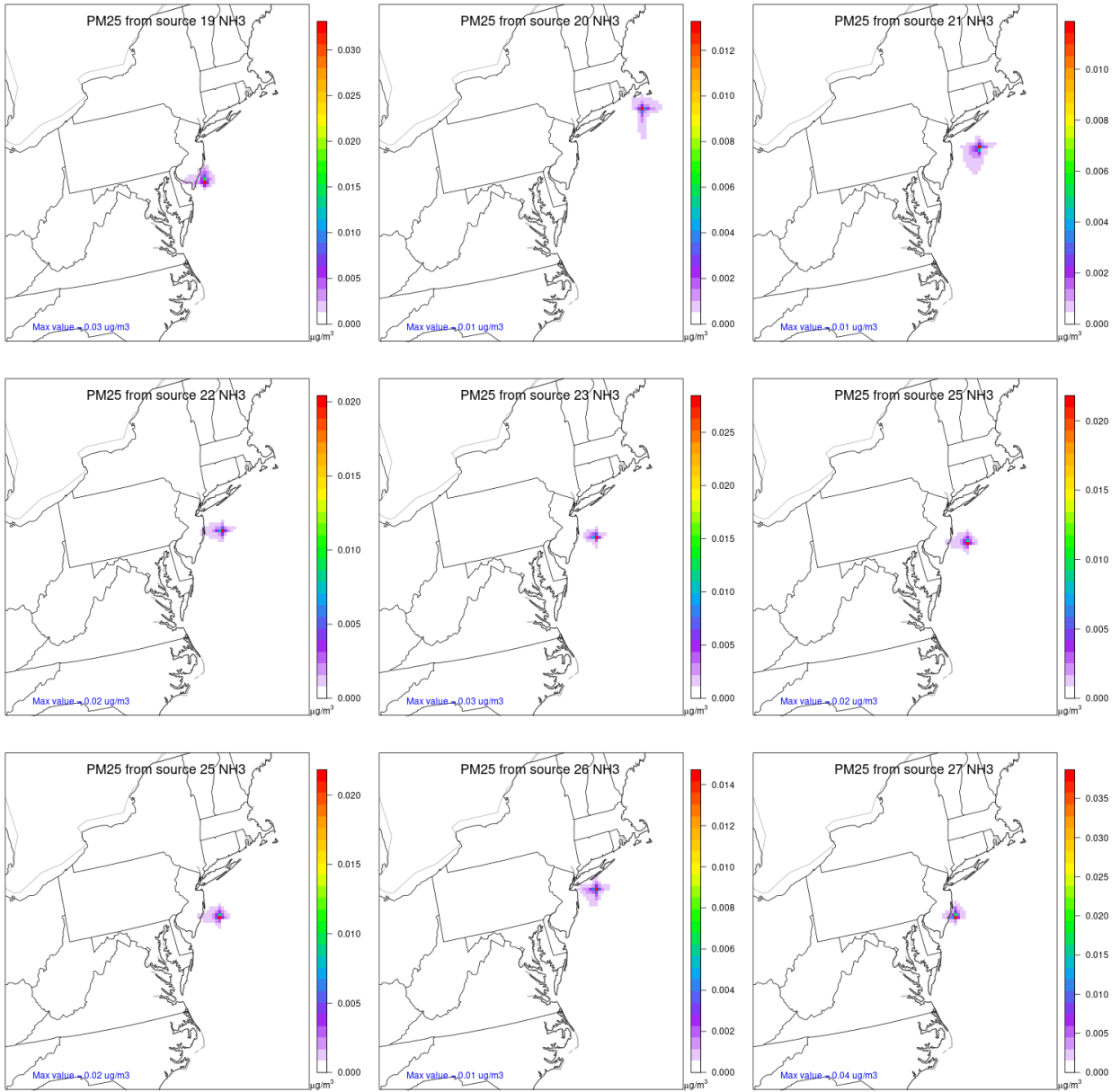


Figure A16. Annual Maximum Daily Average PM_{2.5} impacts from 215 tpy of primary PM_{2.5} emissions from sources 1-9.

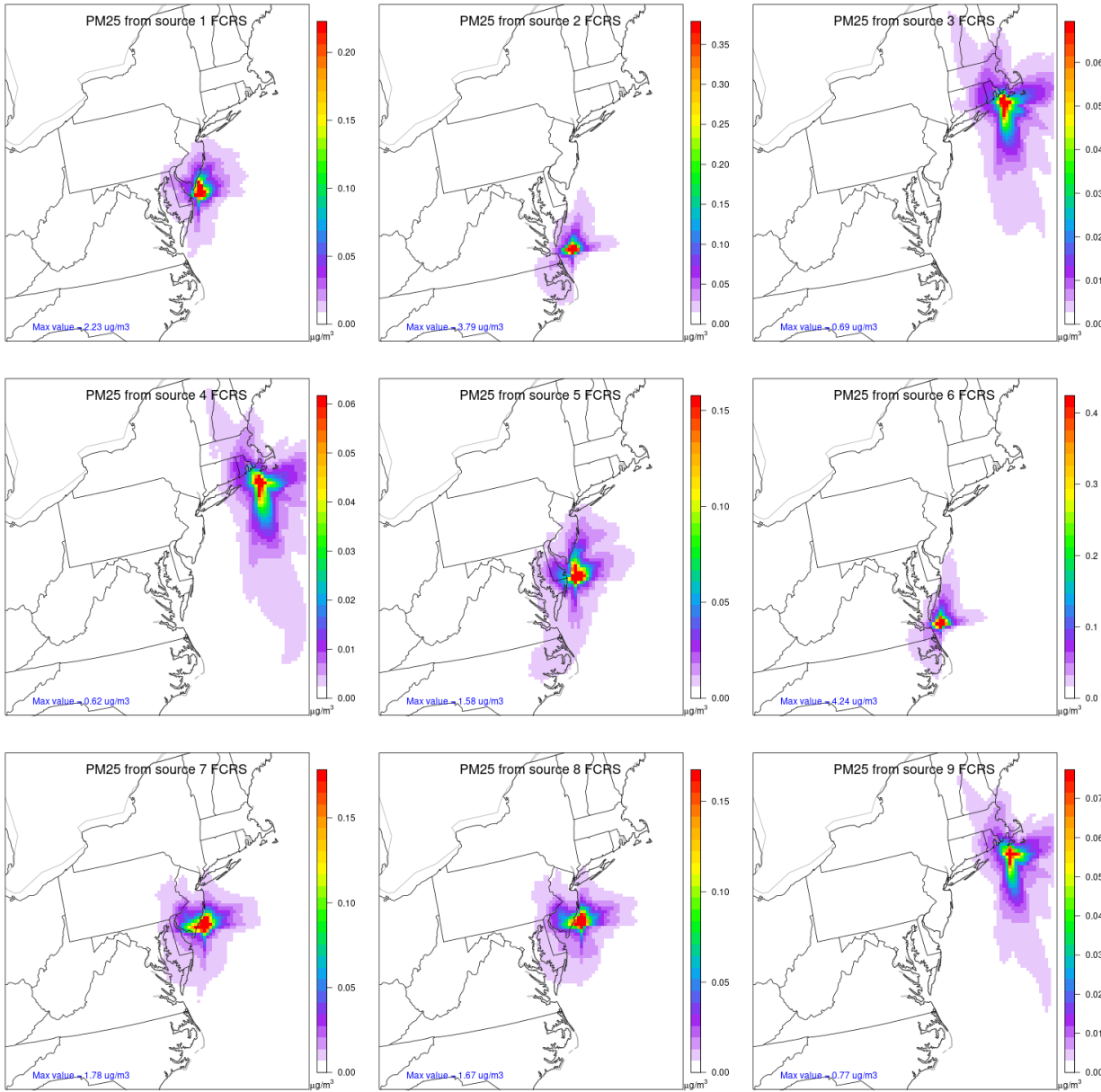


Figure A17. Annual Maximum Daily Average PM_{2.5} impacts from 215 tpy of primary PM_{2.5} emissions from sources 10-18.

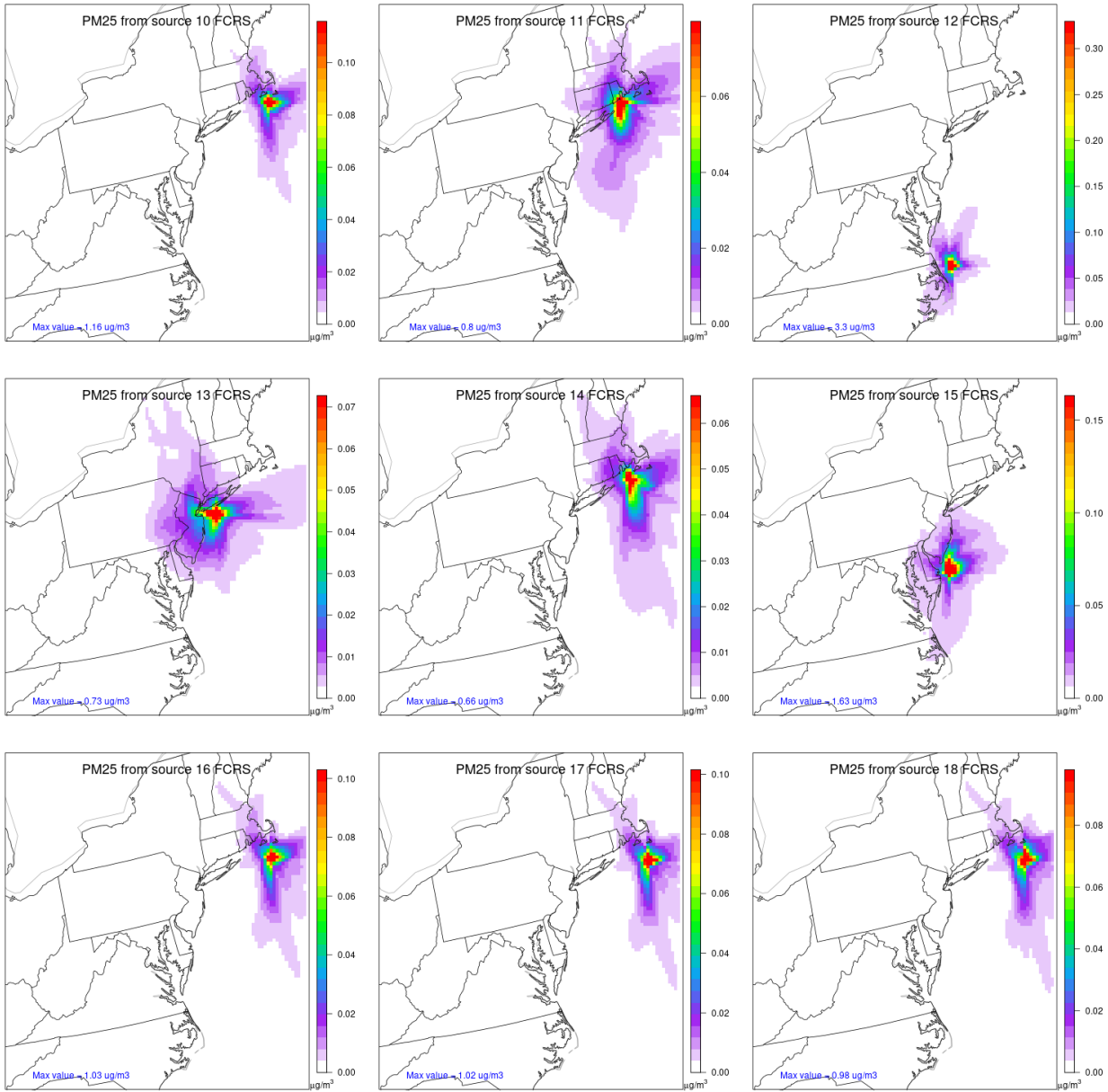


Figure A18. Annual Maximum Daily Average PM_{2.5} impacts from 215 tpy of primary PM_{2.5} emissions from sources 19-27.

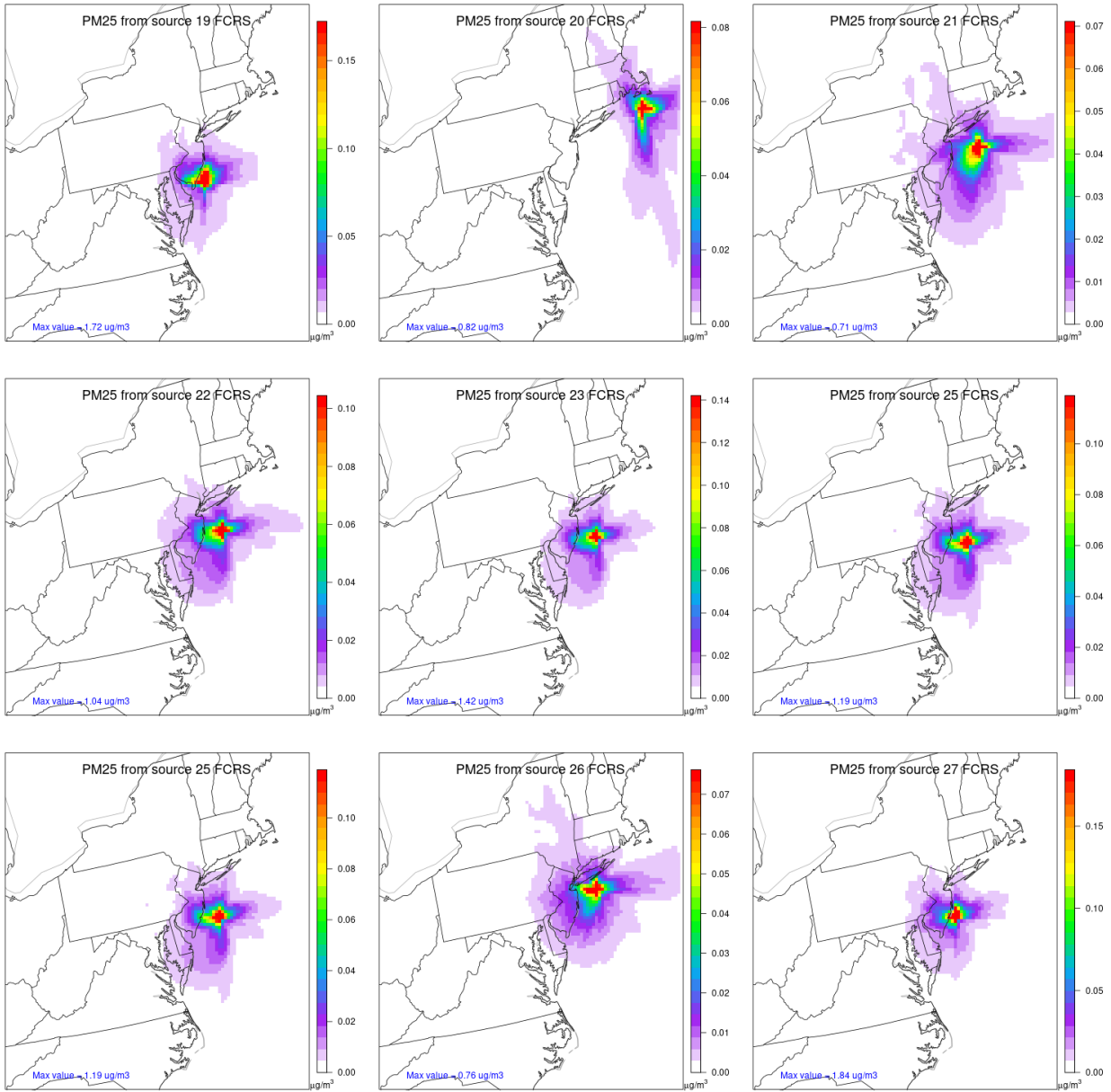


Figure A19. Annual Maximum Daily Average Coarse PM impacts from 215 tpy of coarse PM emissions from sources 1-9.

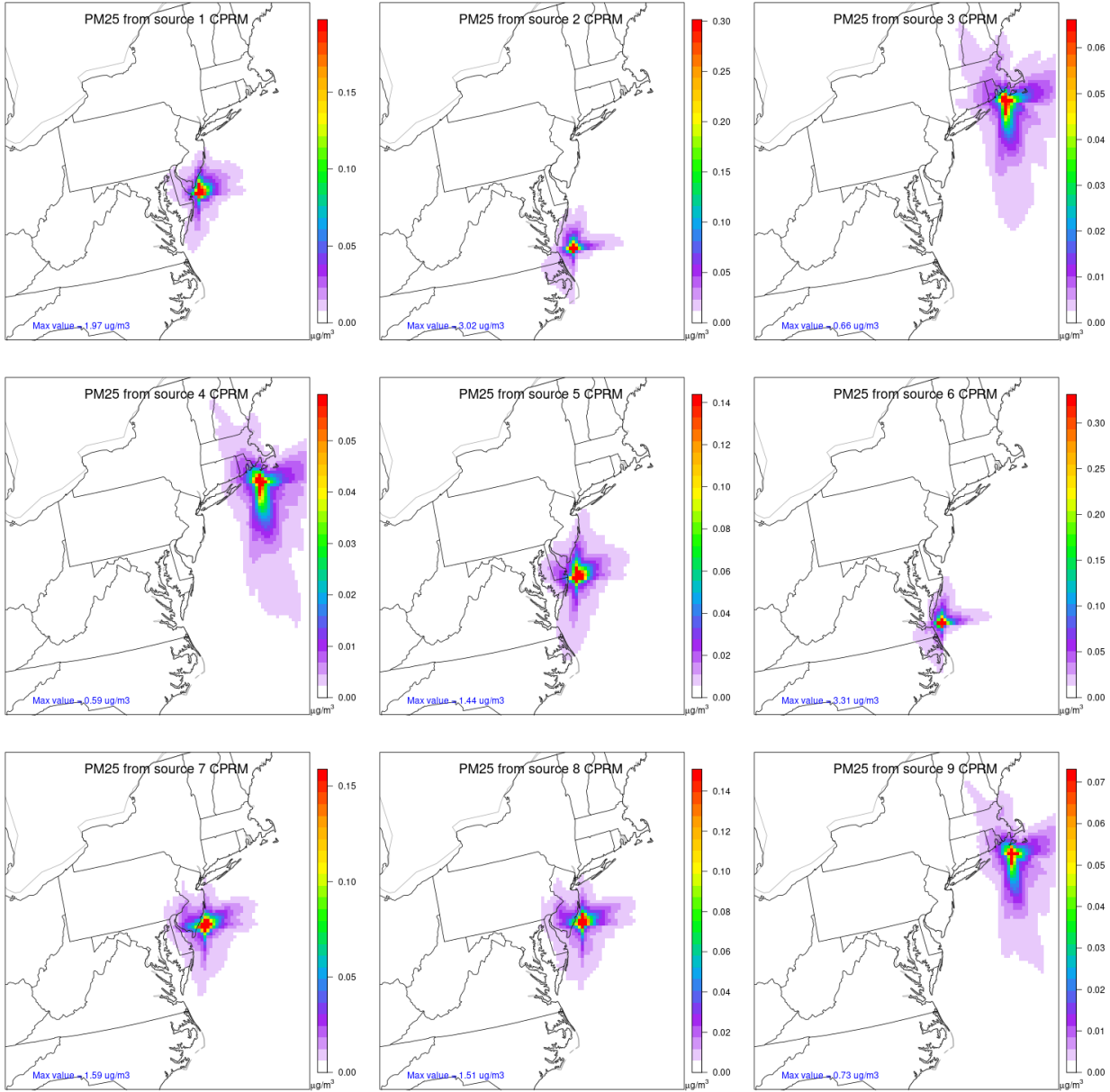


Figure A20. Annual Maximum Daily Average Coarse PM impacts from 215 tpy of coarse PM emissions from sources 10-18.

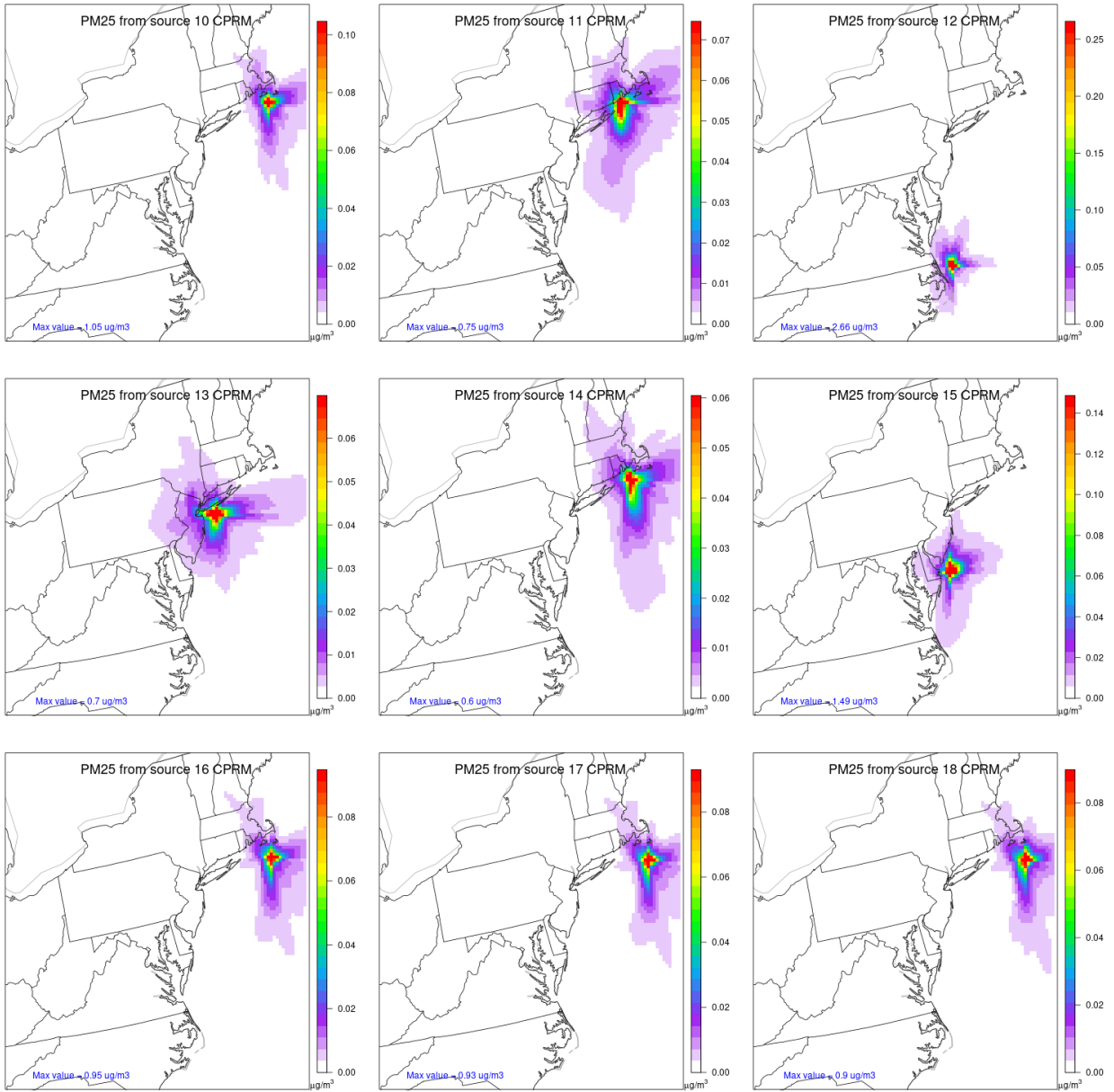
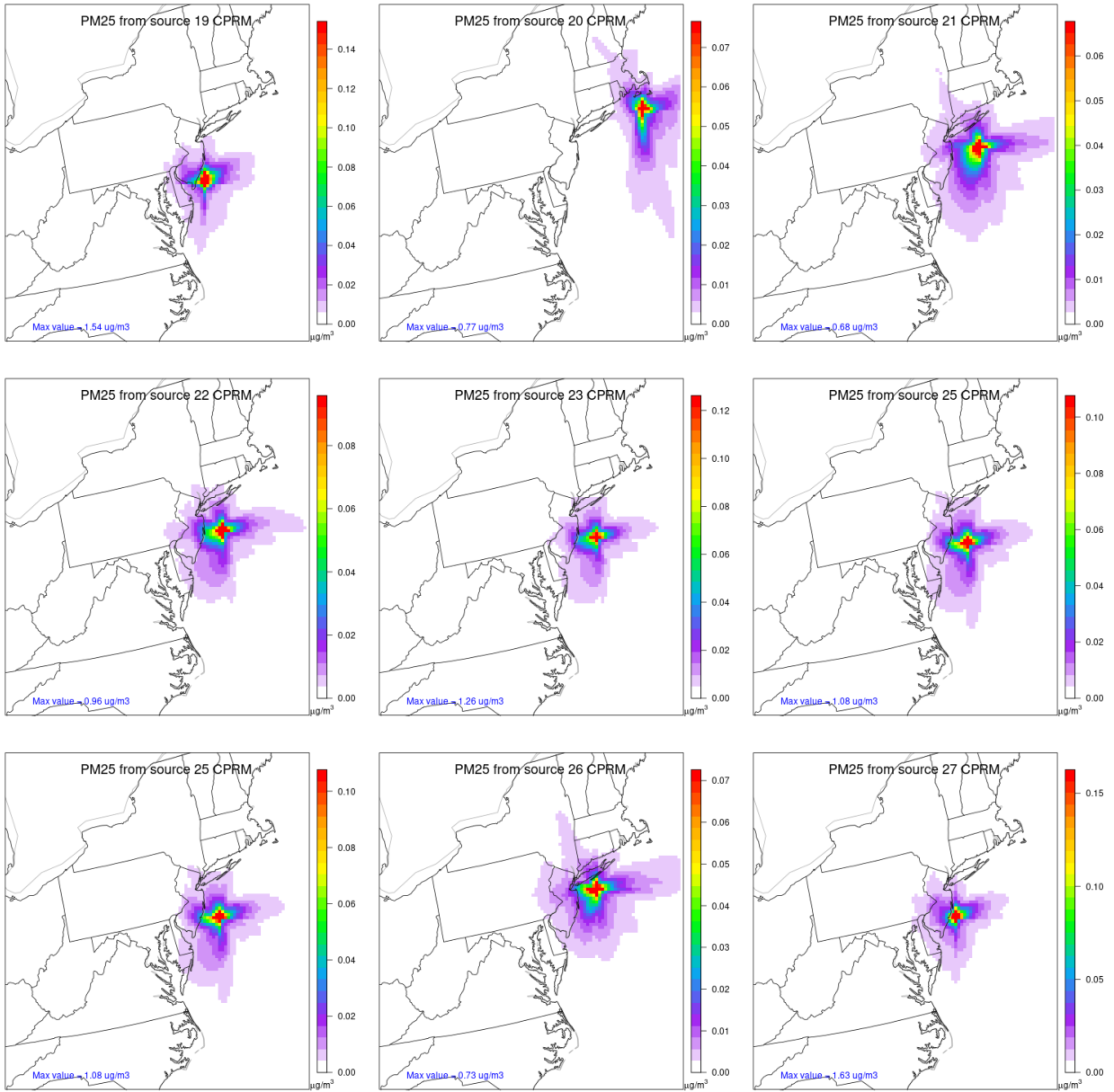


Figure A21. Annual Maximum Daily Average Coarse PM impacts from 215 tpy of coarse PM emissions from sources 19-27.



APPENDIX B

Annual Average Speciated PM_{2.5} Impacts Based on Hypothetical Emission Rates

Figure B1. Annual Average PM_{2.5} sulfate ion impacts from 50 tpy of SO₂ emissions from sources 1-9.

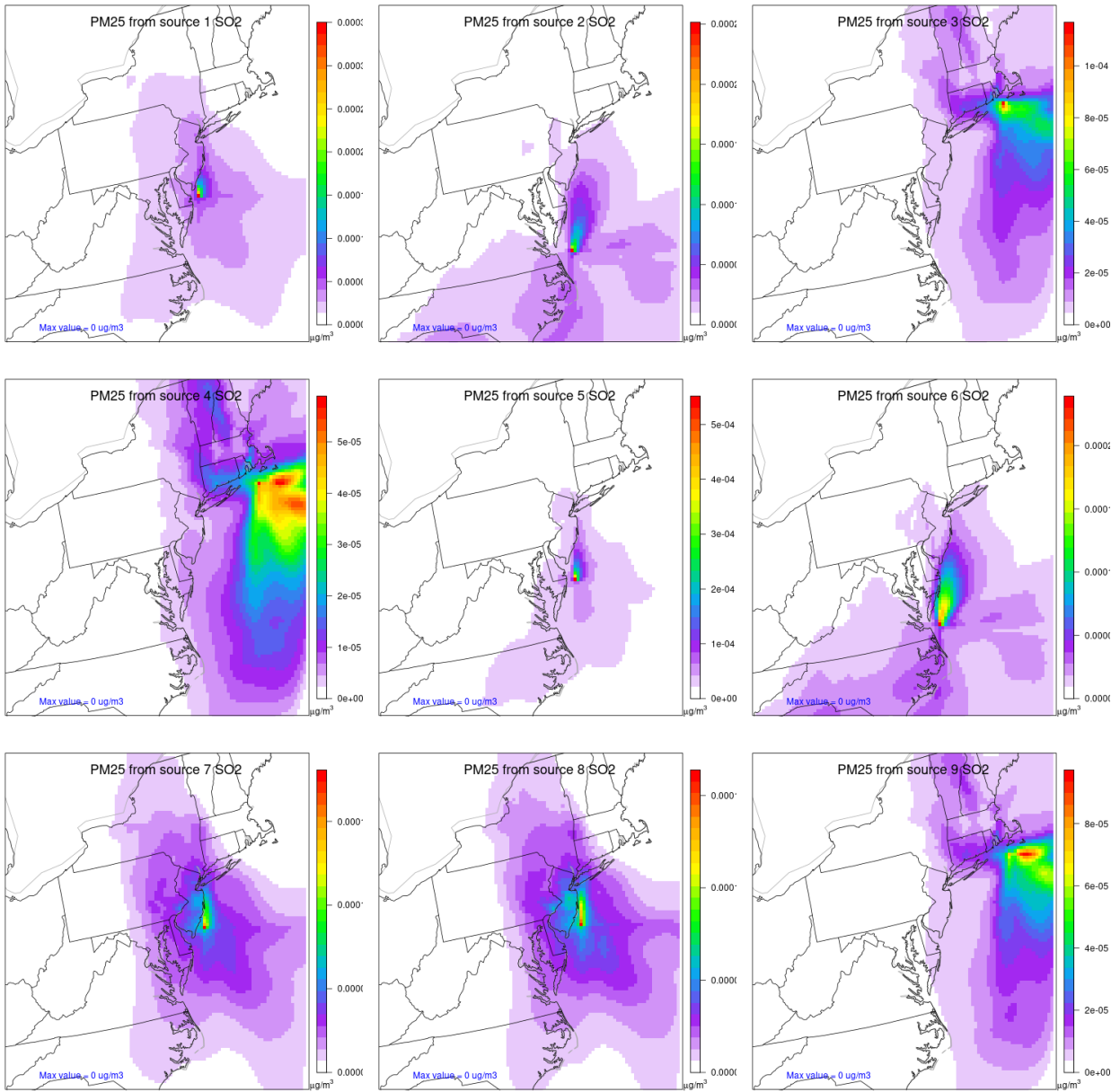


Figure B2. Annual Average PM_{2.5} sulfate ion impacts from 50 tpy of SO₂ emissions from sources 10-18.

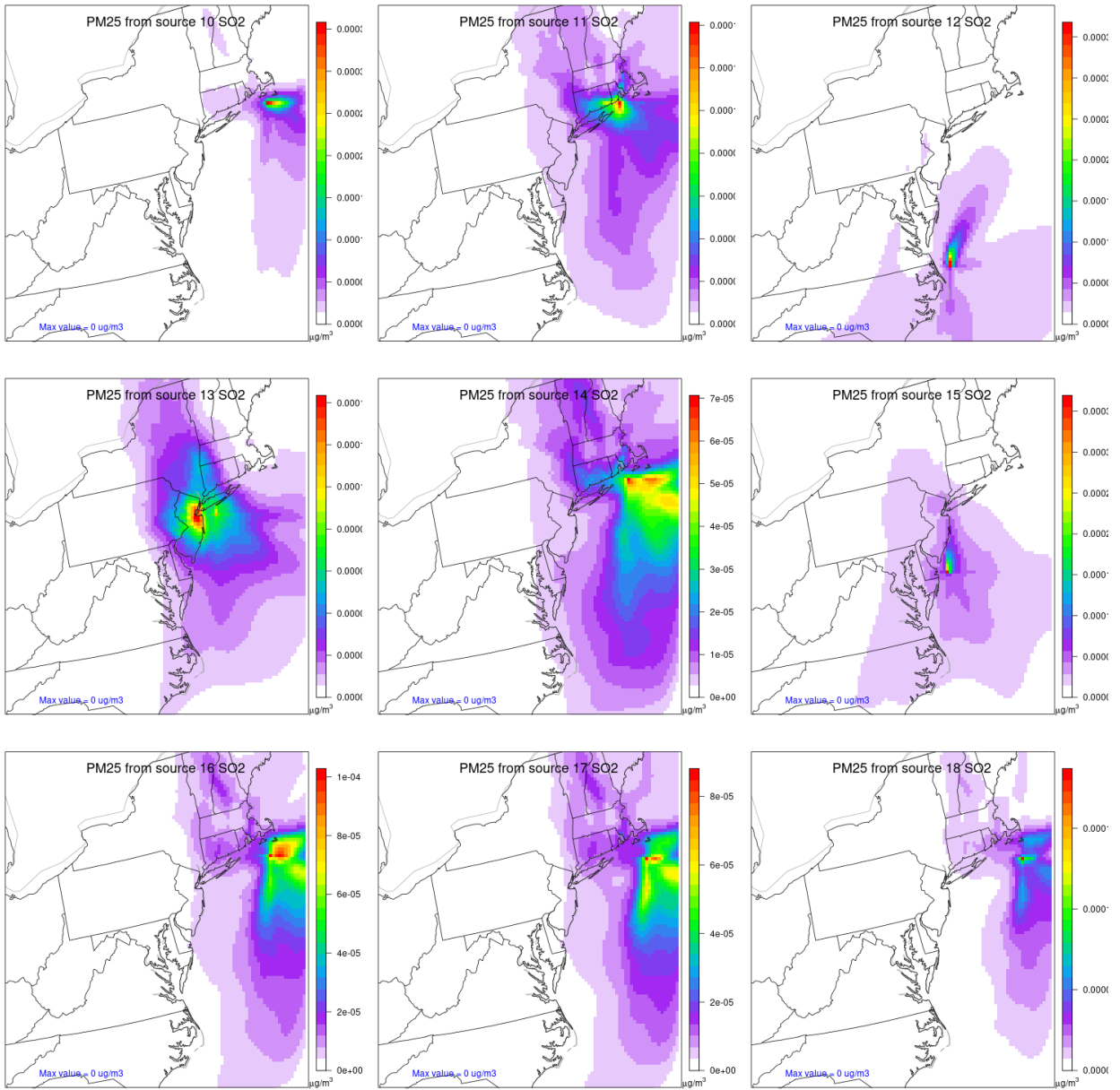


Figure B3. Annual Average PM_{2.5} sulfate ion impacts from 50 tpy of SO₂ emissions from sources 19-27.

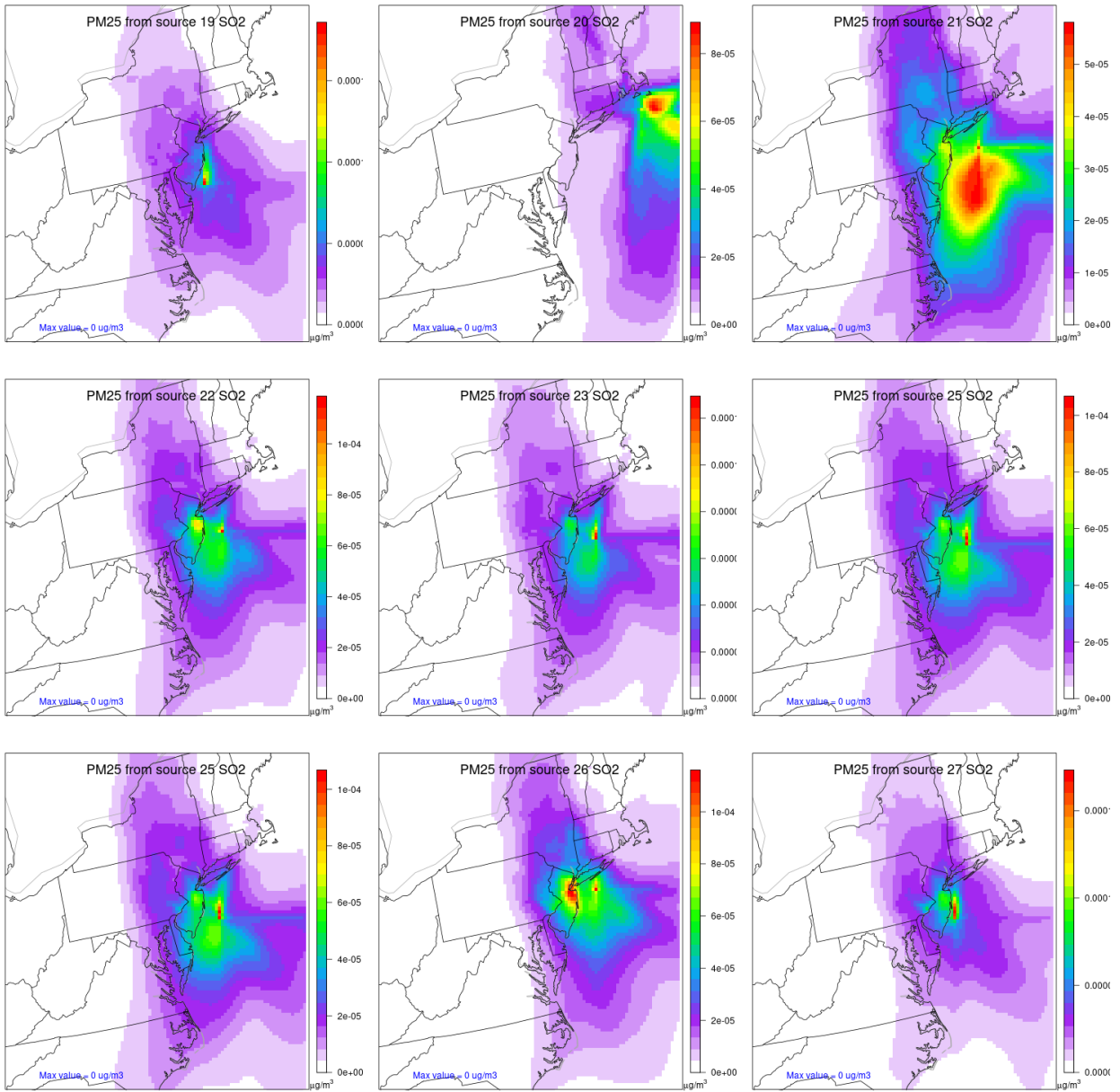


Figure B4. Annual Average PM_{2.5} nitrate ion impacts from 5000 tpy of NO_x emissions from sources 1-9.

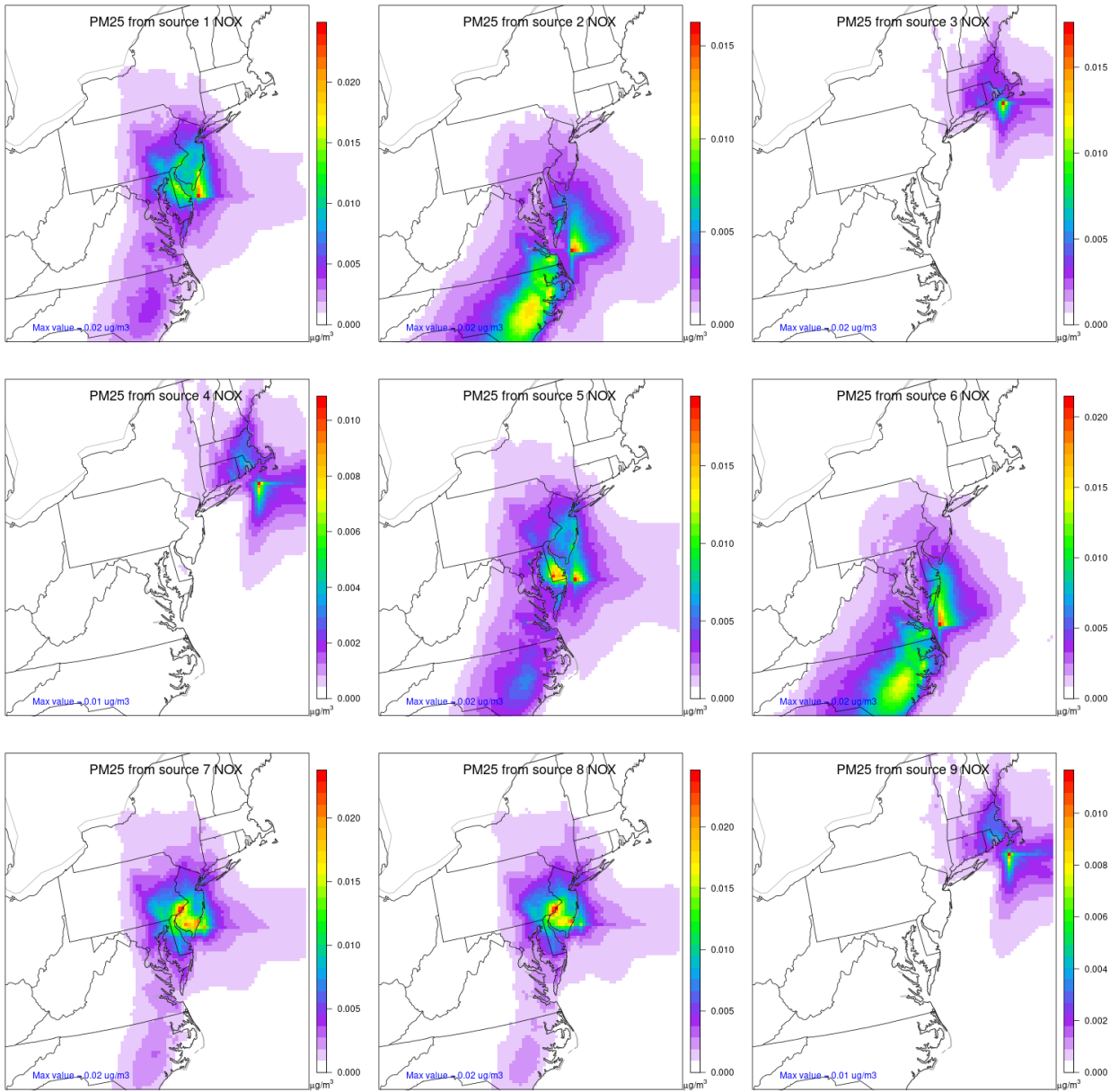


Figure B5. Annual Average PM_{2.5} nitrate ion impacts from 5000 tpy of NO_x emissions from sources 10-18.

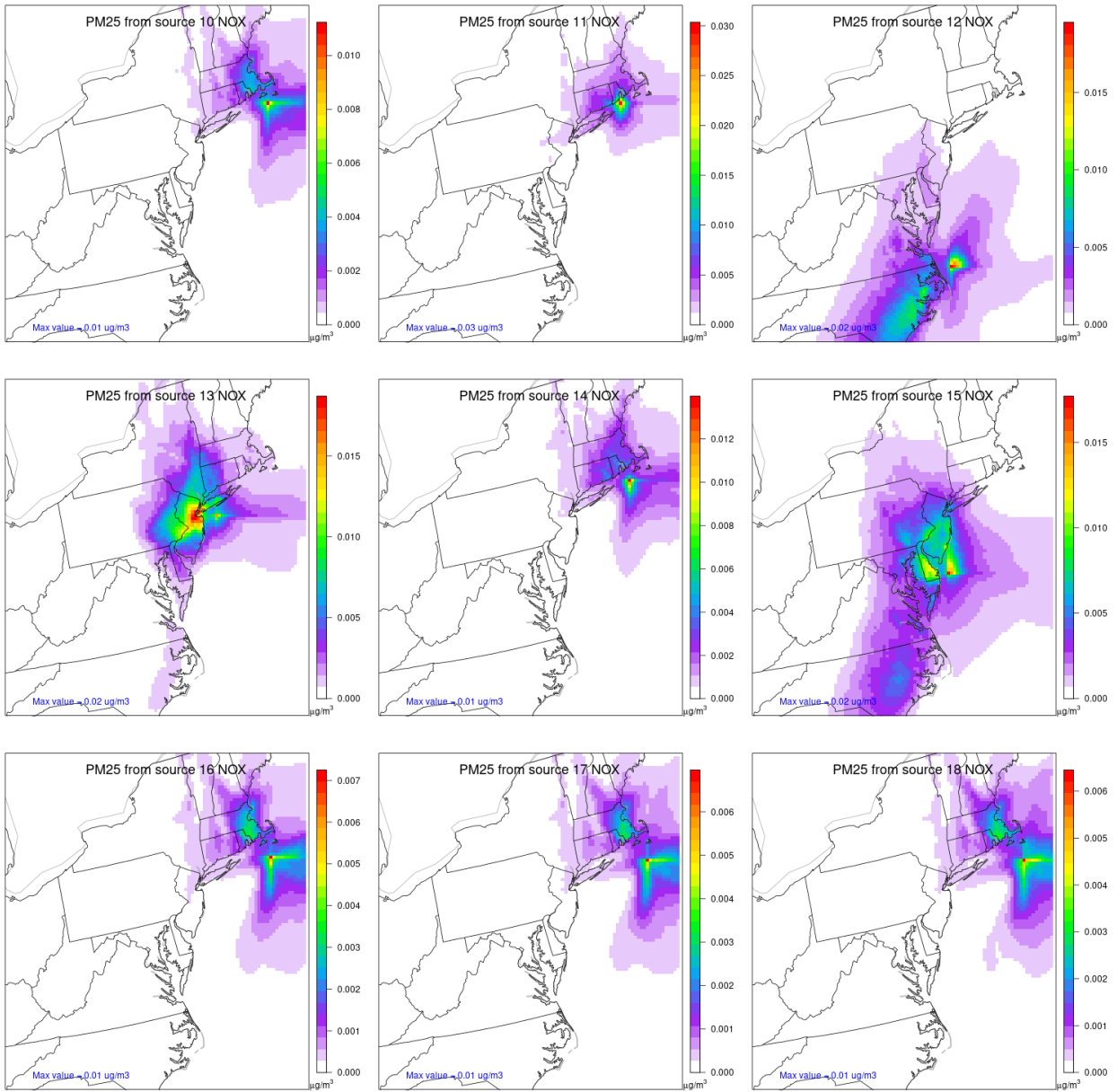


Figure B6. Annual Average PM_{2.5} nitrate ion impacts from 5000 tpy of NO_x emissions from sources 19-27.

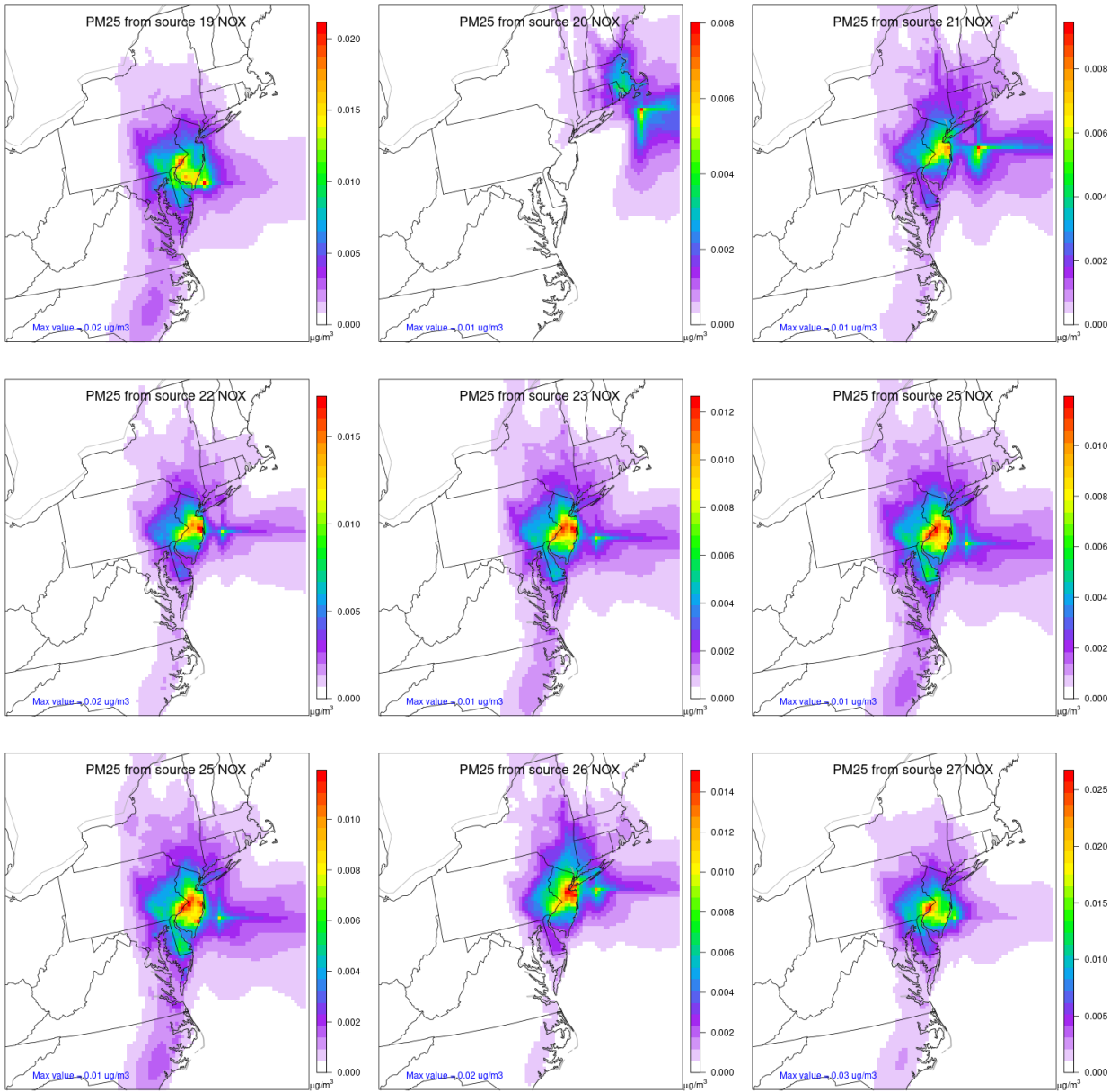


Figure B7. Annual Average PM_{2.5} ammonium ion impacts from 5 tpy of NH₃ emissions from sources 1-9.

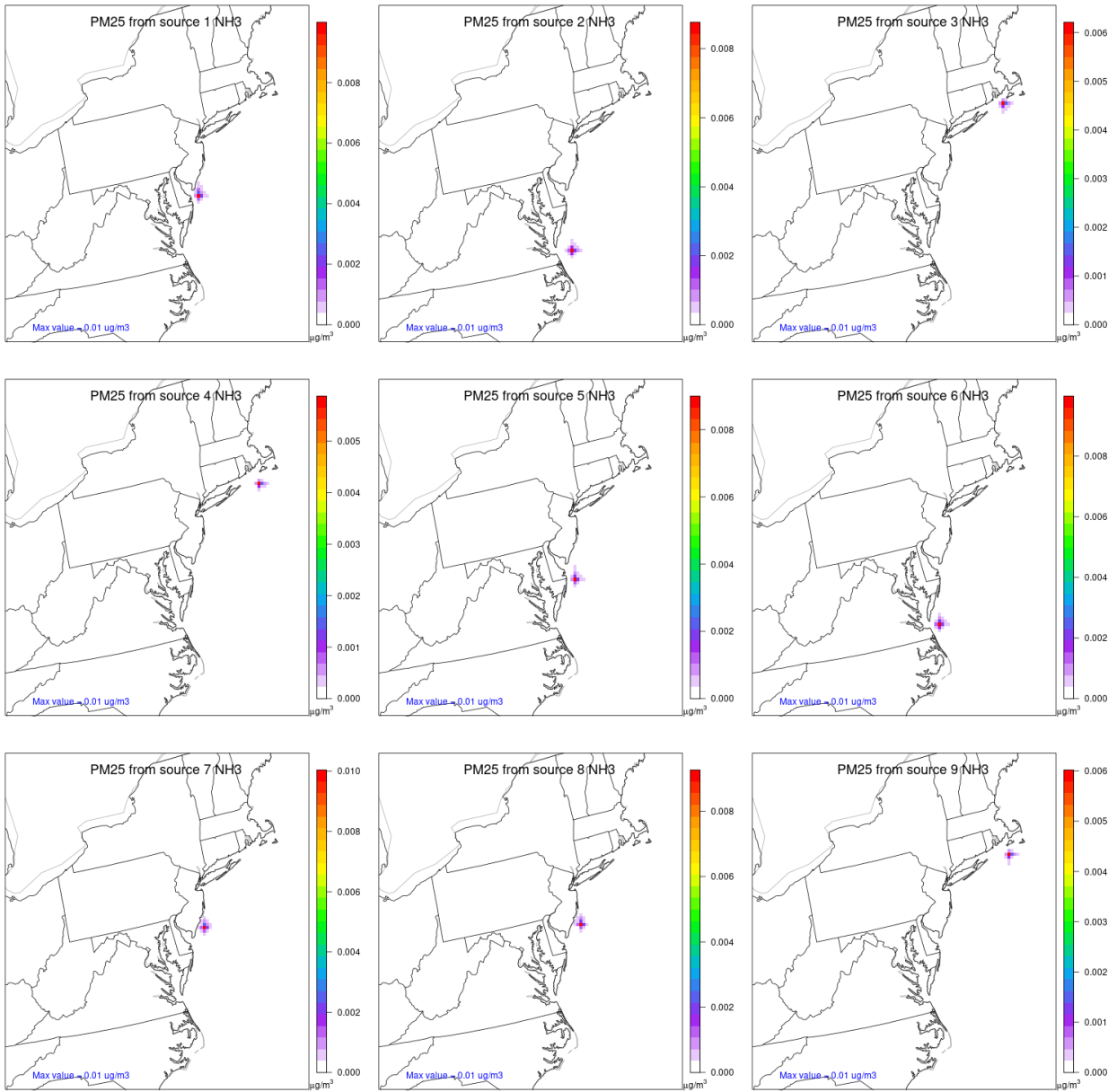


Figure B8. Annual Average PM_{2.5} ammonium ion impacts from 5 tpy of NH₃ emissions from sources 10-18.

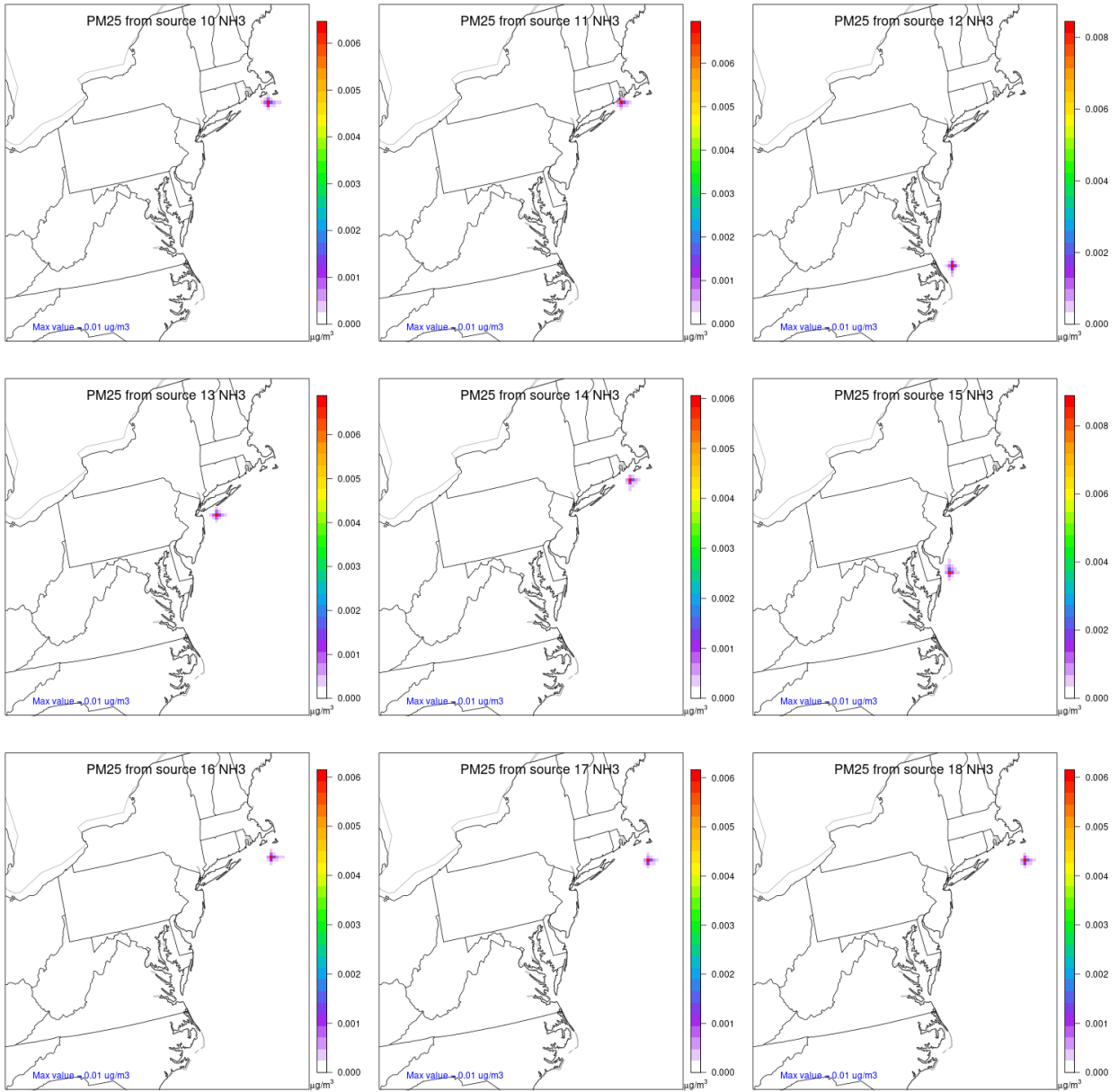


Figure B9. Annual Average PM_{2.5} ammonium ion impacts from 5 tpy of NH₃ emissions from sources 19-27.

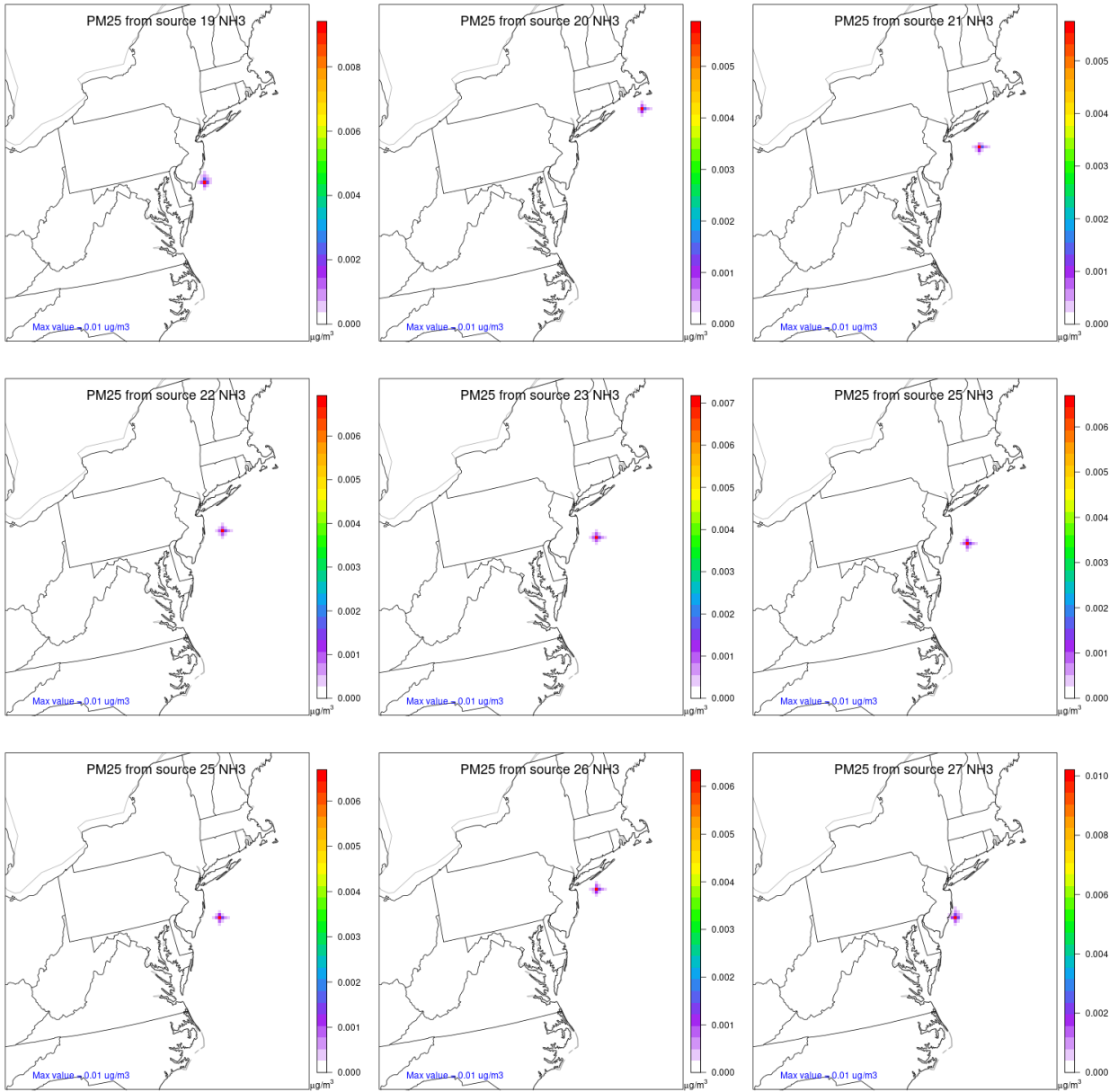


Figure B10. Annual Average PM_{2.5} impacts from 215 tpy of primary PM_{2.5} emissions from sources 1-9.

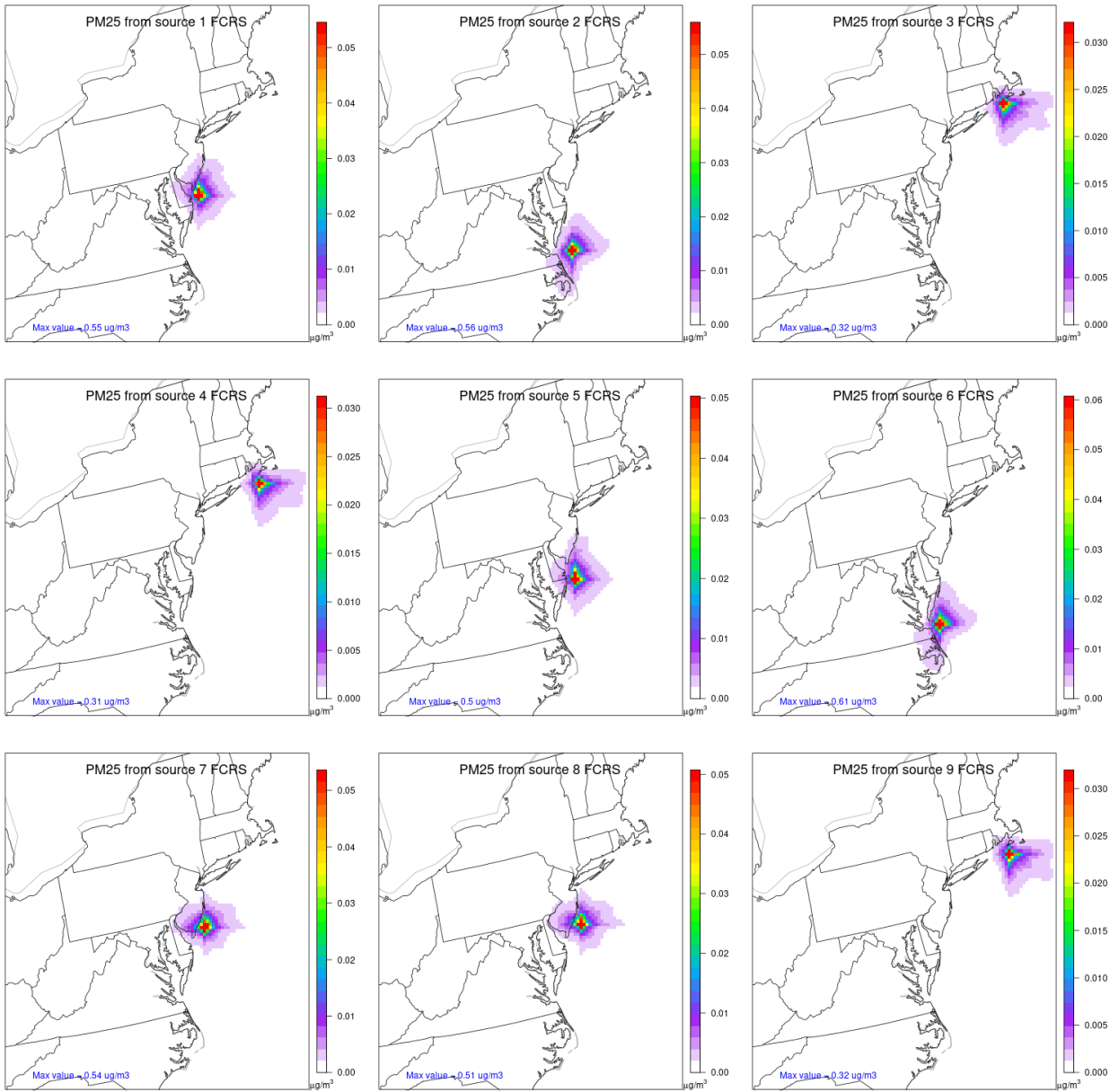


Figure B11. Annual Average PM_{2.5} impacts from 215 tpy of primary PM_{2.5} emissions from sources 10-18.

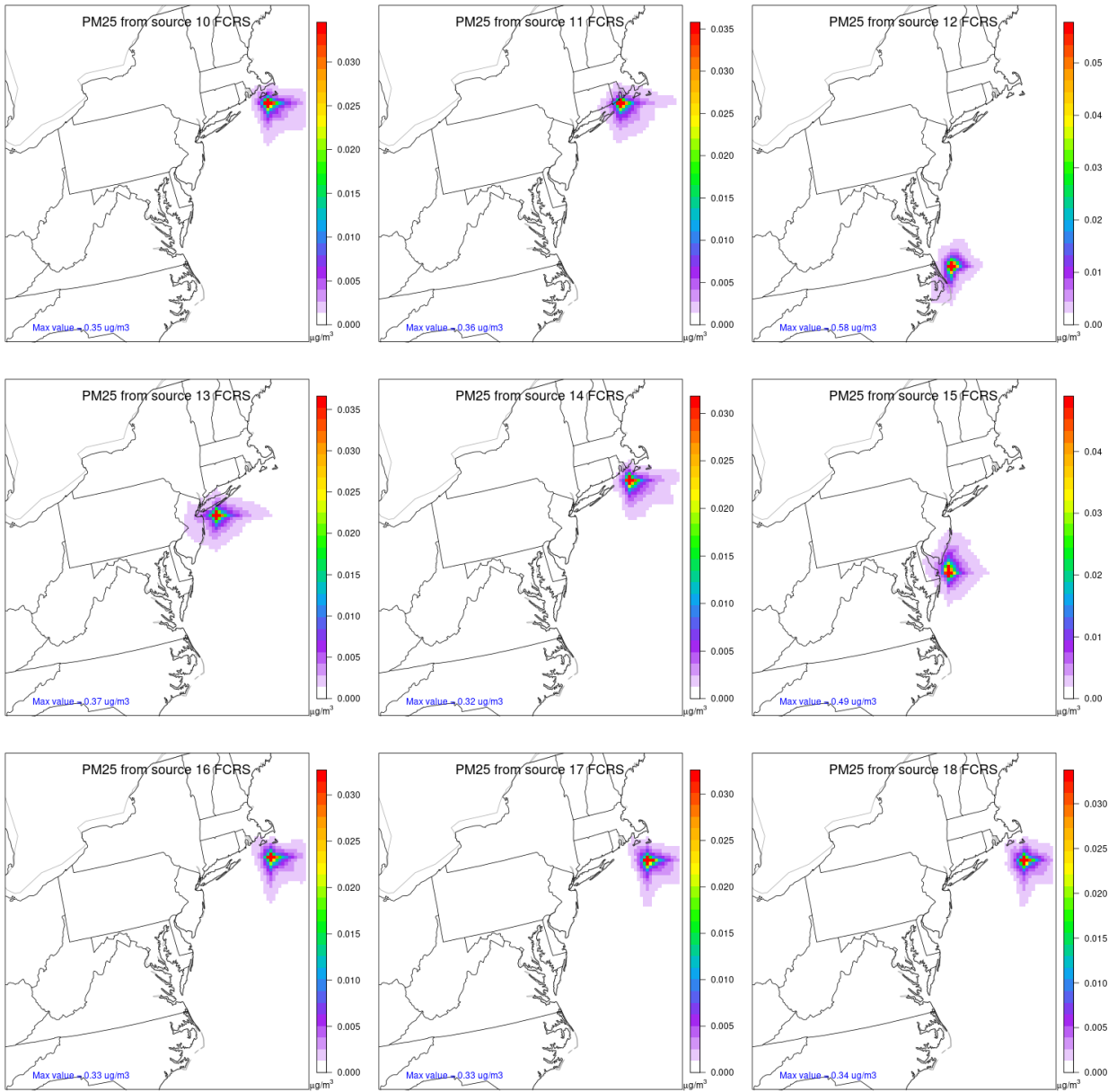


Figure B12. Annual Average PM_{2.5} impacts from 215 tpy of primary PM_{2.5} emissions from sources 19-27.

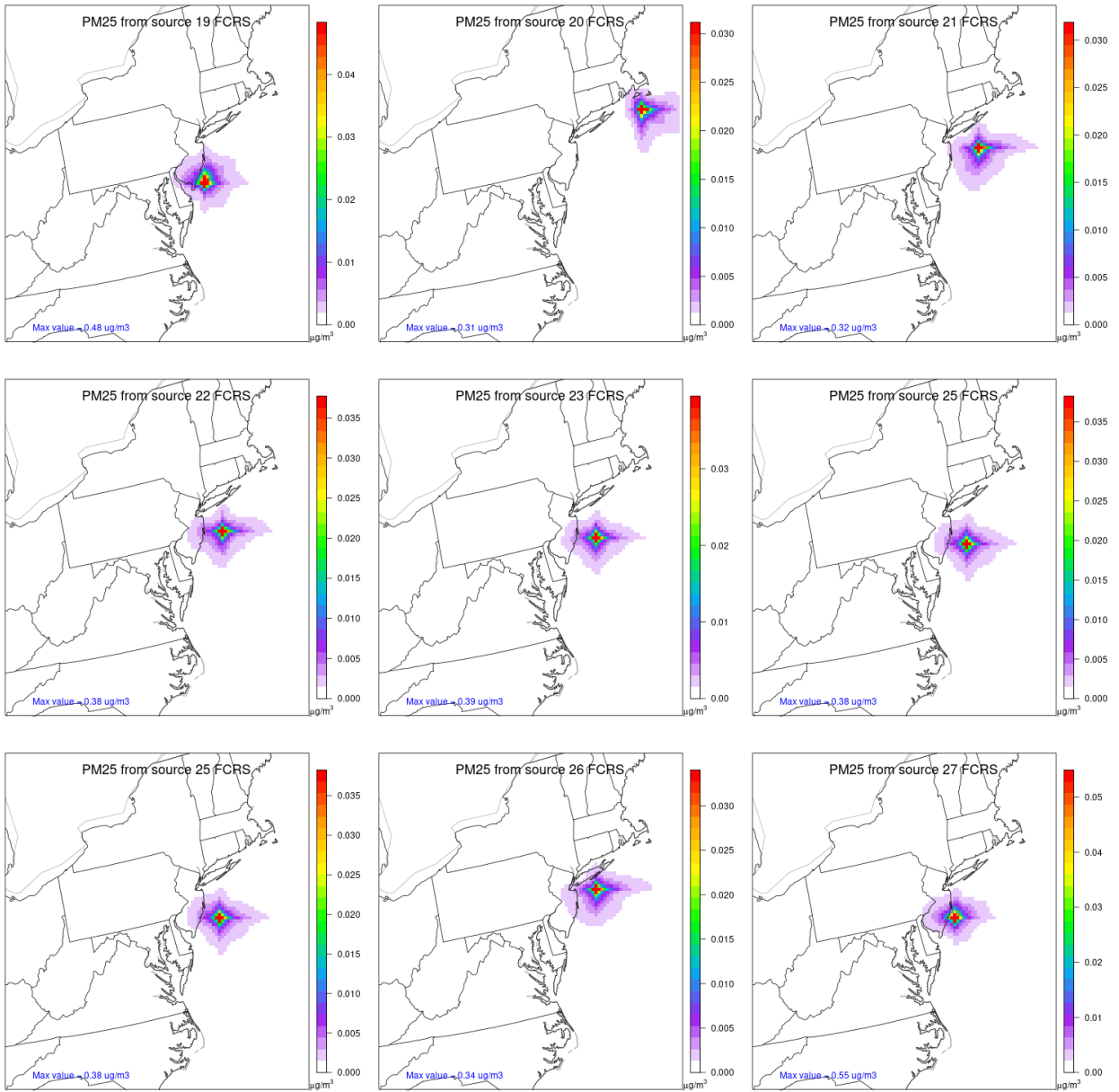


Figure B13. Annual Average Coarse PM impacts from 215 tpy of coarse PM emissions from sources 1-9.

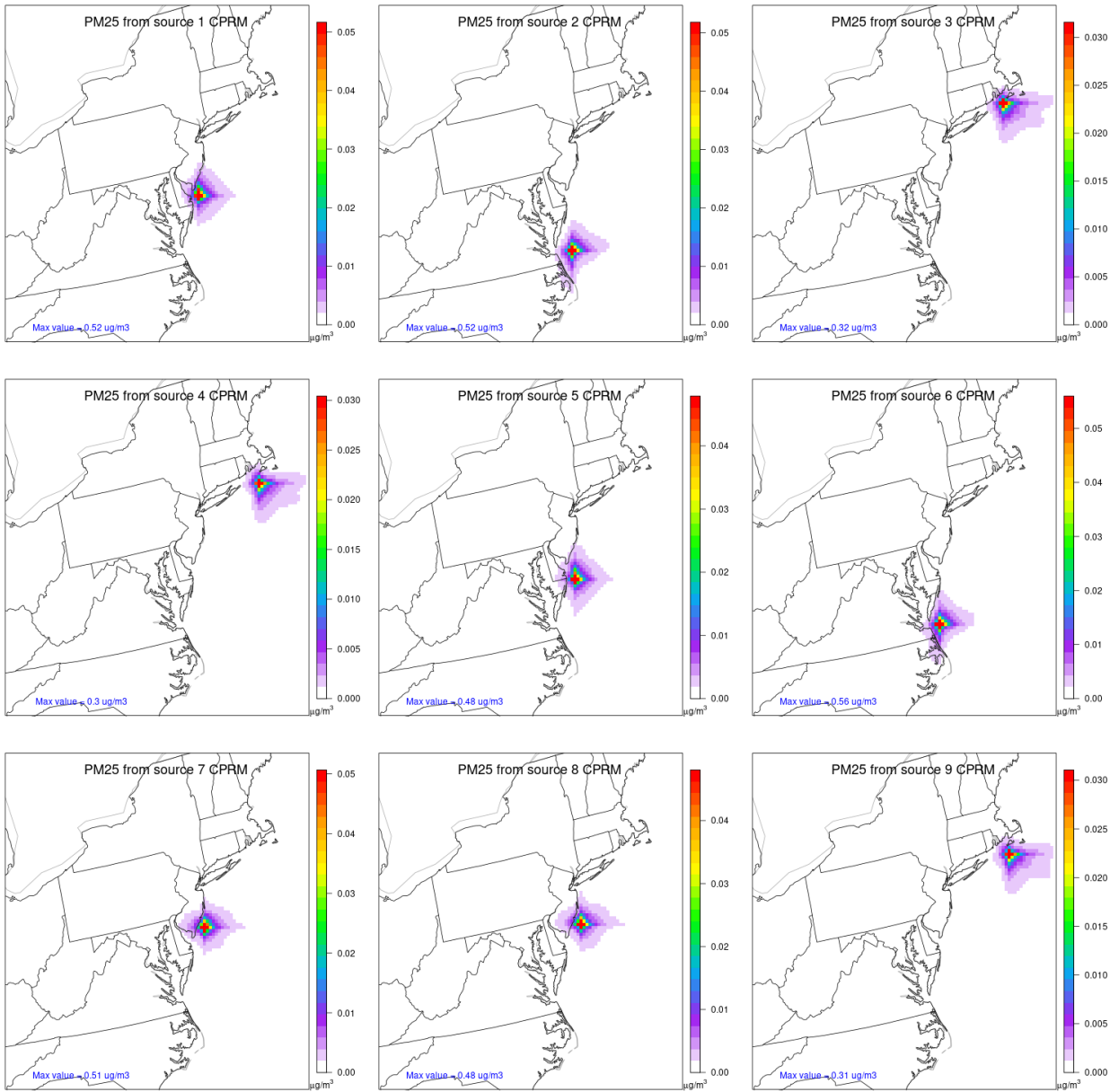


Figure B14. Annual Average Coarse PM impacts from 215 tpy of coarse PM emissions from sources 10-18.

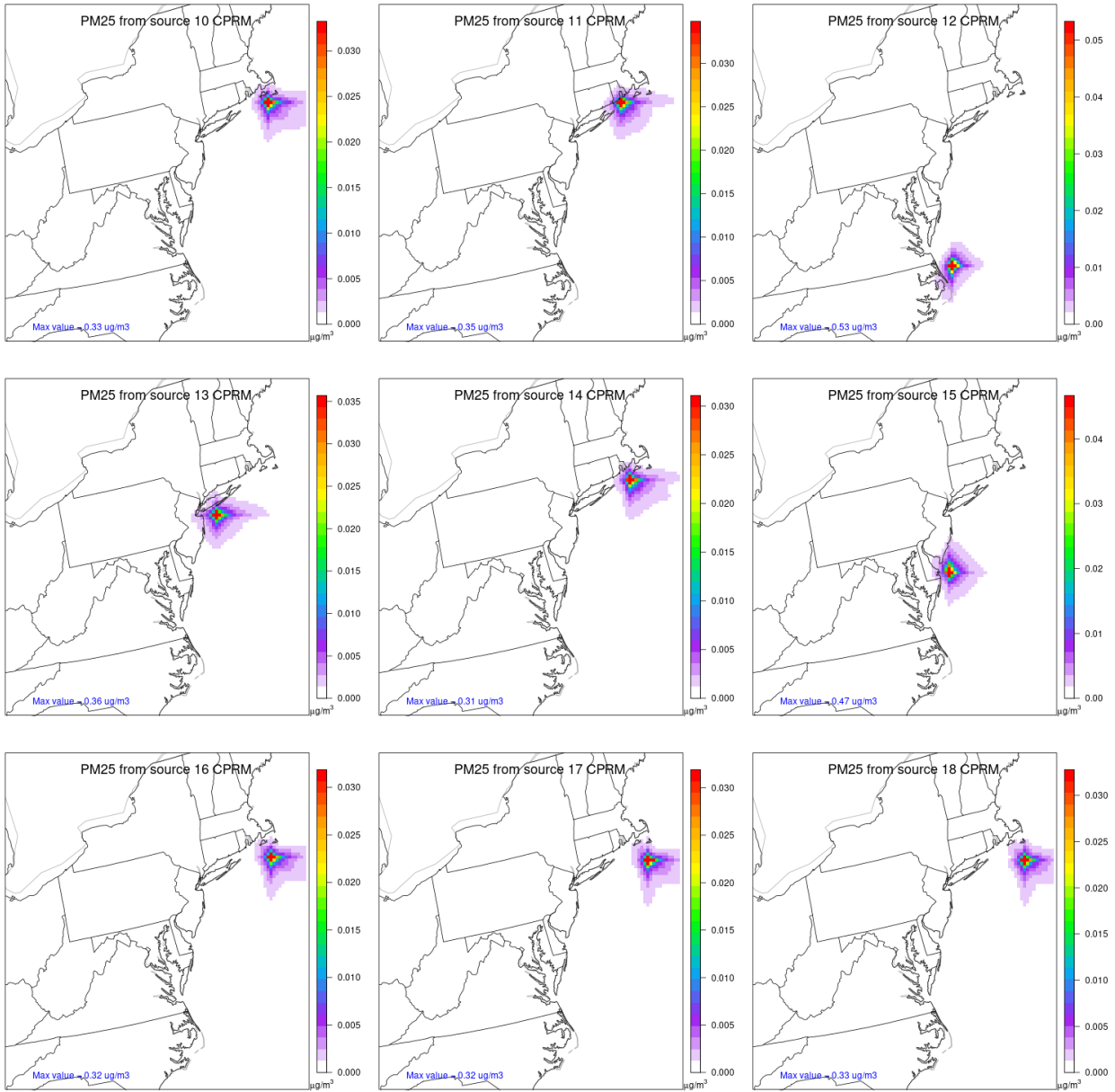
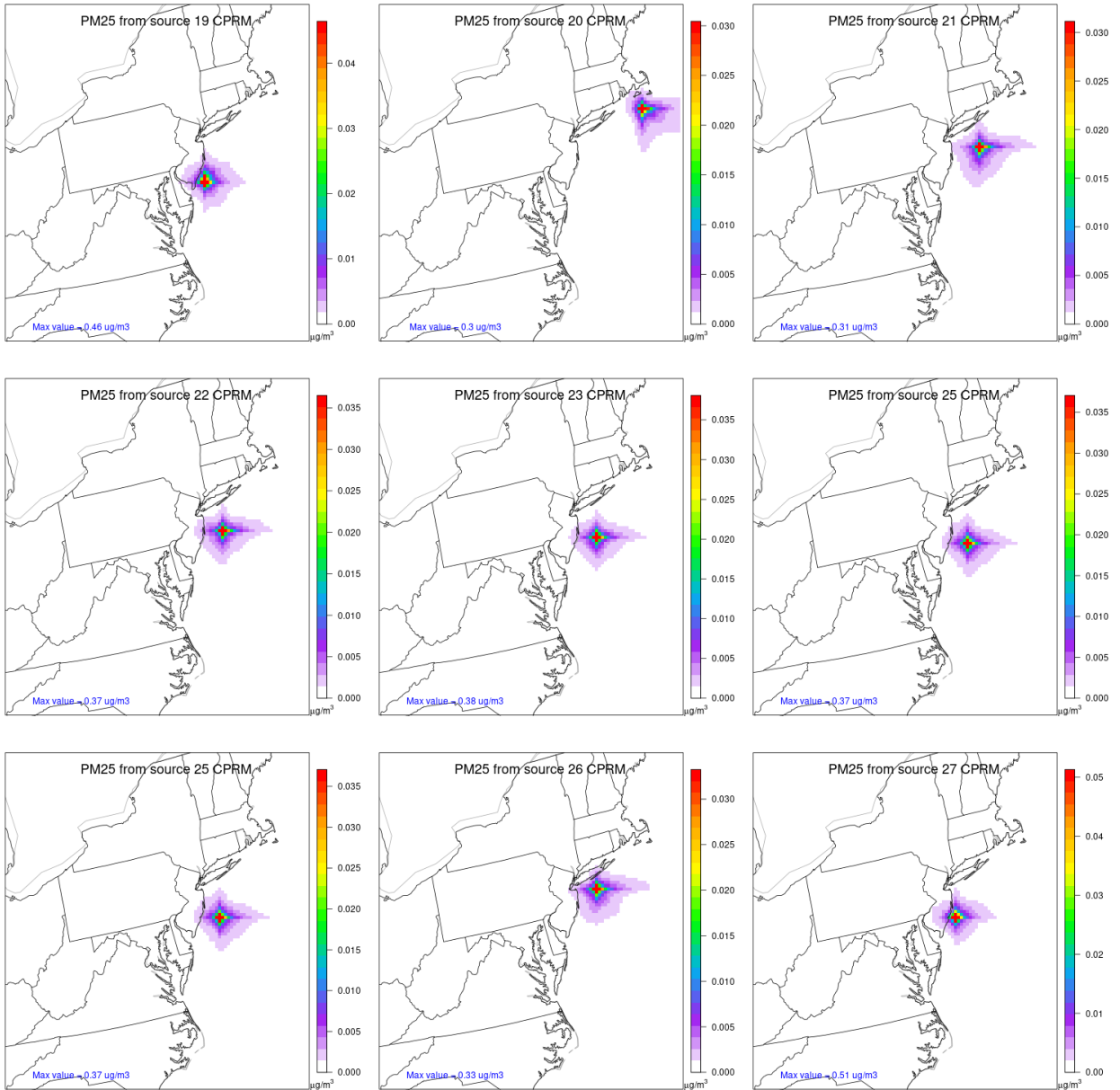


Figure B15. Annual Average Coarse PM impacts from 215 tpy of coarse PM emissions from sources 19-27.



United States
Environmental Protection
Agency

Office of Air Quality Planning and Standards
Air Quality Assessment Division
Research Triangle Park, NC

Publication No. EPA-454/R-22-007
December 2022
